

AD-A031 178 ARMY ENGINEER WATERWAYS EXPERIMENT STATION VICKSBURG MISS F/G 8/3
NUMERICAL ANALYSIS OF TIDAL CIRCULATION FOR LONG BEACH HARBOR. --ETC(U)
SEP 76 D C RANEY

UNCLASSIFIED

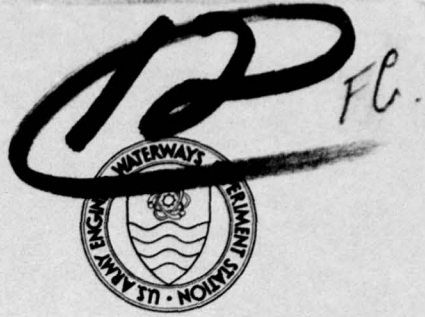
WES-MP-H-76-4-3

NL

1 OF 2
AD A031 178



AD A031178



MISCELLANEOUS PAPER H-76-4

NUMERICAL ANALYSIS OF TIDAL CIRCULATION FOR LONG BEACH HARBOR

Report 3

EXISTING CONDITIONS AND ALTERNATE PLANS FOR PIER J COMPLETION AND TANKER TERMINAL STUDY WITH -82 FT CHANNEL

by

Donald C. Raney

Hydraulics Laboratory

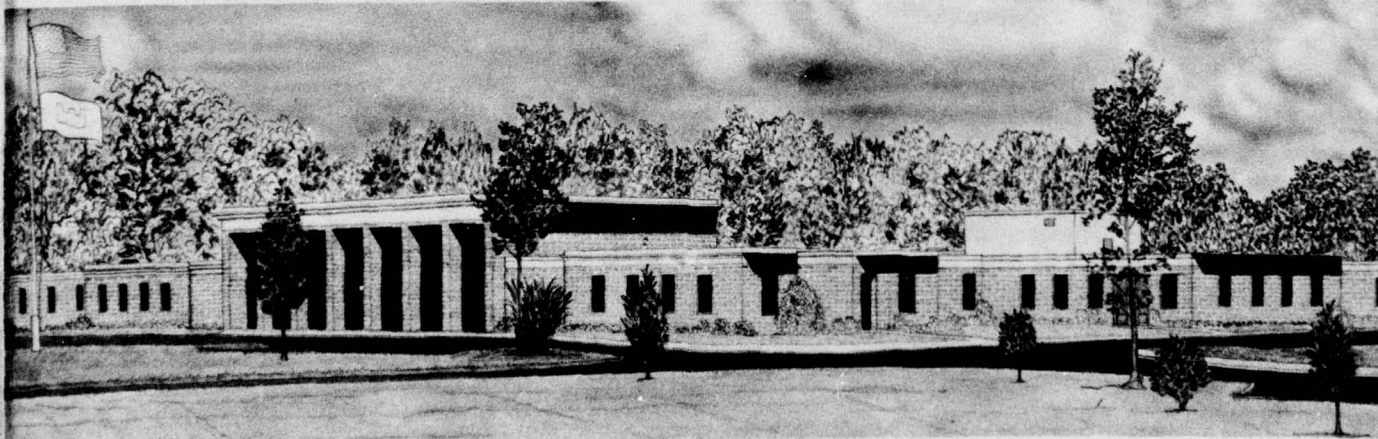
U. S. Army Engineer Waterways Experiment Station

P. O. Box 631, Vicksburg, Miss. 39180

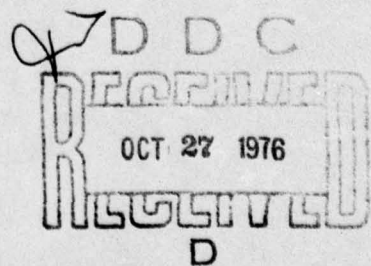
September 1976

Report 3 of a Series

Approved For Public Release; Distribution Unlimited



Prepared for Port of Long Beach
Long Beach, California 90801



**Destroy this report when no longer needed. Do not return
it to the originator.**

Unclassified

SECURITY CLASSIFICATION OF THIS PAGE (When Data Entered)

DD FORM 1 JAN 73 1473 EDITION OF 1 NOV 65 IS OBSOLETE

Unclassified

SECURITY CLASSIFICATION OF THIS PAGE (When Data Entered)

Unclassified

SECURITY CLASSIFICATION OF THIS PAGE(When Data Entered)

20. ABSTRACT (Continued).

tide and velocity data from the prototype and from physical model tests conducted at WES.

For each Pier J modification considered, overall tidal circulation patterns were obtained hourly by vector plots of the tidal velocity at each finite difference cell. The change in overall tidal circulation patterns from those presently existing were also determined. The mass flow rates through the breakwater openings and channels were calculated and compared with those flows currently existing in the harbor. Changes in flow rates as a result of the Pier J modification were identified.

ACCESSION FOR	
NTIS	White Section <input checked="" type="checkbox"/>
DOC	Buff Section <input type="checkbox"/>
UNANNOUNCED	<input type="checkbox"/>
JUSTIFICATION	
BY	
DISTRIBUTION/AVAILABILITY CODES	
BEST	AVAIL. AND/or SPECIAL
P	

D D C
REF ID: A65192
OCT 27 1976
R E S U L T S
D

Unclassified

SECURITY CLASSIFICATION OF THIS PAGE(When Data Entered)

PREFACE

This study was conducted at the U. S. Army Engineer Waterways Experiment Station (WES) with funding provided by the Port of Long Beach, Long Beach, California, under WES Agreement No. 76-8. The study was conducted during the period from November 1975 to April 1976 in the Harbor Wave Action Branch, Wave Dynamics Division, Hydraulics Laboratory, WES, under the direction of Mr. H. B. Simmons, Chief of the Hydraulics Laboratory, Dr. R. W. Whalin, Chief of the Wave Dynamics Division, and Mr. C. E. Chatham, Chief of the Harbor Wave Action Branch.

The study was conducted and this report prepared by Dr. Donald C. Raney, Associate Professor of Engineering Mechanics at the University of Alabama, assigned to WES under an Intergovernmental Personnel Exchange Agreement. Messrs. H. Lee Butler, K. A. Turner, C. W. Coe, L. A. Barnes, and C. R. Curren assisted with various tasks during the investigation.

A significant portion of the numerical computations associated with this study was performed on a CDC-7600 computer at the Los Alamos Scientific Laboratory, Los Alamos, New Mexico, through the cooperation of C-Division.

The following Port of Long Beach personnel visited WES for conferences associated with the study: Messrs. B. N. Hoffmaster, C. T. Johnson, G. H. Porter, R. F. Berbower, and Dr. D. B. Bright.

Directors of WES during the course of this study and the preparation and publication of this report were COL G. H. Hilt, CE, and COL John L. Cannon, CE. Technical Director was Mr. F. R. Brown.

CONTENTS

	<u>Page</u>
PREFACE	1
CONVERSION FACTORS, U. S. CUSTOMARY TO METRIC (SI)	
UNITS OF MEASUREEMENT	3
PART I: INTRODUCTION	4
Objective	4
Background	4
PART II: THE NUMERICAL MODEL	6
Formulation of the Model	6
Application to San Pedro Bay	12
PART III: MODEL VERIFICATION	16
Existing Conditions	16
Plan 1A-2	23
PART IV: ALTERNATE PIER J CONFIGURATIONS	28
Modifications Investigated	28
Results	28
PART V: CONCLUSIONS	35
REFERENCES	36
TABLES 1-3	
PLATES 1-102	
APPENDIX A: NOTATION	

CONVERSION FACTORS, U. S. CUSTOMARY TO METRIC (SI)
UNITS OF MEASUREMENT

U. S. customary units of measurement used in this report can be converted to metric (SI) units as follows:

Multiply	By	To Obtain
feet	0.3048	metres
miles (U. S. statute)	1.609344	kilometres
square miles (U. S. statute)	2.589988	square kilometres
cubic feet	0.02831685	cubic metres
feet per second	0.3048	metres per second
cubic feet per second	0.02831685	cubic metres per second

NUMERICAL ANALYSIS OF TIDAL CIRCULATION FOR LONG BEACH HARBOR

EXISTING CONDITIONS AND ALTERNATE PLANS FOR PIER J COMPLETION
AND TANKER TERMINAL STUDY WITH -82 FT CHANNEL

PART I: INTRODUCTION

Objective

1. The purpose of this phase of the Long Beach Harbor model study was to numerically investigate the impact on existing harbor circulation of alternate master plan Pier J configurations with a -82 ft* channel on tidal circulation.

2. This report describes the application of a previously verified numerical model in a completely predictive mode to evaluate the effect of alternate Pier J configurations and a -82 ft channel on tidal circulation.

Background

3. Los Angeles and Long Beach Harbors are adjacent ports in San Pedro Bay, California. They constitute separate political entities and are administered by separate port authorities. Modifications to the existing harbors have been proposed by both port authorities, the U. S. Army Corps of Engineers, and the city of Long Beach. Proposed modifications are so extensive that a careful examination of their effects on the existing harbor and expanded harbor facilities is required to reduce the possibility of undesirable effects that could prove irreversible or expensive to correct. Therefore, Congress directed the Corps of Engineers to build a physical model of Los Angeles and Long Beach Harbors and to conduct studies of the harbors and proposed modifications.

* A table of factors for converting U. S. customary units of measurement to metric (SI) units is presented on page 3.

Construction of the model at the U. S. Army Engineer Waterways Experiment Station (WES) began in January 1973 and was completed in August of that year.

4. An extensive prototype data collection program (described in detail in Reference 1) was performed to provide data for verification of the physical model and to describe existing conditions in the harbors. The physical model was verified using prototype data and base circulation tests were conducted as reported in Reference 2. In addition, studies of several alternate harbor configurations have been conducted in the physical model. Of particular interest relative to the present study is the harbor configuration referred to as plan 1A-2.³

5. In November 1975, the Port of Long Beach requested WES to conduct a study of the effects on tidal-generated circulation in Los Angeles and Long Beach Harbors produced by proposed modifications of the Pier J complex. Primarily because of time constraints and scheduling problems associated with the physical model, it was decided to conduct the study using a two-dimensional, depth-averaged, numerical model of the hydrodynamic equations. The numerical model would be verified using physical model data for (a) the present harbor configuration and (b) for a proposed modification to the harbor known as plan 1A-2. After model verification, the numerical model would be used to predict the effects on tidal-generated circulation of proposed modification to the Pier J complex. Pier J modifications associated with a tanker terminal project have been previously investigated using the numerical model.^{4,5} The present report is concerned with basically the same Pier J modifications as those considered for the tanker terminal project but with a -82 ft channel.

PART II: THE NUMERICAL MODEL

Formulation of the Model

6. A complete mathematical description of the hydrodynamic flow in a harbor or estuary would require that the velocity and density be completely specified for every point in the system at all times:

$$u = u(x, y, z, t)*$$

$$\rho = \rho(x, y, z, t)$$

where

x = longitudinal coordinate measured along the estuary axis

y = transverse coordinate

z = vertical coordinate

t = time

Unfortunately, with existing computers, a generalized three-dimensional model with the needed time and spatial resolution is not available. Because of the difficulties in formulation and executing a three-dimensional program, researchers have devised a variety of numerical models of various degrees of simplification. In general, the simpler the model the less reliable and less adaptable it is to changing conditions.

7. A two-dimensional approach that produces a pseudothree-dimensional effect was utilized in the numerical investigation. The vertical components of velocity and acceleration are neglected and the general three-dimensional governing hydrodynamic equations are integrated over the water depth. A depth-averaged two-dimensional flow field is obtained but three-dimensional geometry can be considered. The most important approximations used in the model are those of constant density and relatively small variations of velocity over the

* For convenience, symbols and unusual abbreviations are listed and defined in the Notation (Appendix A).

depth, conditions which are reasonably valid in most harbors. Where these conditions are approximately valid, this type of numerical model can provide accurate representations of tidal elevations and velocities. Although the model output is two-dimensional, it has a pseudothree-dimensional character since the actual bathymetric data are used in the calculations. The two-dimensional depth-averaged model appears to be the most sophisticated numerical model presently available for study of tidal circulation in harbors.

8. The rectangular coordinate system used is located in the plane of the undisturbed water surface as shown in Figure 1. The equations

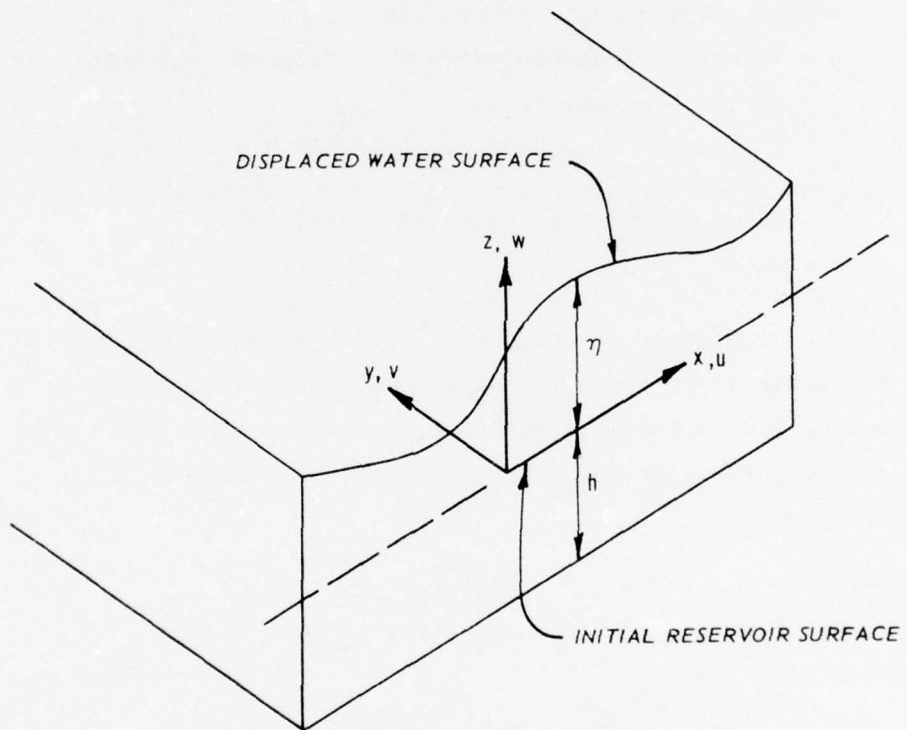


Figure 1. Coordinate system for problem formulation

of motion and the equation of continuity are written as follows:

$$\frac{\partial u}{\partial t} + u \frac{\partial u}{\partial x} + v \frac{\partial u}{\partial y} + g \frac{\partial \eta}{\partial x} - fv = R_x + L_x \quad (1)$$

$$\frac{\partial v}{\partial t} + u \frac{\partial v}{\partial x} + v \frac{\partial v}{\partial y} + g \frac{\partial \eta}{\partial y} + fu = R_y + L_y \quad (2)$$

and

$$\frac{\partial \eta}{\partial t} + \frac{\partial}{\partial x} [(h + \eta)u] + \frac{\partial}{\partial y} [(h + \eta)v] = 0 \quad (3)$$

where

u = depth-averaged velocity component in the x direction

t = time

x, y = rectangular coordinate variables

v = depth-averaged velocity component in the y direction

g = acceleration due to gravity

η = water-level displacement with respect to datum elevation

f = Coriolis parameter

R_x, R_y = the effect of bottom roughness in x and y directions

L_x, L_y = the acceleration effect of the wind stress acting on the water surface in the x and y directions

h = water depth

9. The continuity equation has been obtained by integrating across the water depth and applying kinematic and dynamic boundary conditions at the surface and bottom of the reservoir. The bottom friction terms are represented using a Chezy coefficient in the following form:

$$R_x = \frac{-gu(u^2 + v^2)^{1/2}}{C^2(h + \eta)} \quad (4)$$

$$R_y = \frac{-gv(u^2 + v^2)^{1/2}}{C^2(h + \eta)} \quad (5)$$

where C is the Chezy coefficient. The terms L_x and L_y represent the wind shear stress effect on the water surface. These terms are of the form:

$$L_x = \frac{T_x}{(h + \eta)} \quad (6)$$

$$L_y = \frac{T_y}{(n + \eta)} \quad (7)$$

where T_x and T_y are the wind stress components acting on the water surface.

10. To solve the governing equations, a finite difference approximation of the equations and an alternating direction technique are employed. A space-staggered scheme is used in which velocities, water-level displacement, bottom displacement, and water depth are described at different locations within a grid cell as shown in Figure 2. The first step in the calculation consists of computing u

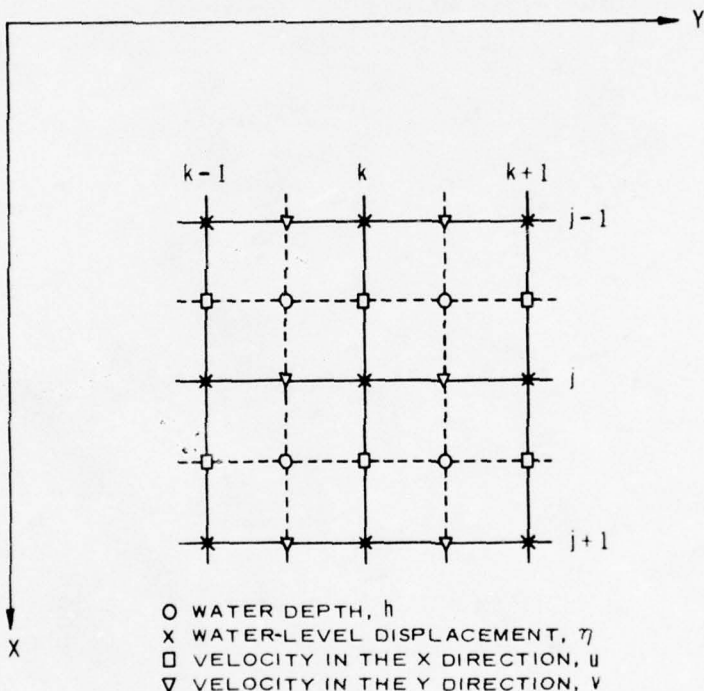


Figure 2. Grid system and variable definition locations

and η implicitly and v explicitly, advancing from time $n\Delta t$ to $(n + 1/2)\Delta t$. The parameter n is an integer representing the time step at which the calculations are being conducted. The second step computes η and v implicitly and u explicitly, advancing from time

$(n + 1/2)\Delta t$ to $(n + 1)\Delta t$. Central differences are used for evaluating all derivatives in the governing equations. The application of these difference approximations gives rise to corresponding difference equations centered about different points within a grid cell. These expressions require the evaluation of certain quantities at locations different from those defined in the grid system. Such quantities are replaced by values computed from a one- and two-dimensional averaging of neighboring values. The time interval Δt is taken as the time required to complete the full cycle in the computational procedure; however, each half cycle is treated by a different set of equations so a system of six operational equations is used. The difference approximations used in the first step of the alternating direction technique are:

$$u^{n+1/2} = u^n - \frac{g}{2} \left(\frac{\Delta t}{\Delta x} \right) \ll \eta_x \gg^{n+1/2} - \frac{1}{4} \left(\frac{\Delta t}{\Delta x} \right) u^{n+1/2} \ll u_x^n \\ - \frac{1}{4} \left(\frac{\Delta t}{\Delta y} \right) v^n \ll u_y^n \gg + \frac{1}{2} \Delta t (R_x + L_x)^n \text{ at } j+1/2, k \quad (8)$$

and

$$\eta^{n+1/2} = \eta^n - \frac{1}{2} \left(\frac{\Delta t}{\Delta x} \right) \ll [(\bar{h} + \bar{\eta})u]_x \gg^{n+1/2} - \frac{1}{2} \left(\frac{\Delta t}{\Delta y} \right) \ll [(\bar{h} + \bar{\eta})v]_y \gg^n \\ \text{at } j, k \quad (9)$$

where superscripts refer to multiples of time increments. For simplicity of notation, some terms have been maintained in differential form within angle brackets $\langle \rangle$ or double brackets $\ll \gg$. The differential forms are defined by the examples:

$$\ll \eta_x(j, k) \gg = \eta_{j+1/2, k} - \eta_{j-1/2, k} \quad (10)$$

$$\ll u_x(j, k) \gg = u_{j+1, k} - u_{j-1, k} \quad (11)$$

11. These two equations can be solved simultaneously for quantities $u^{n+1/2}$ and $\eta^{n+1/2}$ along a grid line k . The additional velocity component $v^{n+1/2}$ can be determined explicitly from the expression

$$v^{n+1/2} = v^n - \frac{g}{2} \left(\frac{\Delta t}{\Delta y} \right) \ll \eta_y \gg^n - \frac{1}{4} \left(\frac{\Delta t}{\Delta x} \right) \bar{u}^{n+1/2} \ll v_x \gg^n - \frac{1}{4} \left(\frac{\Delta t}{\Delta y} \right) v^{n+1/2} \ll v_y \gg^n + \frac{1}{2} \Delta t (R_y + L_y)^n \quad \text{at } j, k+1/2 \quad (12)$$

The equations for the second step of the alternating direction technique are:

$$v^{n+1} = v^{n+1/2} - \frac{g}{2} \left(\frac{\Delta t}{\Delta y} \right) \ll \eta_y \gg^{n+1} - \frac{1}{4} \left(\frac{\Delta t}{\Delta x} \right) \bar{u}^{n+1/2} \ll v_x \gg^{n+1/2} - \frac{1}{4} \left(\frac{\Delta t}{\Delta y} \right) v^{n+1} \ll v_y \gg^{n+1/2} + \frac{1}{2} \Delta t (R_y + L_y)^{n+1/2} \quad \text{at } j, k+1/2 \quad (13)$$

and

$$\eta^{n+1} = \eta^{n+1/2} - \frac{1}{2} \left(\frac{\Delta t}{\Delta x} \right) \ll \left[\frac{(h+\eta)}{2} u \right]_x \gg^{n+1/2} - \frac{1}{2} \left(\frac{\Delta t}{\Delta y} \right) \ll \left[\frac{(h+\eta)}{2} v \right]_y \gg^{n+1} \quad \text{at } j, k \quad (14)$$

These equations are solved simultaneously for the quantities $v^{n+1/2}$ and $\eta^{n+1/2}$ along a grid line j . The additional velocity component $u^{n+1/2}$ can be determined explicitly from the expression

$$u^{n+1} = u^{n+1/2} - \frac{g}{2} \left(\frac{\Delta t}{\Delta x} \right) \ll \eta_x \gg^{n+1/2} - \frac{1}{4} \left(\frac{\Delta t}{\Delta x} \right) u^{n+1} \ll u_x \gg^{n+1/2} - \frac{1}{4} \left(\frac{\Delta t}{\Delta y} \right) \bar{v}^{n+1} \ll u_y \gg^{n+1/2} + \frac{1}{2} \Delta t (R_x + L_x)^{n+1/2} \quad \text{at } j+1/2, k \quad (15)$$

12. The formulation of the problem in this way (ADI method) considerably simplifies the computational procedure. The implicit equations are solved simultaneously during each half time step. However, with this formulation scheme the coefficient matrix is tridiagonal

and a relatively simple solution procedure is available.

13. Two types of boundaries are involved in the calculations: the solid boundaries at fixed coastlines and the artificial tidal input boundaries arising from the need to truncate the region of computation (in order to minimize computational time requirements).

14. A condition of complete reflection is adopted at solid boundaries. While some dissipation does occur at the shoreline, this should not be significant in this application. The actual boundary condition for the solid boundary can be written as

$$\vec{V}_n = 0 \quad (16)$$

where \vec{V}_n denotes the normal component of velocity.

15. Artificial tidal boundaries were used in the model to describe the tidal action that occurs at the ocean computational boundaries. These boundaries must be accurately defined since the tides applied at these boundaries represent the major forcing function driving the hydrodynamic system. The water-surface elevation time history for the desired tidal cycle is specified at each such boundary and applied during the operation of the model.

Application to San Pedro Bay

16. San Pedro Bay is formed by the curvature and indentation of the southern California coastline (Figure 3). Sheltered to the west by Point Fermin, the bay is open to the south and southeast except for the slight protection offered by Catalina Island. Originally an open bay, the protection afforded by its orientation has been augmented by an 8-mile-long breakwater extending from Point Fermin eastward to near Seal Beach.

17. The breakwater consists of three sections. The San Pedro breakwater (oldest of the three) is 11,000 ft long and extends from the shoreline east of Point Fermin to Angel's Gate, which is the 2,100-ft-wide navigation opening for Los Angeles Harbor. The Middle breakwater

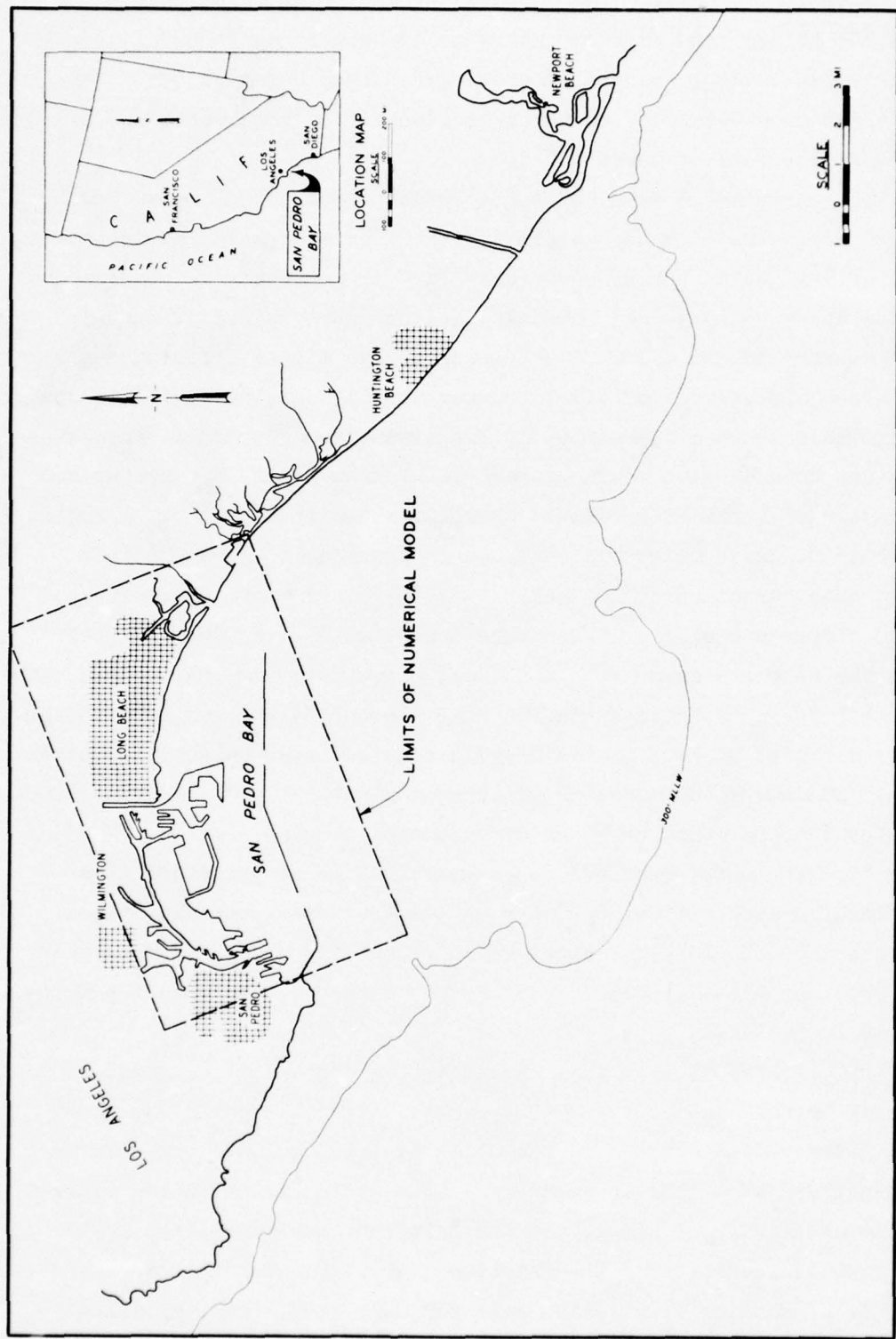


Figure 3. Site map and limits of numerical model

is 18,500 ft long and extends from Angel's Gate to Queen's Gate, which is the 1,800-ft-wide navigation opening for Long Beach Harbor. The Long Beach breakwater is the third section of the breakwater and extends 13,350 ft due east of Queen's Gate.

18. A detailed study of the circulation patterns in San Pedro Bay was necessary in order to predict the effect on circulation patterns of changes in harbor configuration. To get the required resolution of the harbor basins, channels, and proposed modifications it was necessary to use a 300-ft step size in the finite difference grid. For proper application of tidal boundary conditions the region of study was extended seaward approximately 1.4 miles from the Middle breakwater. The tidal boundary was taken as parallel to the Middle breakwater and the region of application of the model is shown in Figure 3. A region of about 60 square miles was included in the model coverage with a finite grid dimension of 101 cells by 199 cells or approximately 20,000 finite difference cells. There were approximately 12,000 water cells where the velocity components and tidal elevations were calculated each time step during a tidal cycle. A time step of 45 sec was used in the numerical model so a 25-hr tidal cycle required 2000 calculation time steps. The numerical model required approximately 1-1/4 hr of CDC-7600 computer time to simulate 25 hr of prototype time.

19. The model required approximately 5 hr of prototype time (15 min of computer time) to "warm up" due to transients associated with starting the model. Actual calculations for a 25-hr tidal cycle required approximately 1.5 hr of CDC-7600 computer time when the warm-up time is included.

20. Preparation of the input data for the numerical model is extensive since each of the 20,000 finite difference cells requires certain input data concerning the cell characteristics. The cell must be identified as a land or water cell, the depth of the water relative to some datum must be given, and the friction characteristics of the cell must be identified. The friction characteristics are expressed in terms of Manning's n which vary for mud, sand, rock, shoaling areas, vegetation in marsh areas, etc.

21. After the input data have been prepared, the desired tidal cycle is applied to the model and the results are examined and compared with prototype and physical model results. The model parameters are then adjusted until the desired agreement exists between the numerical model and known data.

PART III: MODEL VERIFICATION

Existing Conditions

22. Before any numerical model can be applied as a predictive tool with a reasonable degree of confidence it must be verified. It must demonstrate an ability to produce results that agree with known data for existing conditions. The numerical model was verified by comparing the results with data obtained from the previously verified physical model of Los Angeles and Long Beach Harbors.² This technique was used because of the ready availability of sufficient data of the required quality and quantity. A typical spring tide with a 7.1-ft diurnal range was one of the tides used in the original base tests on the physical model.

Tidal elevations

23. From physical model tests, surface elevation data were available at 13 locations and velocity data were available at 7 ranges (a total of 22 gages) as a function of time for an entire tidal cycle. Locations of these gages are shown in Figure 4. In addition, photographs of surface velocity patterns at hourly intervals were available.

24. The input data were prepared for the numerical model and the 7.1-ft diurnal spring tide was applied at the tidal input boundary. Results were compared with the physical model data and parameters in the numerical model were adjusted to bring the numerical results into agreement with the physical model results.

25. Tidal elevations calculated from the numerical model were compared with physical model data at 13 locations distributed throughout Los Angeles and Long Beach Harbors, and the results are shown in Plates 1-5. The numerical results and physical model results are essentially identical at all gages. This result coincides with past experience which has indicated that tidal elevations are reproduced extremely well by the two-dimensional depth-averaged numerical model.

Tidal velocities

26. Reproducing tidal velocities is a much more difficult

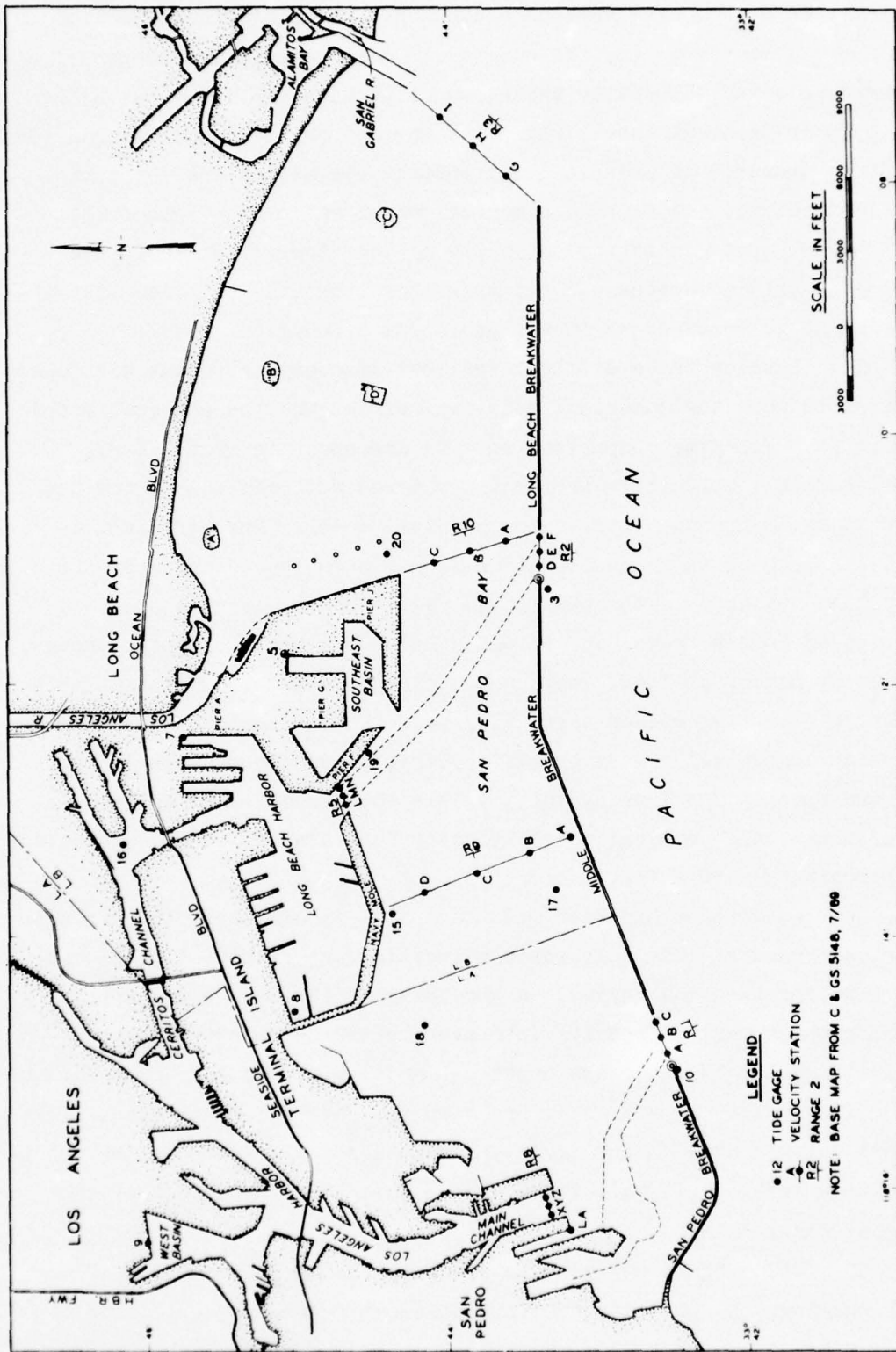


Figure 4. Gage locations for circulation study

problem than reproducing surface elevations. This difficulty arises from several sources: (a) the numerical model calculates a depth-averaged velocity, an entity which cannot be directly measured in the prototype or physical model; (b) prototype and physical model velocities cannot be measured as accurately as surface elevations due to instrument limitations; and (c) the numerical model calculates velocities at discrete points in the hydrodynamic system, therefore the finite difference grid locations will in general not exactly coincide with the location of velocity gages in the prototype or physical model.

27. Despite these difficulties, satisfactory agreement was found to exist between the numerical model velocities and the physical model velocities. Velocity comparison results are shown in Plates 6-27; numerical model velocities are shown compared with the velocities measured at the midpoint depth in the physical model. The agreement is particularly good when consideration is given to the accuracy of the velocities measured in the physical model. The low current speeds experienced in San Pedro Bay are often below the threshold of standard laboratory meters so floats were used to measure model currents. This measuring technique yields a velocity value which, rather than being an instantaneous value at a specific point, is somewhat averaged over time and space. Considering the possible sources of error in the measurements, the physical model velocity data are considered accurate to approximately ± 0.2 fps.

28. No attempt has been made to draw a smooth curve through the numerical results. The calculated velocities are simply plotted each half hour for the tidal cycle. A smoothing of the data would appear to bring the numerical results into even better agreement with the physical model data since the numerical model picks up some fluctuations in the flow which are not as apparent in the physical model data. This is particularly true in the Cerritos Channel gages. These rather short-period fluctuations in velocity would tend to be filtered out of the physical model data.

29. The overall bay circulation patterns were obtained from the numerical model by plotting the instantaneous depth-averaged velocity

at each point in the bay as a vector at specific times during the tidal cycle. The direction and length of the vector indicate the direction and magnitude of the velocity; a vector plot is illustrated in Figure 5. These results were compared with surface current pattern photographs from the physical model tests. In order to facilitate a direct comparison of results, the vector plots from the numerical model were reproduced to the same large scale used in the surface current photographs. The vector plots have therefore been published as a separate report.⁶ The overall circulation patterns observed in the physical model were reproduced reasonably well in the numerical model. This is particularly true when it is recognized that surface currents were observed in the physical model while the numerical model produced depth-averaged velocities. The major gyres observed in the physical model are present in the numerical model results and extend over essentially the same spatial region. The complete extent of the gyres in the numerical model are difficult to ascertain when the vectors are plotted to the scale needed to observe the major circulation patterns in the entire bay. Thus, the large gyre east of the Angel's Gate opening (Figure 5) appears to be smaller in spatial extent than that observed in the physical model. However, a larger scale plot of this region (Figure 6) clearly illustrates the actual extent of the gyre to be very similar to that observed in the physical model. This is also the case for the other major gyres although in some cases the center of the gyre may be shifted somewhat from that observed in the physical model. Any apparent differences in the strength of the gyres between the two models may be associated with variation in the strength of the gyre between the surface strength and an average strength over the water depth.

Volumetric flow rates

30. The volumetric flow rate across the various velocity ranges was also calculated, and results are compared with physical model data in Plates 28-32. The apparent discharge across a range was calculated using the total current velocity regardless of its orientation relative to the velocity range; the adjusted discharge across a range was calculated using the velocity component normal to the range (Figure 7).

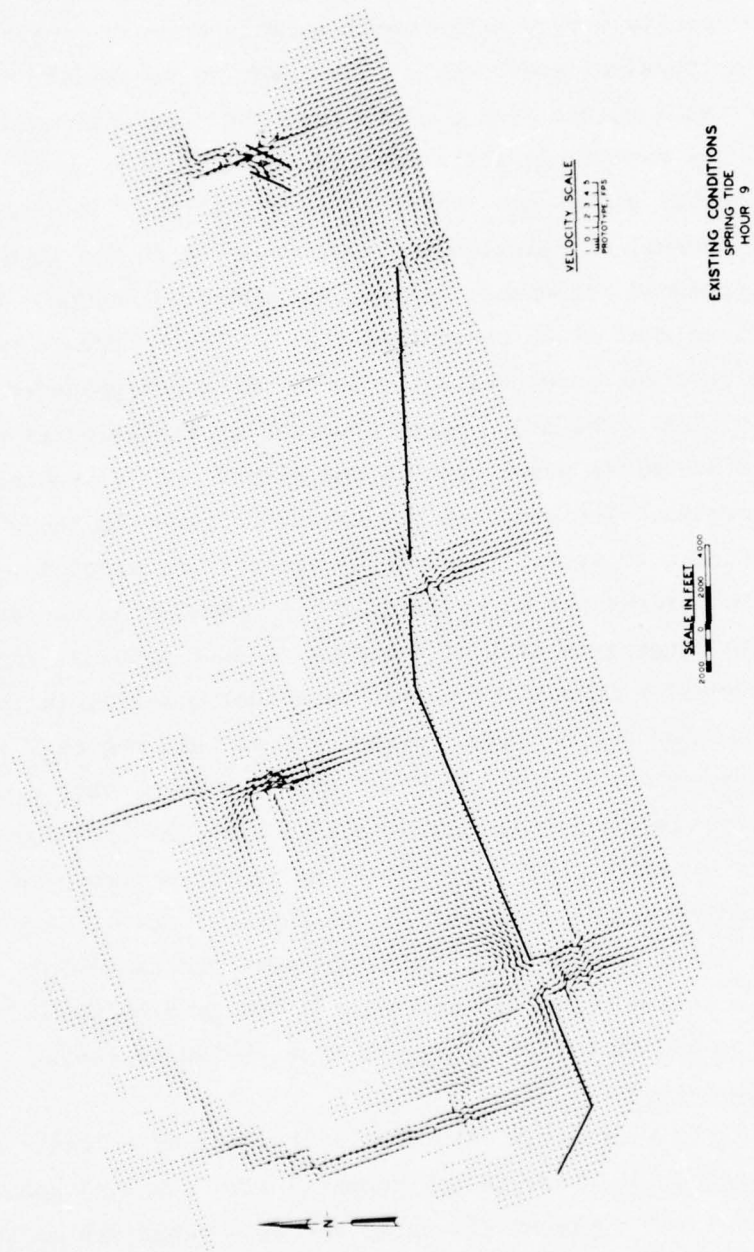


Figure 5. Velocity vector plot of tidal circulation patterns
for existing conditions

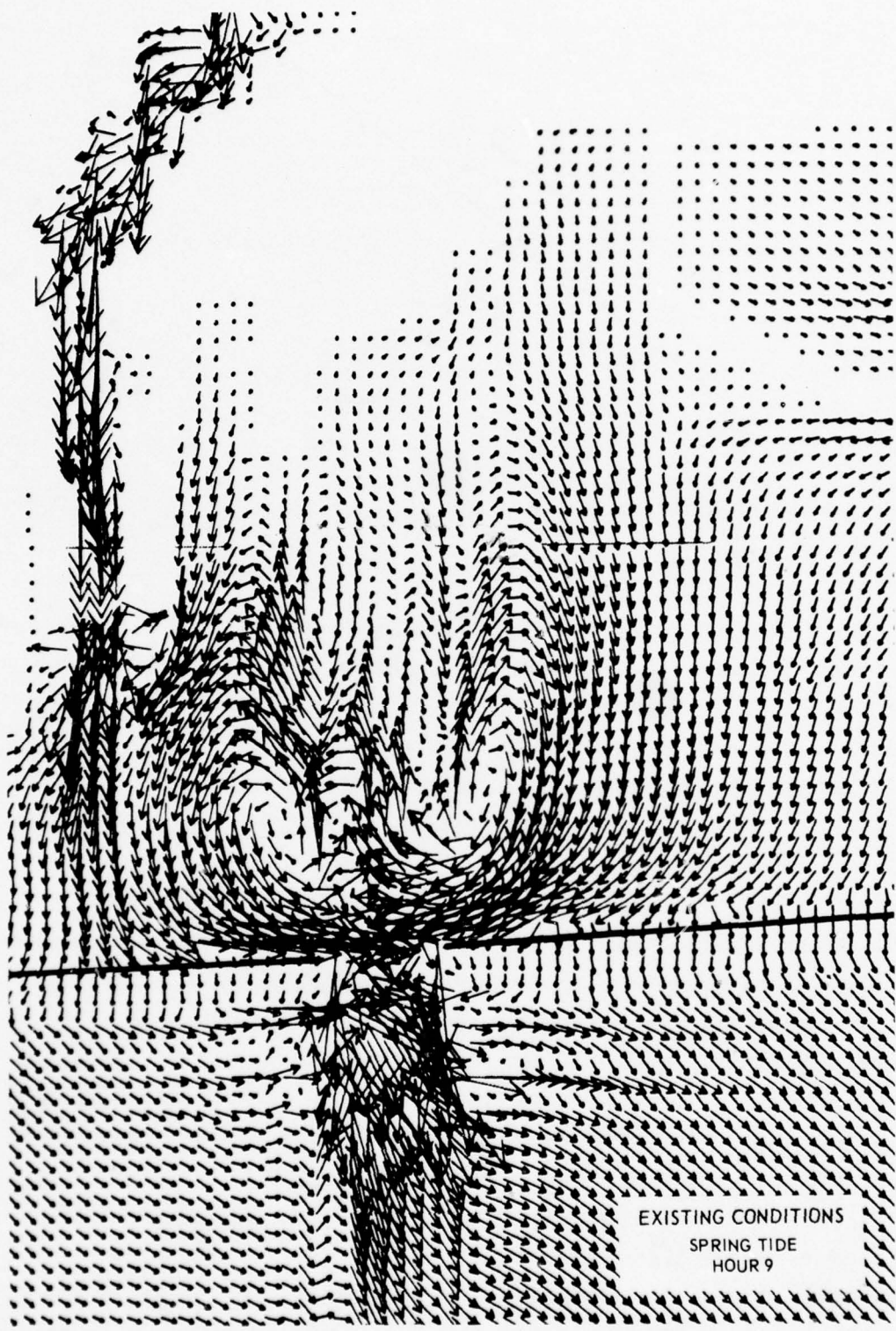
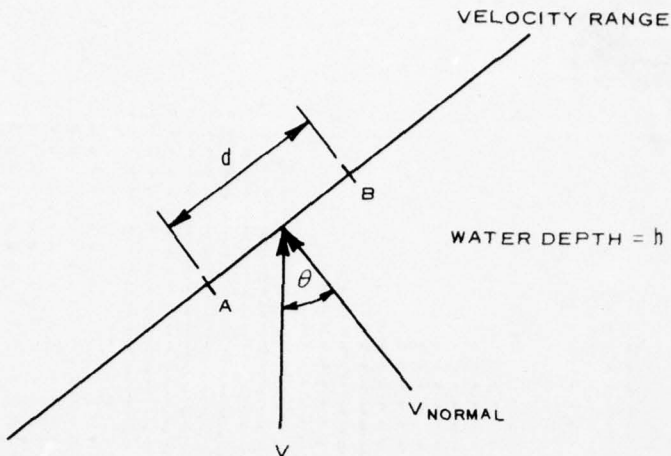


Figure 6. Large-scale vector plot of tidal circulation patterns east of Angel's Gate for existing conditions



$$\text{APPARENT FLOW ACROSS AB} = (V) (d) (h)$$

$$\text{ADJUSTED FLOW ACROSS AB} = (V_{\text{NORMAL}}) (d) (h)$$

Figure 7. Apparent and adjusted discharge

31. The adjusted discharge will obviously always be less than the apparent discharge, the ratio of the two quantities being the cosine of the angle θ . If the flow across the velocity range is essentially normal to the range, then the two quantities are approximately equal. This was the case at ranges 3, 5, and 8 in this investigation.

32. If the volumetric flow rates are integrated over the entire tidal cycle, then a net flow through the range is obtained. The net flows obtained in the numerical model and from the physical model are compared in Table 1. The net flows are small numerically in comparison with the gross volumetric flow; therefore, small percentage errors or variations in the gross flows may appear large compared with the net flows. For this reason, the net flow values are not considered exact and should be used only to indicate flow trends. Net adjusted flows were calculated using the numerical model and net apparent flows were obtained in the physical model which is primarily responsible for the differences observed at ranges 1 and 2. The primary reason for the difference observed at range 3 was the use of only three gages to calculate the flow across the range in the physical model while velocity values at seven locations along the range were used in the numerical

calculations. The results at ranges 5 and 8 agree extremely well. Considering the indicated qualifications concerning the accuracy of the net flow calculations, the agreement between the numerical and physical model results is very satisfactory.

33. From the numerical model there appears to be a net westward flow in Cerritos Channel of approximately $64 \text{ by } 10^6$ cu ft/tidal cycle. This is based on the flow across range 8 which should be more accurate than that across range 5 because of flow conditions crossing the velocity range. The physical model results indicate a westward flow of approximately $50 \text{ by } 10^6$ cu ft/tidal cycle across range 8. There is a net flow through the breakwater which can be obtained by summing the net flows across ranges 1, 2, and 3.

Plan 1A-2

34. To get an estimate of the ability of the verified numerical model to predict the effect on harbor circulation of modification to the harbor, the model was applied to the master plan 1A-2 configuration. The only changes made in the input to the numerical model were the changes in geometry associated with plan 1A-2 as shown in Figure 8. The 7.1-ft diurnal spring tide was used in the numerical model. The calculated results were then compared with physical model data obtained in a previous study.³

35. Comparisons of tidal elevations are shown in Plates 33-37. As was the case for the existing conditions comparison, the tidal elevations are essentially identical.

36. Velocities are compared in Plates 38-55. Basically the same type velocity agreement is obtained for plan 1A-2 as was obtained in the original model verification. The numerical model appeared to do a good job of predicting the tidal velocities for the modified harbor.

37. Vector plots of the overall bay circulation patterns for plan 1A-2 were also obtained; a sample plot is shown in Figure 9. To make the changes in circulation patterns produced by the modification more apparent, vector plots were made of the velocity differences.

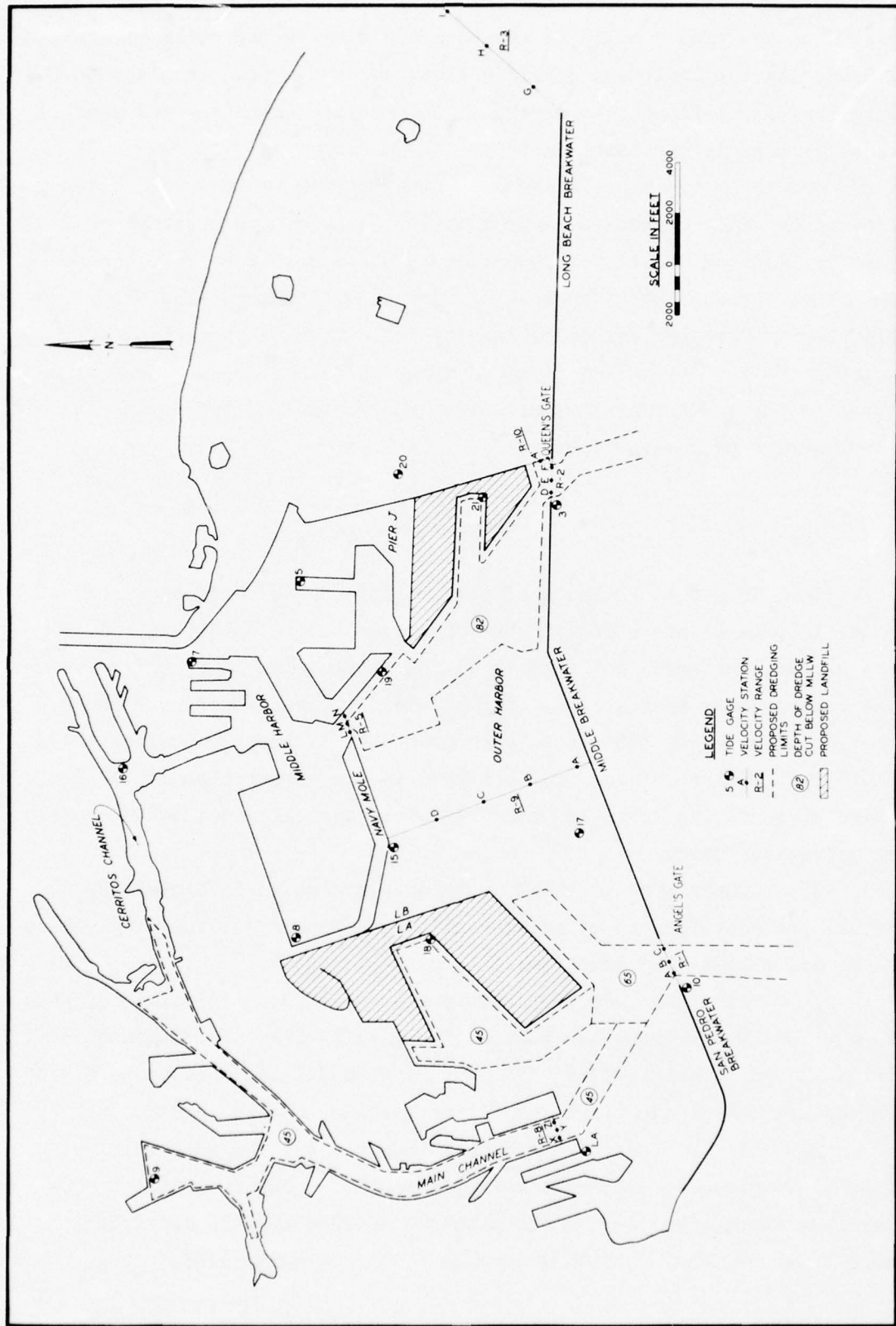


Figure 8. Plan 1A-2

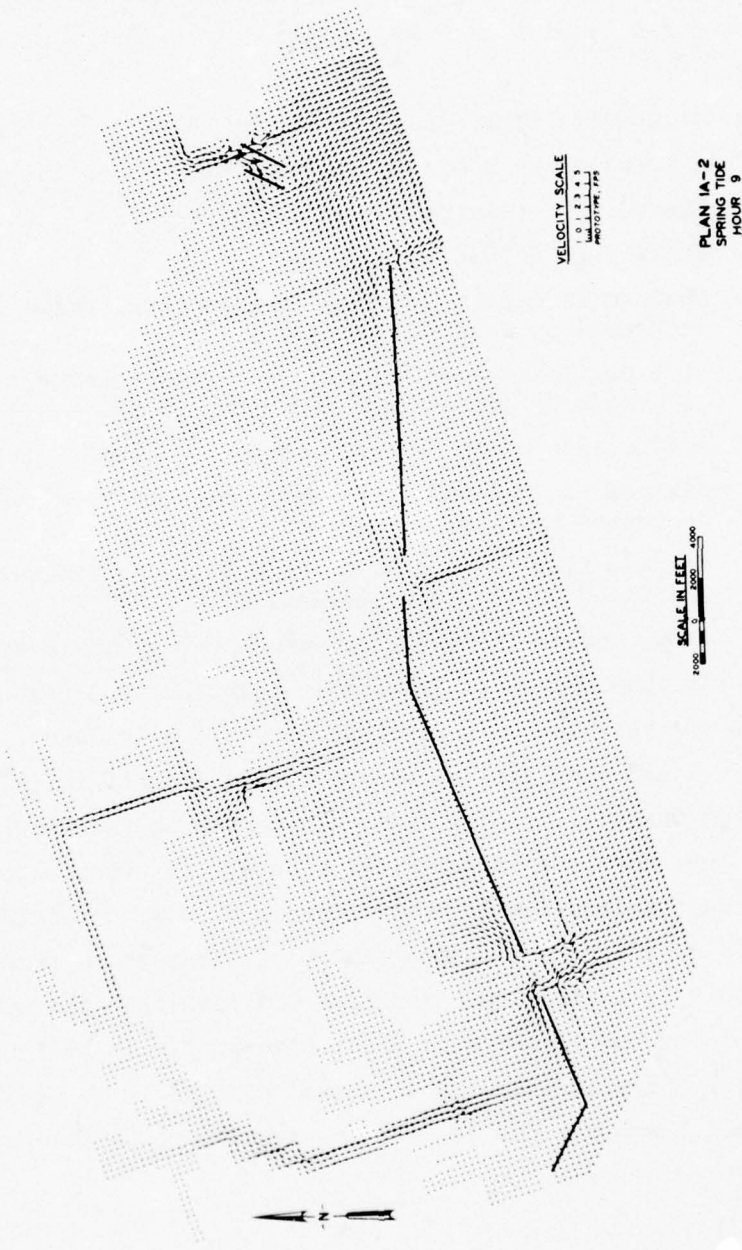


Figure 9. Velocity vector plot of tidal circulation patterns for plan 1A-2

These plots reflect the velocity differences in the bay produced by the plan 1A-2 modifications to the harbor; a sample plot is shown in Figure 10. Large-scale vector plots for plan 1A-2 and for the velocity differences produced by plan 1A-2 are included in Report 4 of this series of reports.⁶

38. The volumetric flow rates across the velocity ranges also were calculated; results are shown in Plates 56-60. When the plan 1A-2 results were compared with results for existing conditions, the following major changes were noted:

- a. Maximum flow rates through Angel's Gate (range 1) were increased by about 10 percent.
- b. Maximum flow rates through Queen's Gate (range 2) were decreased by approximately 50 percent.
- c. Little change was produced at range 3 (East End).
- d. Maximum flow rates across range 5 (Navy Mole) were decreased by about 25 percent.
- e. Maximum flow rates across range 8 (L. A. Channel) were increased by about 20 percent.

39. Net flows across the velocity ranges were calculated and are compared with the physical model results in Table 2. The most significant result is the reversal of the net westward flow in Cerritos Channel. Both the physical and numerical models predicted a small eastward net flow in Cerritos Channel for plan 1A-2. In comparing the net flows obtained from the numerical and physical models, the previous statements concerning the accuracy of these numbers must be considered. These net flows should be considered only to indicate flow trends.

40. Results obtained from plan 1A-2 indicate that the numerical model is capable of being used as a predictive tool. It will apparently yield essentially the same results as those which would be obtained from the physical model and can now be used to investigate the proposed modifications to Pier J.



Figure 10. Tidal circulation velocity differences produced by plan 1A-2

PART IV: ALTERNATE PIER J CONFIGURATIONS

Modifications Investigated

41. The two basic modifications of Pier J, STFP 2 (-82 ft channel) and STFP 3 (-82 ft channel), considered in this investigation are shown in Figures 11 and 12. The dredging scheme to obtain a -82 ft channel is shown in Figure 11. Two cases were actually considered for STFP 2 (-82 ft channel), a 300- and a 600-ft opening in the eastern end of the breakwater protecting the anchorage area. The three modifications indicated as STFP 2 (300, -82 ft channel), STFP 2 (600, -82 ft channel), and STFP 3 (-82 ft channel) were all considered for a 7.1-ft diurnal spring tide. The tide was applied to the verified model, and the model was used to predict circulation patterns resulting for each potential modification to Pier J.

Results

42. The tidal elevations and velocities were compared with those obtained for the existing conditions at the various gage locations. Except for local effects around the Pier J modification configurations themselves, STFP 2 (300, -82 ft channel), STFP 2 (600, -82 ft channel), and STFP 3 (-82 ft channel) all produced essentially the same overall tidal circulation results as the existing condition. Their effects upon the total circulation patterns for the bay were almost identical. The tidal elevations and velocities produced by STFP 2 (600, -82 ft channel), are presented in Plates 61-87 as being typical of all three cases.

43. To properly interpret the results, the effect upon velocity of the changed depths in the dredged areas should be recognized. The relationship between depth-averaged velocity and volumetric flow rate is not the same for existing conditions and for the modifications. Depth-averaged velocity for the modifications may be less than that for existing conditions even though the volumetric flow rate through the

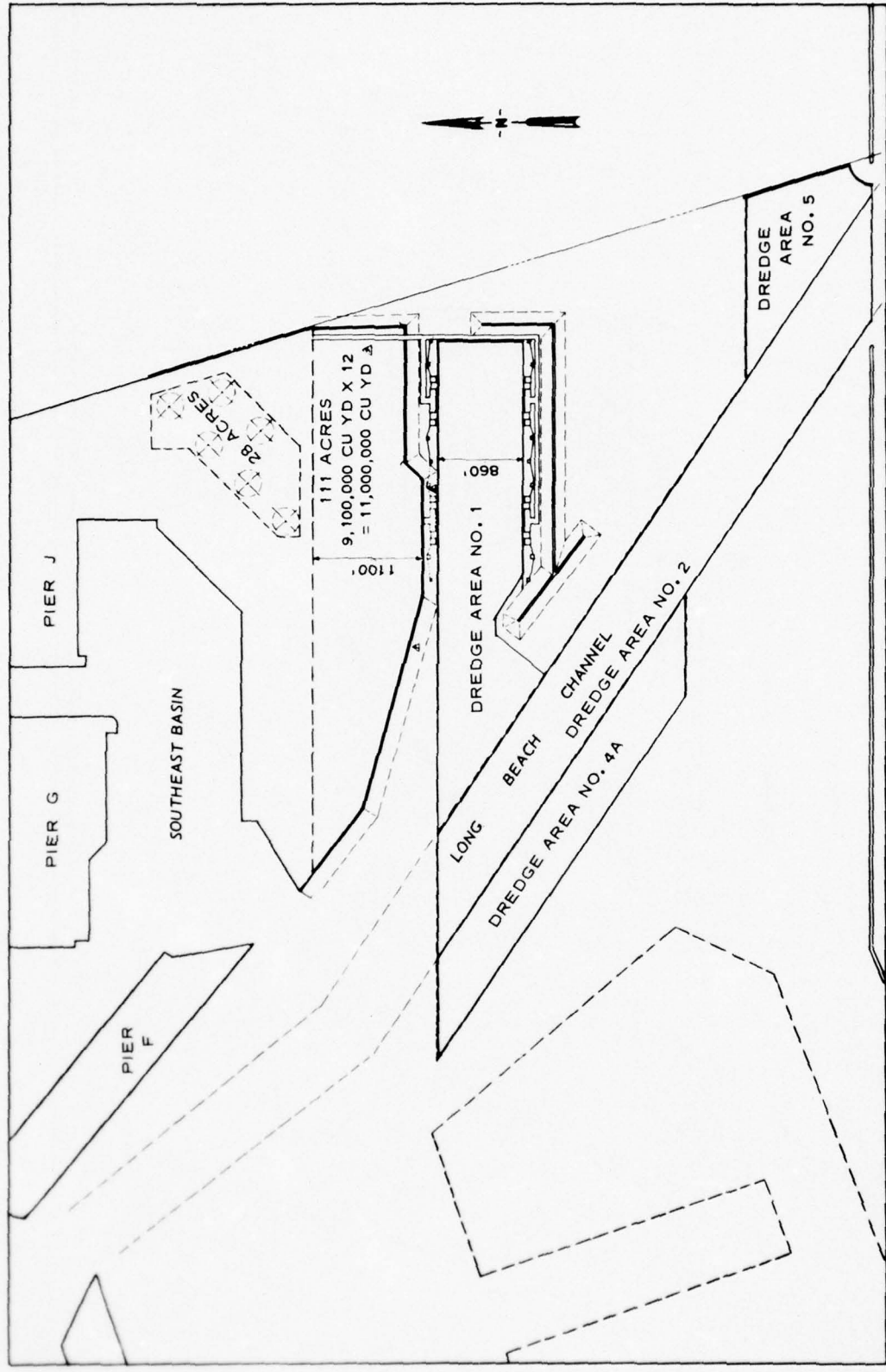


Figure 11. STEP 2 with dredging for -82 ft channel

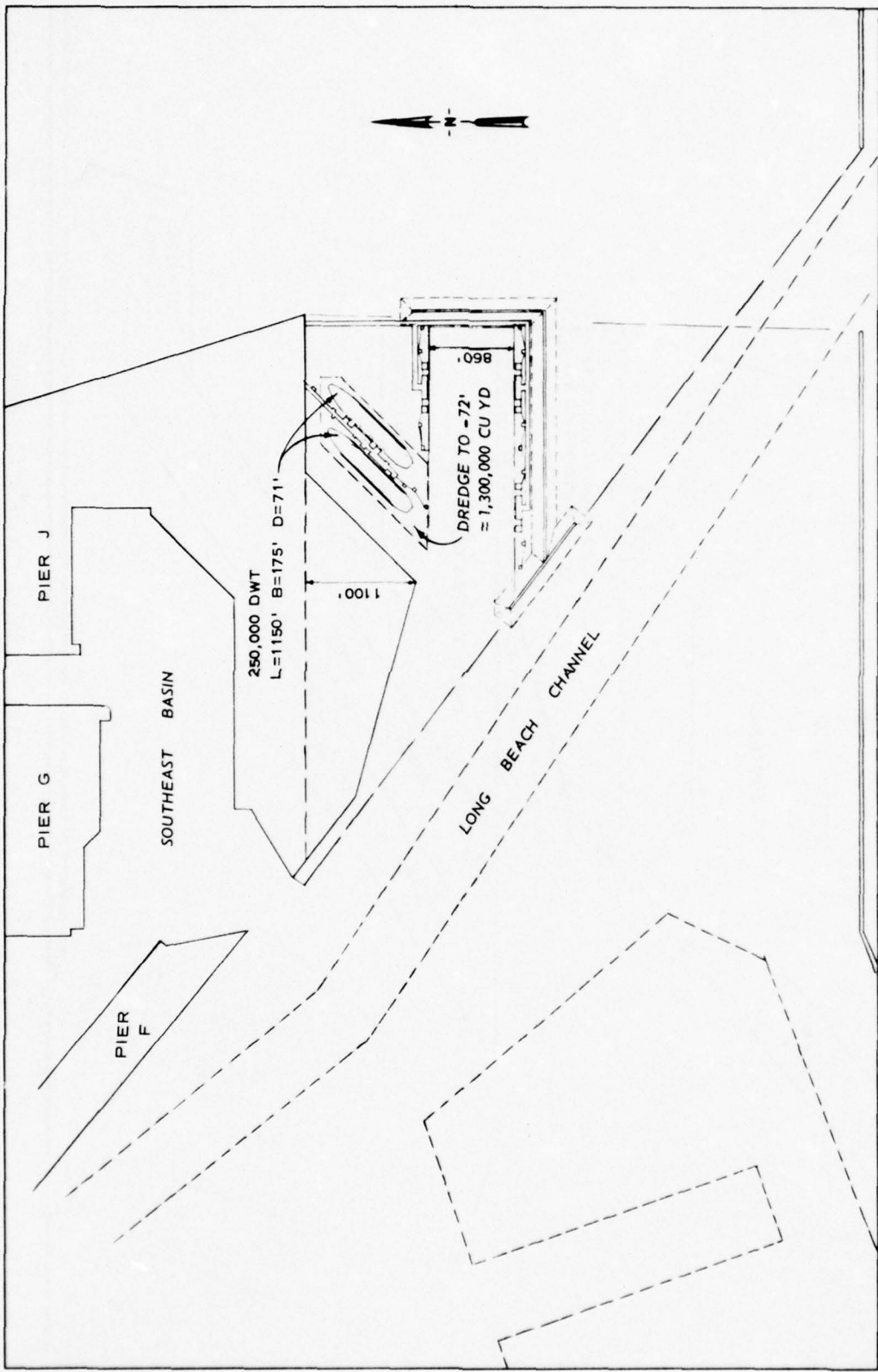


Figure 12. STFP 3

finite difference cell is greater. This results from the greater depths in the dredged areas of the modifications. This qualification is limited to the dredged regions and affects only velocity ranges 2 and 10 and vector plots of overall tidal circulation in the dredged portion of the bay. For example, while velocities at range 2 are observed to be lower than those for existing conditions, there is a slight increase in the volumetric flow rate through this range for the modifications considered.

44. Plates 61-65 show that the tidal elevations were not changed by the Pier J modifications. Plates 66-87 show that except for ranges 2 and 10, velocities at the gage locations were changed only slightly. As indicated previously, velocity changes at ranges 2 and 10 were primarily associated with a change in depth rather than a change in volumetric flow rate. Appreciable changes occurred in velocity patterns, however, in the local Pier J area which differ somewhat for the three cases investigated. The vector plots of the circulation patterns for STFP 2 (300, -82 ft channel), STFP 2 (600, -82 ft channel), and STFP 3 (-82 ft channel) as well as the vector plots indicating changes in circulation patterns from the existing conditions are presented in Report 4 of this series.⁶ Examples of these vector plots are shown in Figures 13 and 14.

45. The volumetric flow rates across the velocity ranges are presented in Plates 88-102. Again, all three cases yield essentially the same results and these results differ only slightly from the existing conditions. The slight increase in flow rate through range 2 is noted although the velocity is less than existing conditions. The following specific observations were made from these results:

- a. Volumetric flow rates across ranges 5 and 8 were essentially identical with those for existing conditions.
- b. A slight increase occurred in the volumetric flow rates across range 1 (approximately a 4% increase at the maximum flow rate).
- c. An increase occurred in the volumetric flow rates through range 2, approximately a 7-1/2% increase at the maximum flow rate).
- d. A slight decrease occurred in the volumetric flow rate across range 3 (approximately 3-1/2% at the maximum flow rate).



Figure 13. Velocity vector plots of tidal circulation patterns for STFP 3 (-82 ft channel)

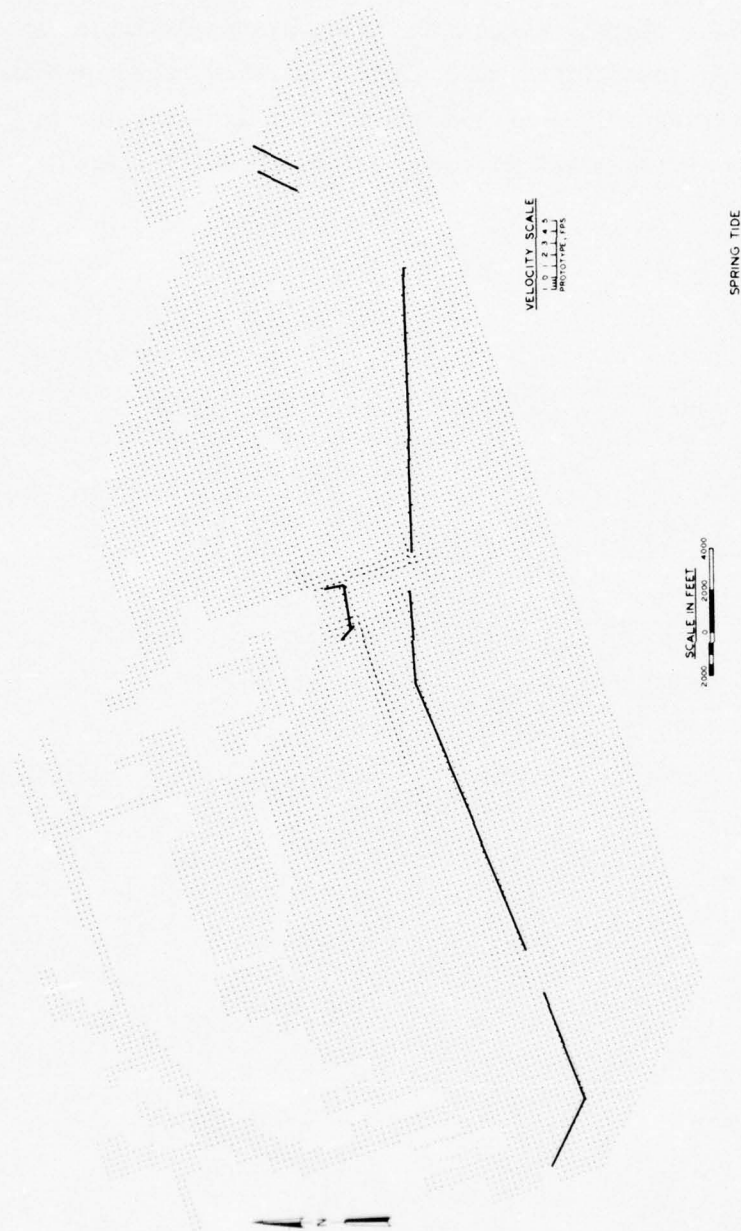


Figure 14. Tidal circulation velocity difference produced by STFP 2
(300, -82 ft channel)

46. Net flows across the velocity ranges are indicated in Table 3. The net westward flow in Cerritos Channel for all three modifications was essentially identical with existing conditions. The net flow through Angel's Gate for all three modifications was essentially identical with existing conditions. The net flow (flood) through Queen's Gate has been increased by about 12% and the net flow across range 3 has been changed from a very small net ebb to a small net flood.

PART V: CONCLUSIONS

47. The Pier J modifications considered in this investigation resulted in only minor overall changes to tidal circulation in the Los Angeles and Long Beach Harbors complex. The primary circulation changes are local in nature. All three modifications--STFP 2 (300, -82 ft channel), STFP 2 (600, -82 ft channel), and STFP 3 (-82 ft channel)--produced essentially the same overall effect on tidal circulation. Specific conclusions concerning the changes in tidal circulation produced by the Pier J modifications are as follows:

- a. A very slight increase in flow through the Angel's Gate opening.
- b. A small increase in flow through the Queen's Gate opening.
- c. A small decrease in flow around the end of the Long Beach breakwater.
- d. No effect on flow in Cerritos Channel. The net westward flow in Cerritos Channel appears to be retained at essentially the same magnitude as for existing conditions.
- e. Little effect northeast of the Queen's Gate opening except in the immediate vicinity of the actual modifications.
- f. Changes in the velocity patterns northwest of the Queen's Gate opening. These changes are primarily confined to the Long Beach portion of the harbor complex, and principally involve the direction of the flow rather than the volume of flow.

REFERENCES

1. Pickett, E. B., Durham, D. L., and McAnally, W. H., Jr., "Los Angeles and Long Beach Harbors Model Study; Prototype Data Acquisition and Observations," Technical Report H-75-4, Report 1, Jun 1975, U. S. Army Engineer Waterways Experiment Station, CE, Vicksburg, Miss.
2. McAnally, W. H., Jr., "Los Angeles and Long Beach Harbors Model Study; Tidal Verification and Base Circulation Tests," Technical Report H-75-4, Report 5, Sep 1975, U. S. Army Engineer Waterways Experiment Station, CE, Vicksburg, Miss.
3. _____, "Los Angeles-Long Beach Harbors Model Study; Interim Analysis of Tidal Circulation Tests of Plan 1A-2," Oct 1975, U. S. Army Engineer Waterways Experiment Station, CE, Vicksburg, Miss.
4. Raney, D. C., "Numerical Analysis of Tidal Circulation for Long Beach Harbor; Existing Conditions and Alternate Plans for Pier J Completion and Tanker Terminal Study," Miscellaneous Paper H-76-4, Report 1, Sep 1976, U. S. Army Engineer Waterways Experiment Station, CE, Vicksburg, Miss.
5. _____, "Numerical Analysis of Tidal Circulation for Long Beach Harbor; Tidal Circulation Velocity Patterns for Existing Conditions and Alternate Master Plan Pier-J Configurations for SOHIO Project," Miscellaneous Paper H-76-4, Report 2, Mar 1976, U. S. Army Engineer Waterways Experiment Station, CE, Vicksburg, Miss.
6. _____, "Numerical Analysis of Tidal Circulation for Long Beach Harbor; Tidal Circulation Velocity Patterns for Existing Conditions and Alternate Master Plan Pier-J Configurations with -82-Ft Channel," Miscellaneous Paper H-76-4, Report 4, May 1976, U. S. Army Engineer Waterways Experiment Station, CE, Vicksburg, Miss.

Table 1
Net Discharge per Tidal Cycle for Existing Conditions

Range	Physical Model		Numerical Model	
	Apparent Net Discharge	10^6 cu ft	Adjusted Net Discharge	10^6 cu ft
1		+1230		+446
2		+520		+641
3		-1700		-146
5		-40		+53
8		-50		-64

Note: + = net flood condition; - = net ebb condition.

Table 2
Net Discharge per Tidal Cycle for Plan 1A-2

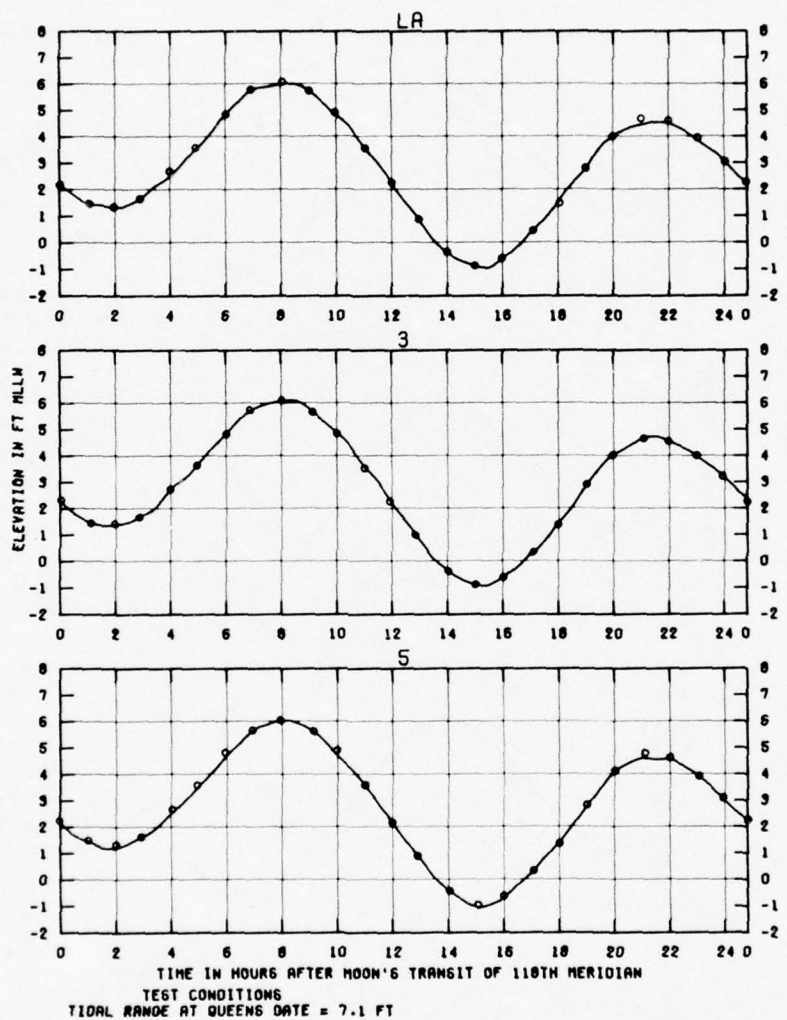
Range	Physical Model		Numerical Model	
	Apparent Net Discharge	10^6 cu ft	Adjusted Net Discharge	10^6 cu ft
1		+1090		+218
2		+80		+698
3		+480		+223
5		-160		+13.2
8		+80		+31.1

Note: + = net flood condition; - = net ebb condition.

Table 3
Numerical Model Adjusted Net Discharge
per Tidal Cycle, 10^6 cu ft

	Velocity Range				
	1	2	3	5	8
Existing	446	641	-35.3	22.2	-64
Plan 1A-2	218	698	223	13.2	31.1
STFP 2 (300), -82 ft channel	431	820	71.8	25.2	-67.2
STFP 2 (600), -82 ft channel	435	819	71.3	24.2	-67.1
STFP 3, -82 ft channel	427	829	81.2	24	-63.6

Note: - = net ebb condition.



TIDAL ELEVATIONS
BASE TEST
SPRING TIDE

STATIONS
LA, 3, AND 5

LEGEND
— PHYSICAL MODEL RESULTS
○ DEPTH-AVERAGED NUMERICAL MODEL RESULTS

PLATE 1

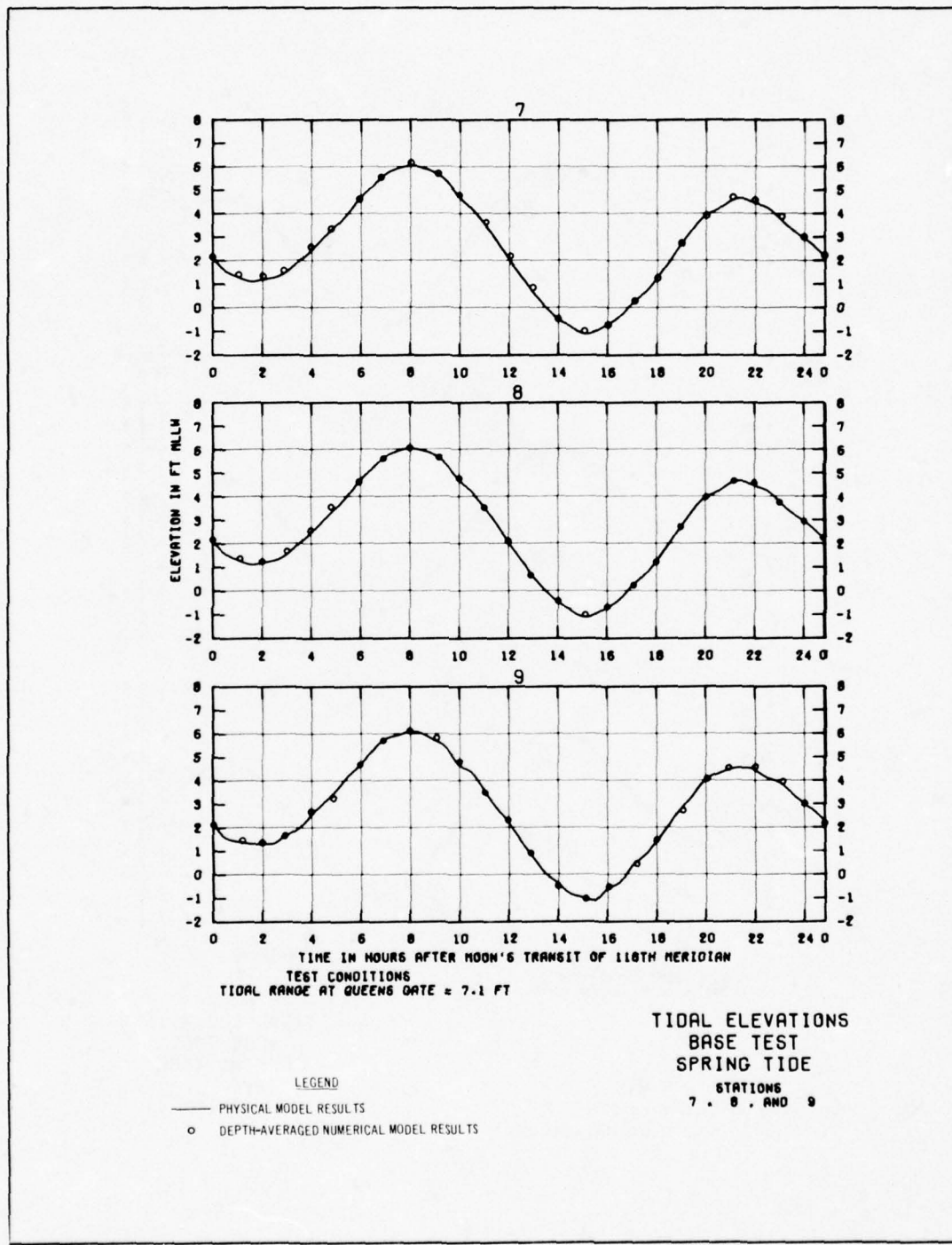
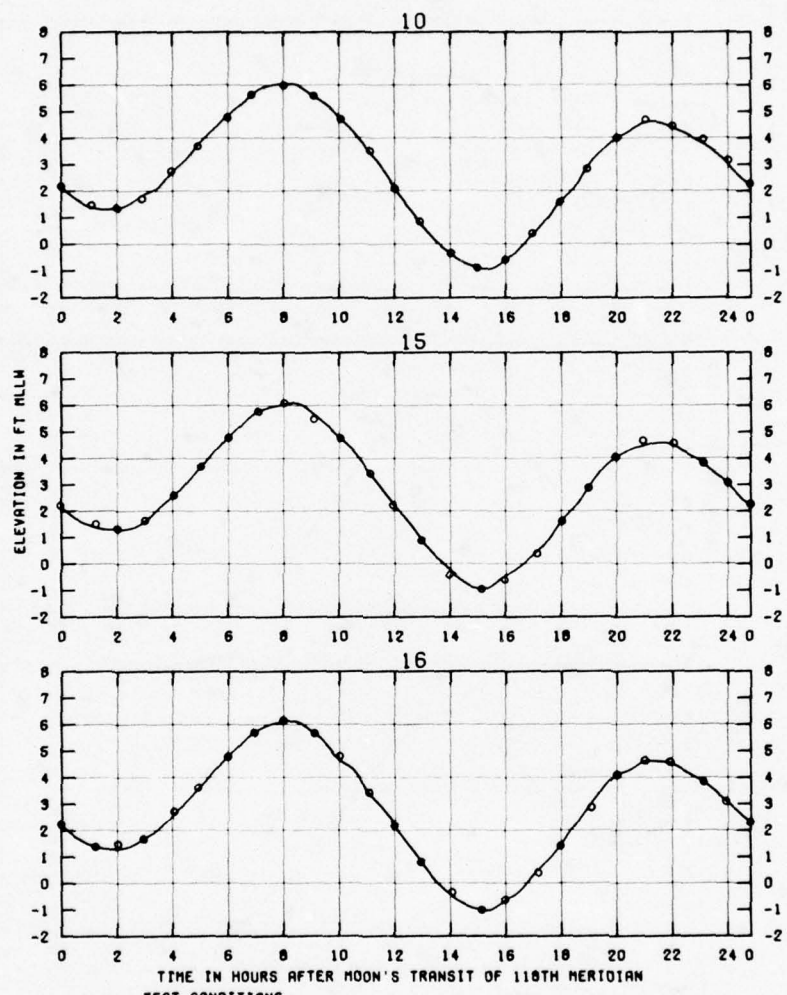


PLATE 2



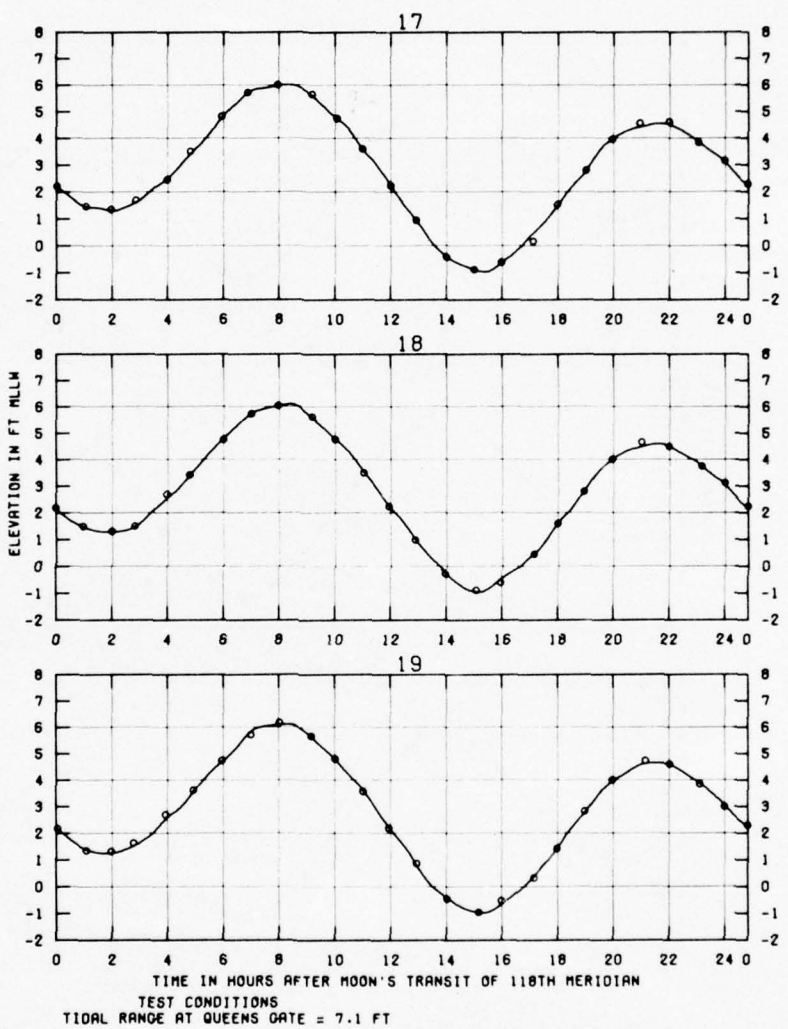
TEST CONDITIONS
TIDAL RANGE AT QUEENS DATE = 7.1 FT

TIDAL ELEVATIONS
BASE TEST
SPRING TIDE

STATIONS
10, 15, AND 16

LEGEND

- PHYSICAL MODEL RESULTS
- DEPTH-AVERAGED NUMERICAL MODEL RESULTS

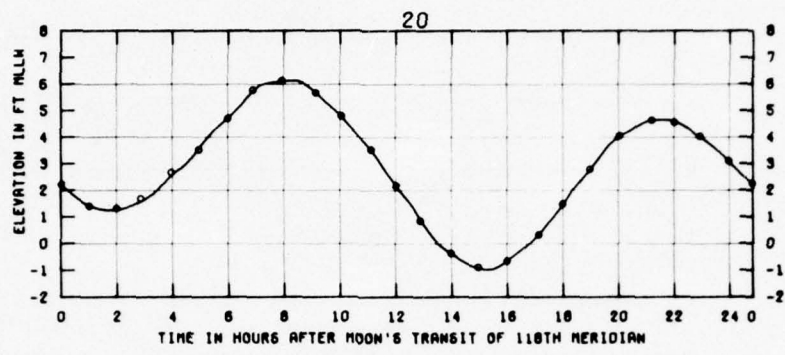


TIDAL ELEVATIONS
BASE TEST
SPRING TIDE

LEGEND

— PHYSICAL MODEL RESULTS
○ DEPTH-AVERAGED NUMERICAL MODEL RESULTS

STATIONS
17, 18, AND 19



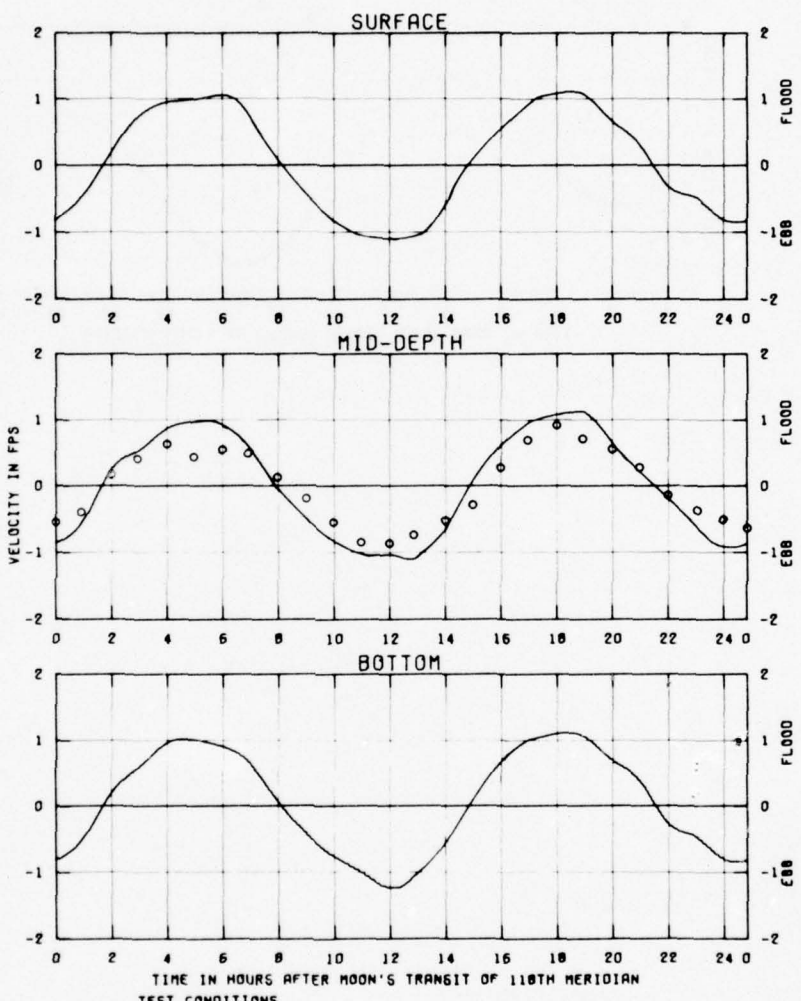
TEST CONDITIONS
TIDAL RANGE AT QUEENS DATE = 7.1 FT

TIDAL ELEVATIONS
BASE TEST
SPRING TIDE

STATION
20

LEGEND
— PHYSICAL MODEL RESULTS
○ DEPTH-AVERAGED NUMERICAL MODEL RESULTS

PLATE 5



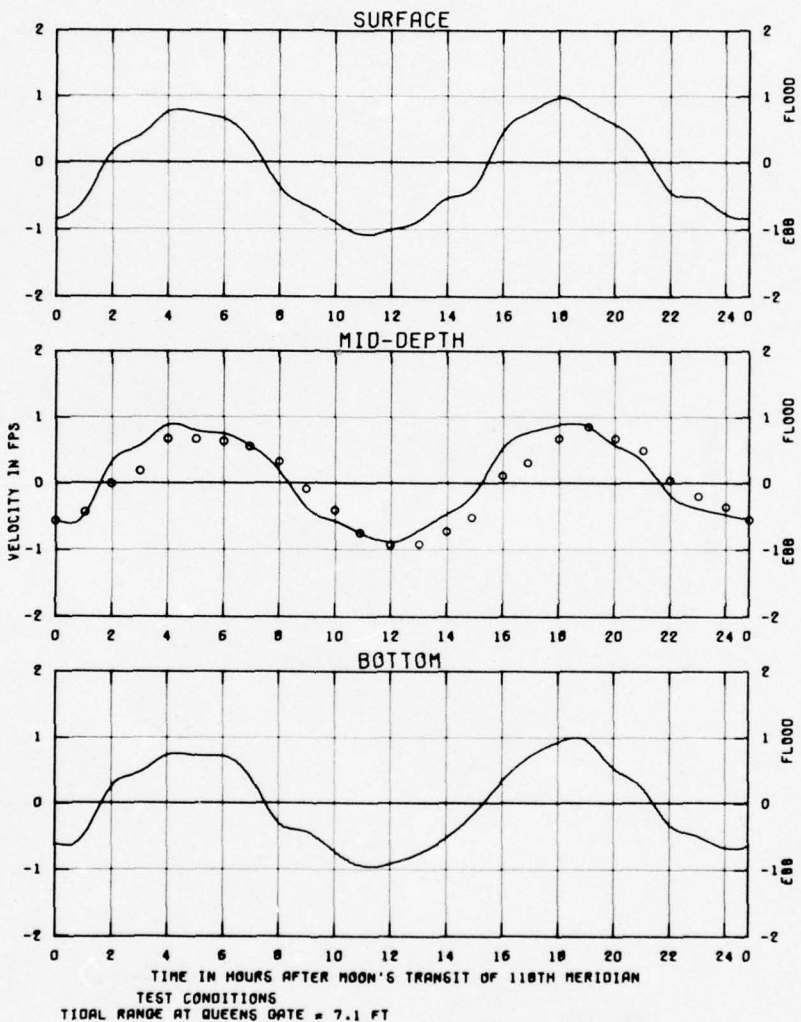
TEST CONDITIONS
TIDAL RANGE AT QUEENS DATE = 7.1 FT

VELOCITIES
BASE TEST
SPRING TIDE

STATION
1A

LEGEND

- PHYSICAL MODEL RESULTS
- DEPTH-AVERAGED NUMERICAL MODEL RESULTS

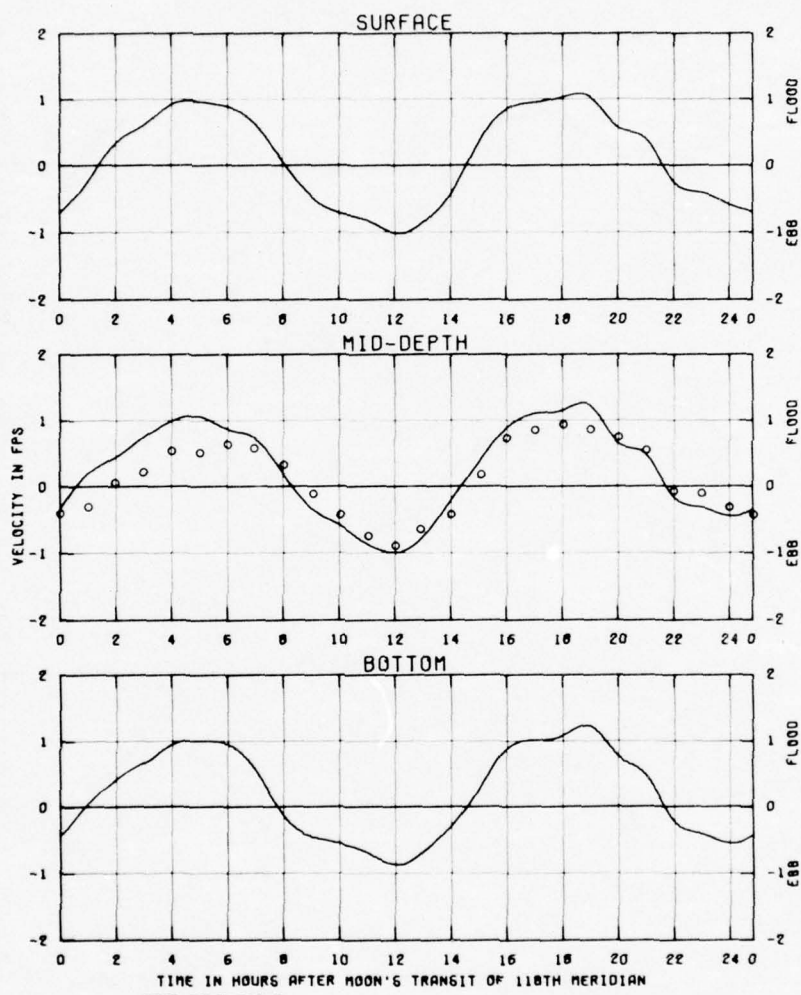


VELOCITIES
BASE TEST
SPRING TIDE

STATION
10

LEGEND
— PHYSICAL MODEL RESULTS
○ DEPTH-AVERAGED NUMERICAL MODEL RESULTS

PLATE 7



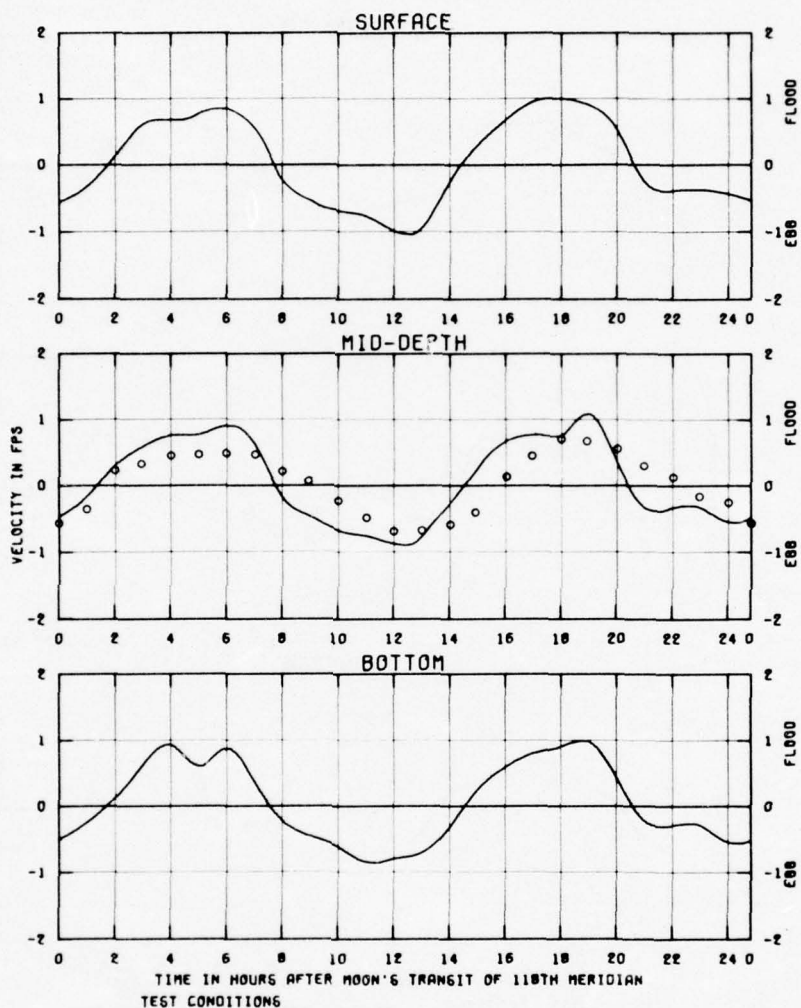
VELOCITIES
BASE TEST
SPRING TIDE

STATION
1C

LEGEND

- PHYSICAL MODEL RESULTS
- DEPTH-AVERAGED NUMERICAL MODEL RESULTS

PLATE 8



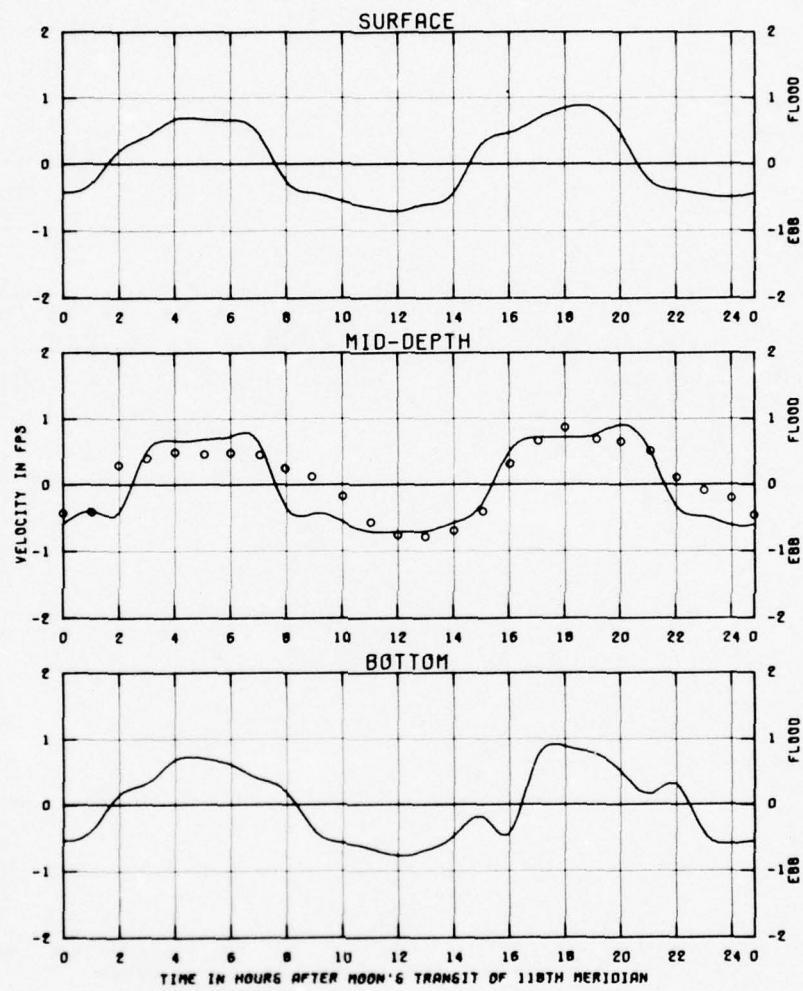
VELOCITIES
BASE TEST
SPRING TIDE

STATION
20

LEGEND

- PHYSICAL MODEL RESULTS
- DEPTH-AVERAGED NUMERICAL MODEL RESULTS

PLATE 9



VELOCITIES
BASE TEST
SPRING TIDE

STATION
2C

LEGEND

- PHYSICAL MODEL RESULTS
- DEPTH-AVERAGED NUMERICAL MODEL RESULTS

PLATE 10

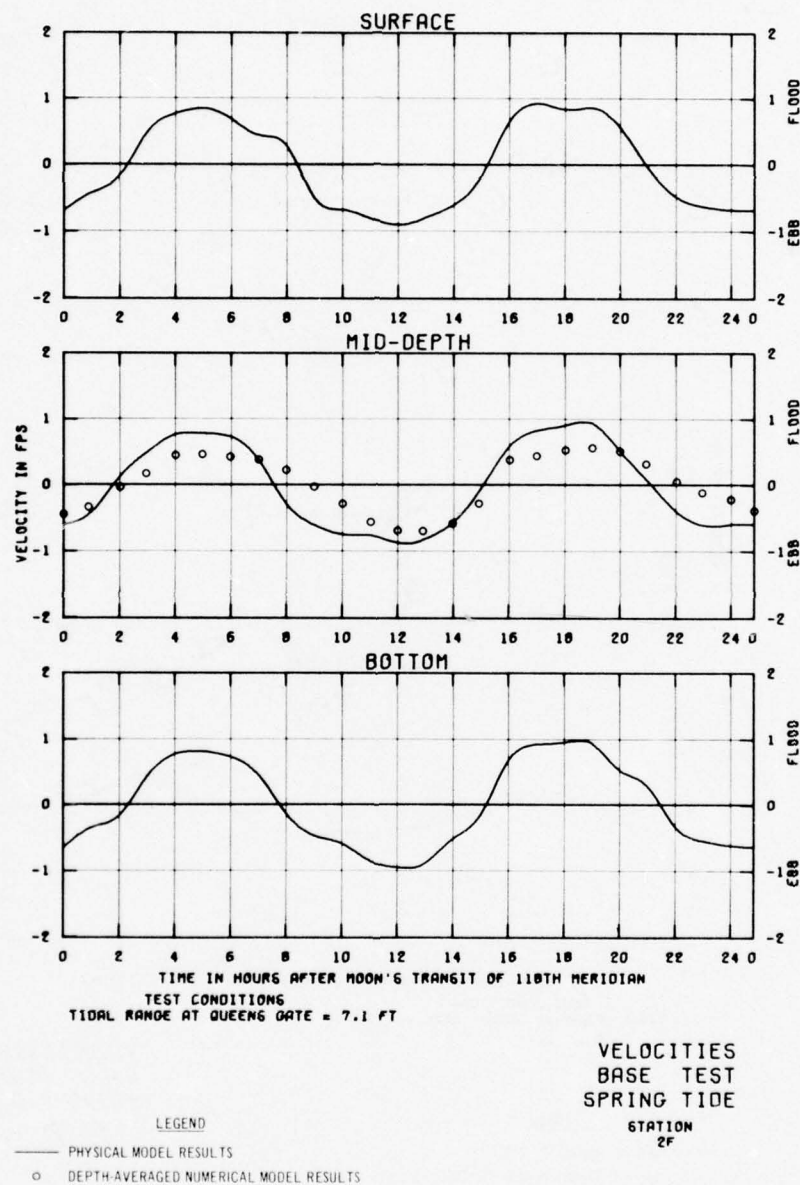
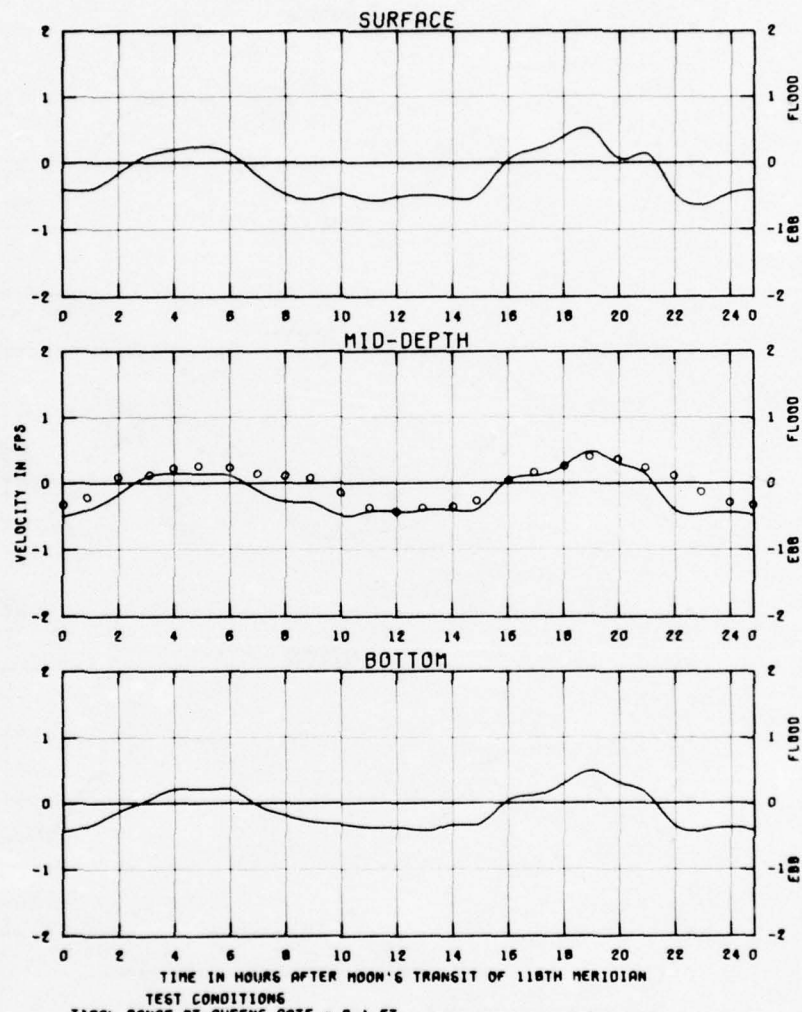


PLATE 11



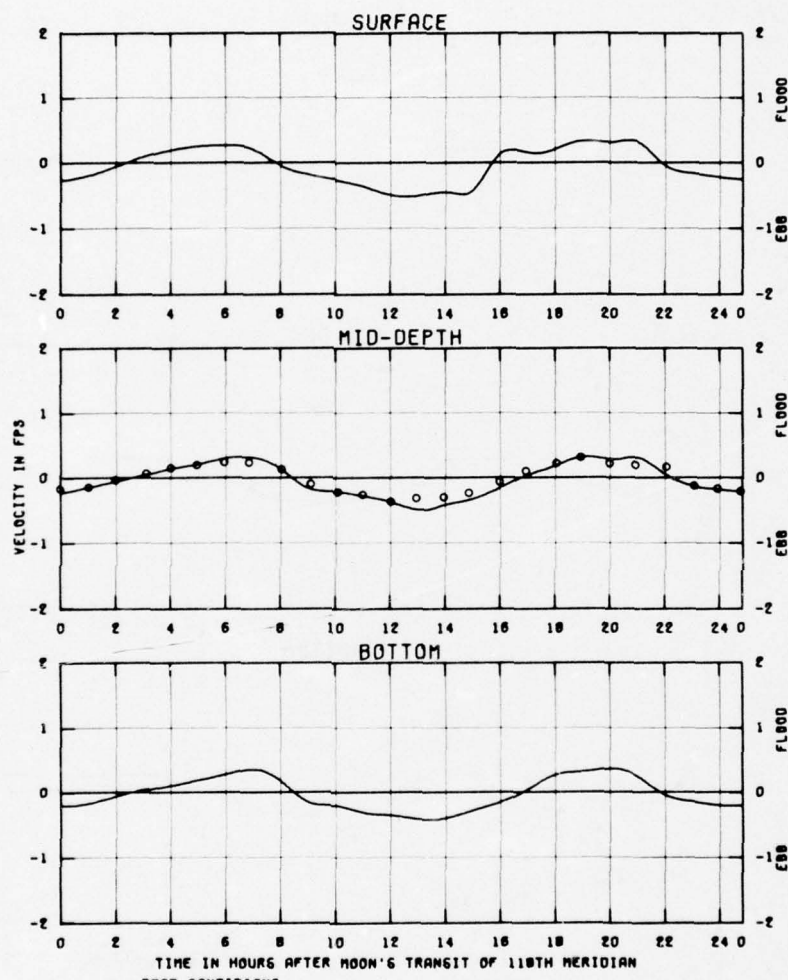
VELOCITIES
BASE TEST
SPRING TIDE

STATION
3G

LEGEND

— PHYSICAL MODEL RESULTS
○ DEPTH-AVERAGED NUMERICAL MODEL RESULTS

PLATE 12



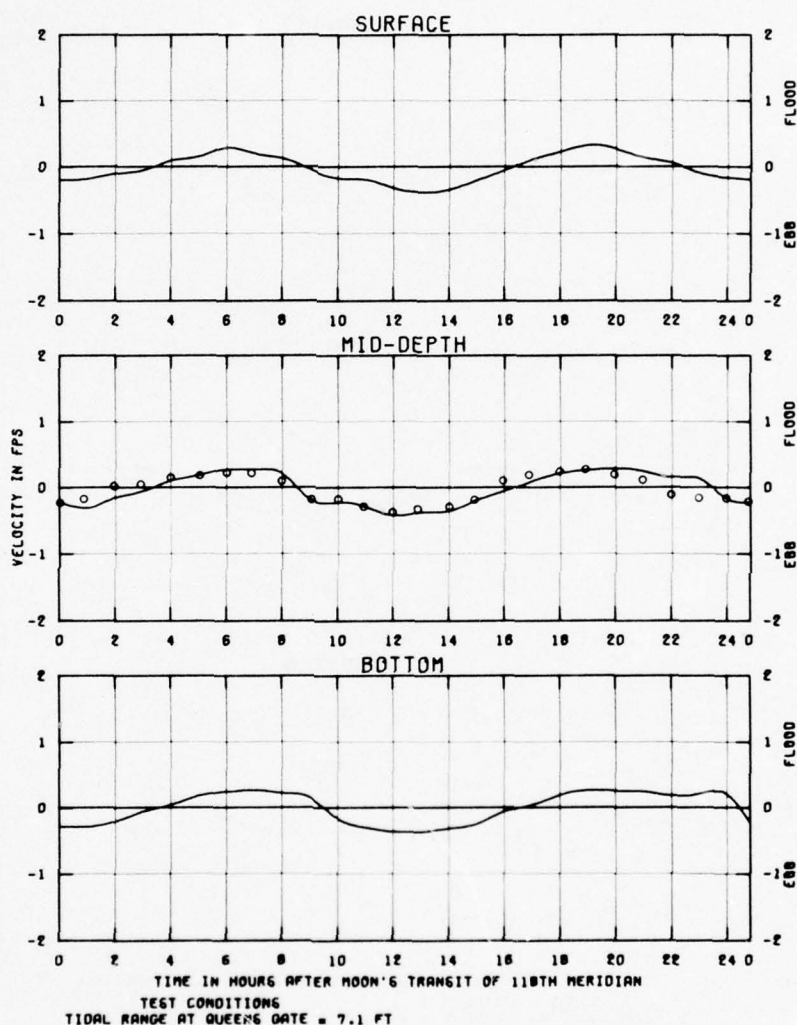
TEST CONDITIONS
TIDAL RANGE AT QUEENS DATE = 7.1 FT

VELOCITIES
BASE TEST
SPRING TIDE

STATION
SM

LEGEND

- PHYSICAL MODEL RESULTS
- DEPTH-AVERAGED NUMERICAL MODEL RESULTS



VELOCITIES
BASE TEST
SPRING TIDE

STATION
31

LEGEND
— PHYSICAL MODEL RESULTS
○ DEPTH-AVERAGED NUMERICAL MODEL RESULTS

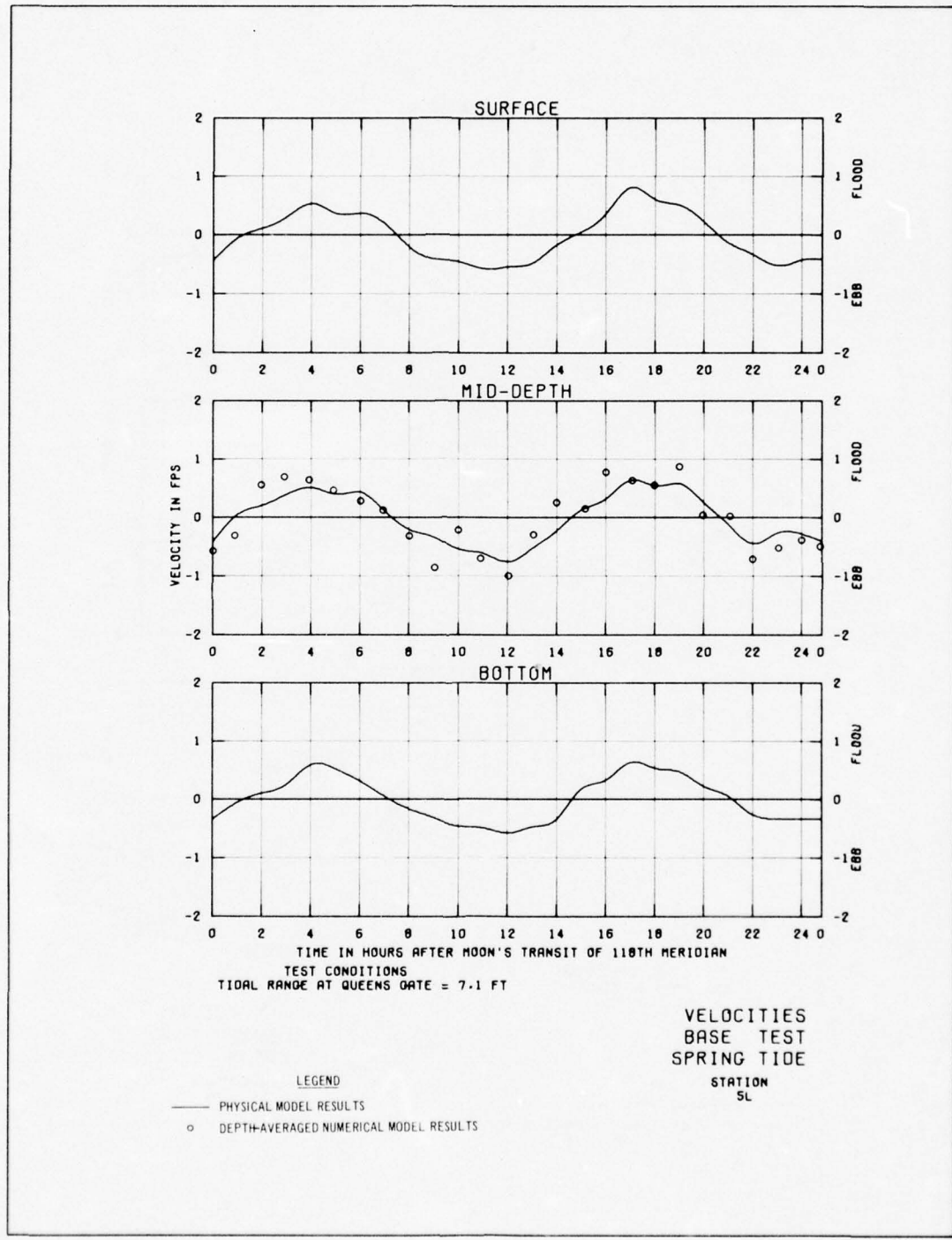
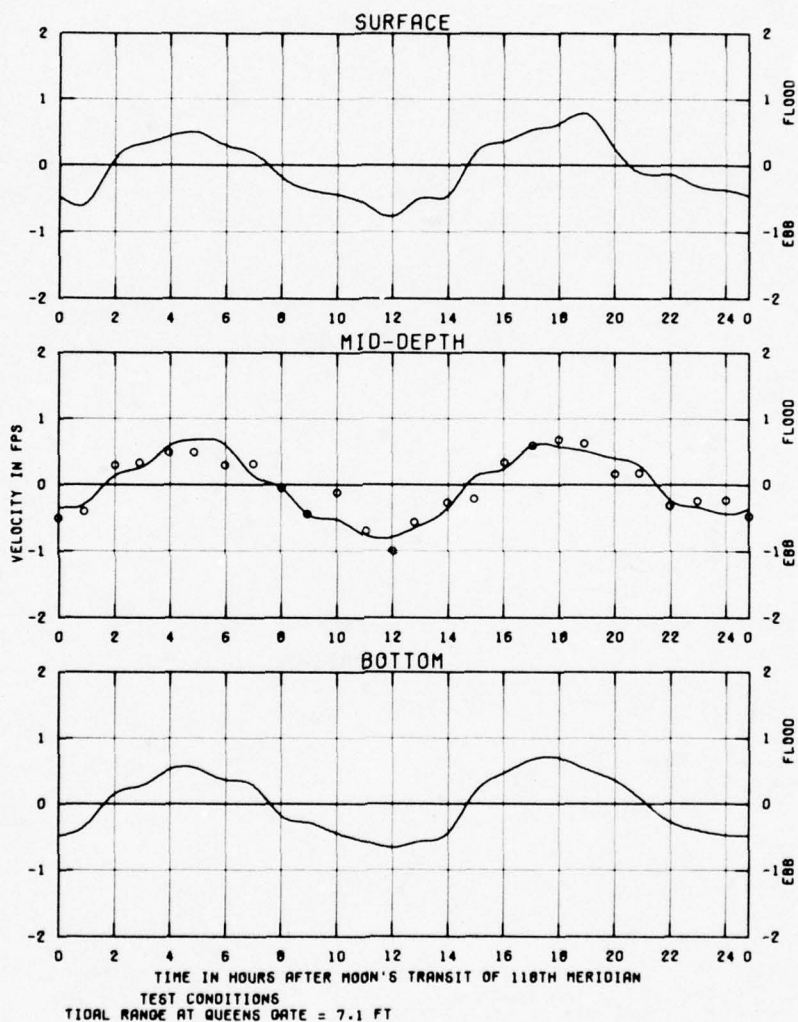


PLATE 15

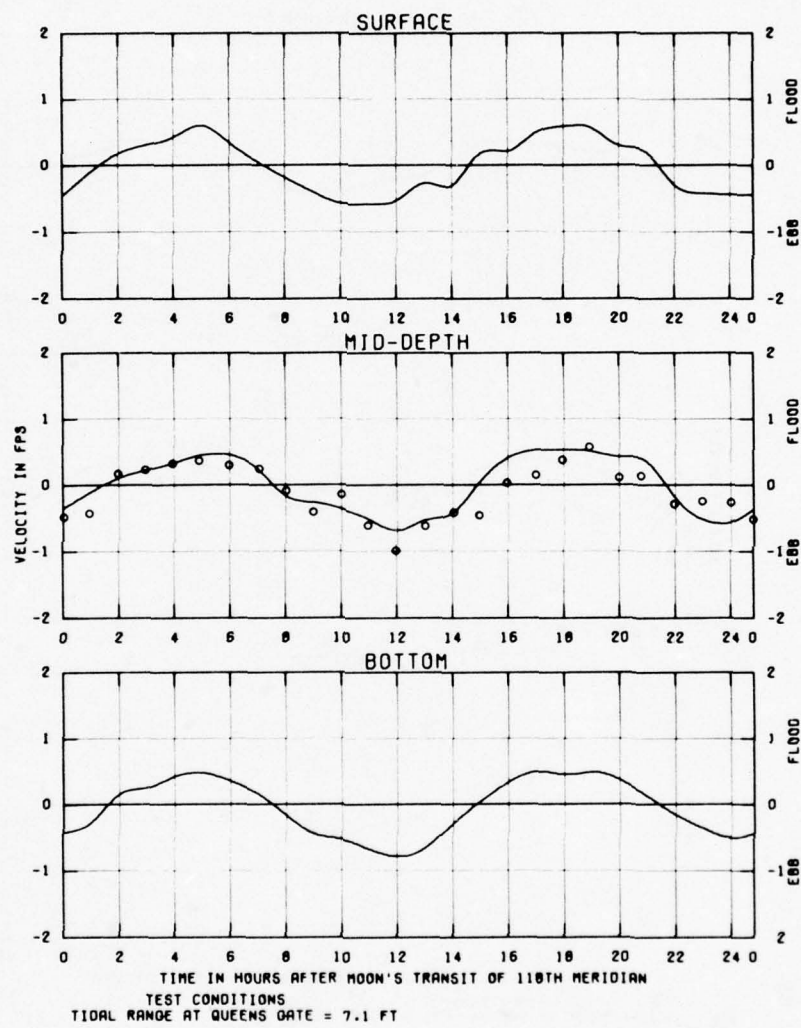


LEGEND

- PHYSICAL MODEL RESULTS
- DEPTH-AVERAGED NUMERICAL MODEL RESULTS

VELOCITIES
BASE TEST
SPRING TIDE

STATION
SM



VELOCITIES
BASE TEST
SPRING TIDE

STATION

5M

LEGEND

- PHYSICAL MODEL RESULTS
- DEPTH-AVERAGED NUMERICAL MODEL RESULTS

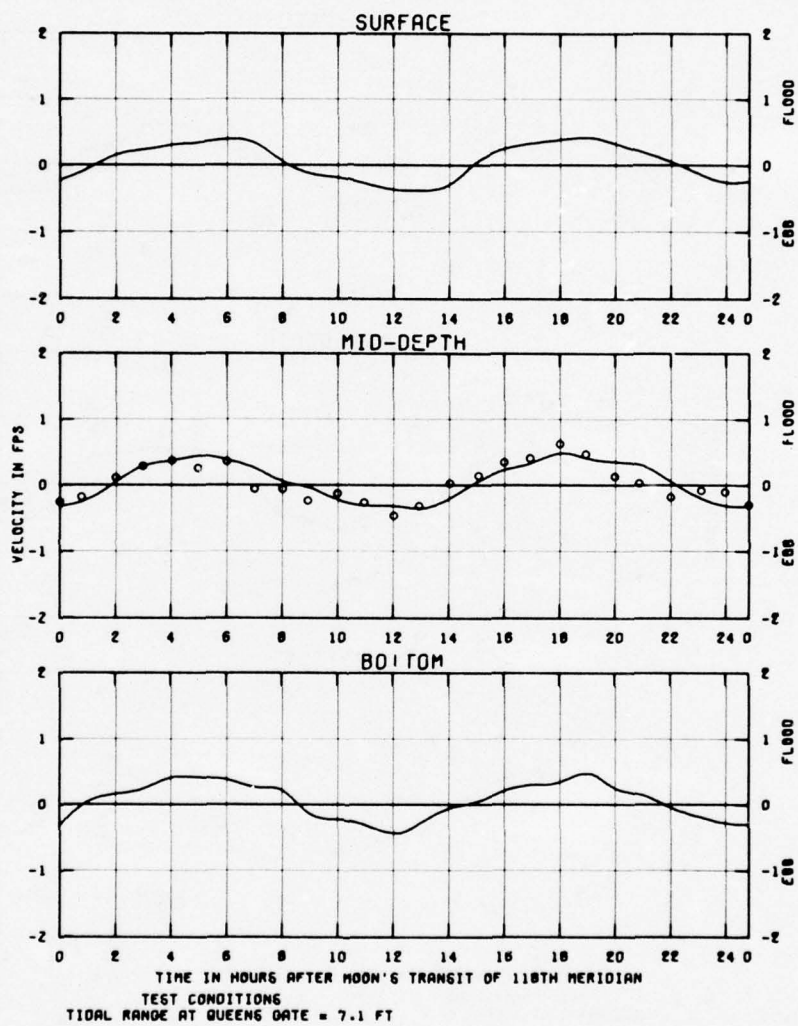
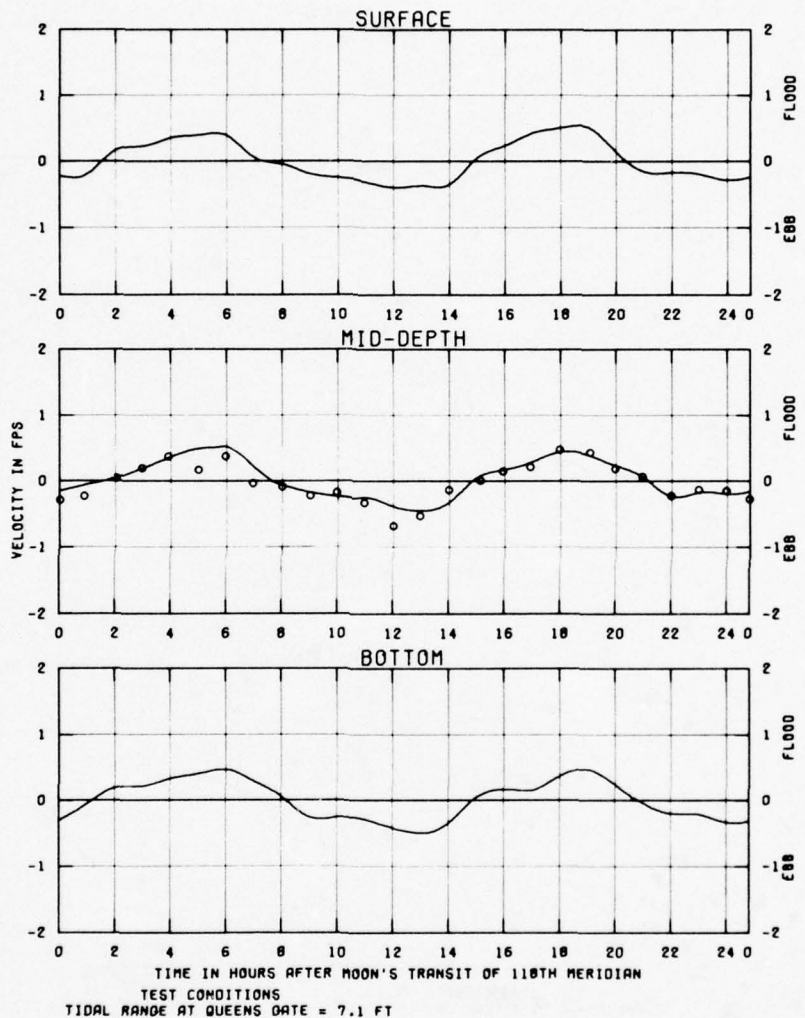


PLATE 18

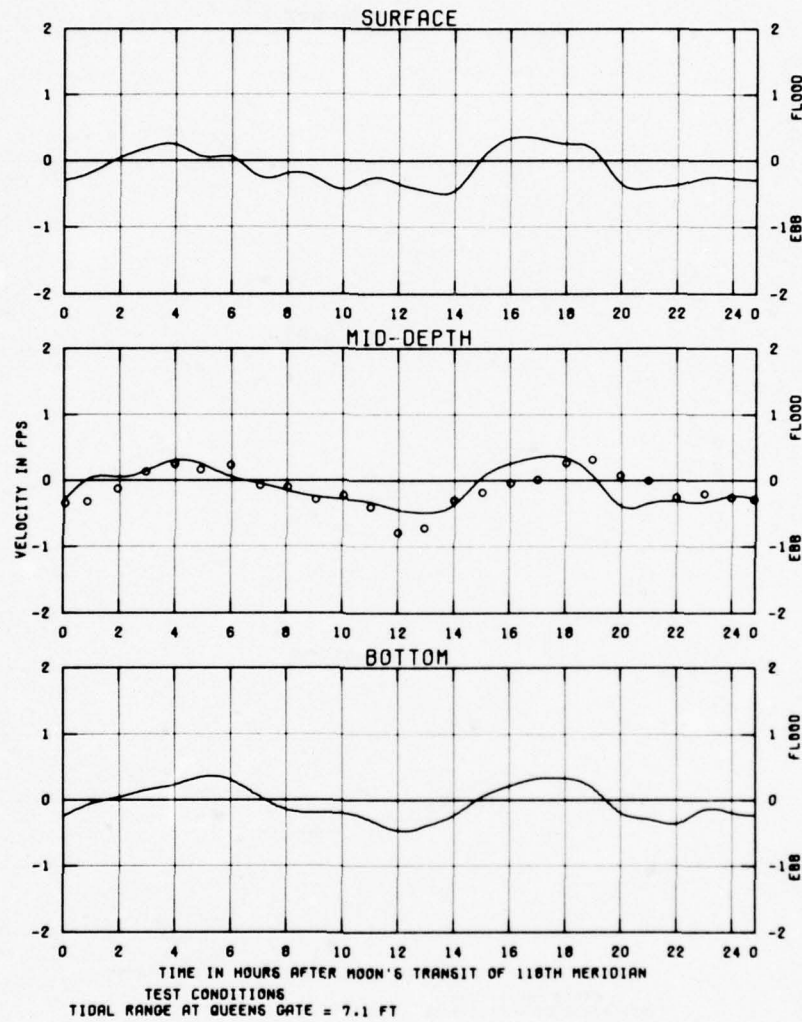


VELOCITIES
BASE TEST
SPRING TIDE

STATION
BY

LEGEND

- PHYSICAL MODEL RESULTS
- DEPTH-AVERAGED NUMERICAL MODEL RESULTS



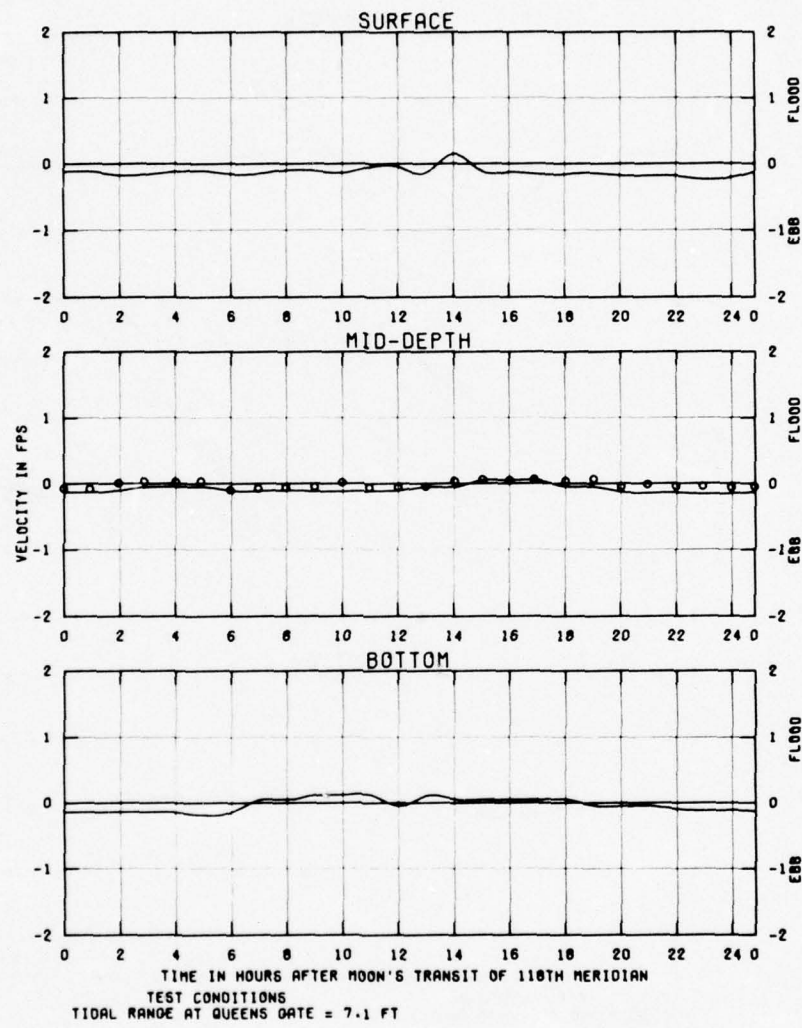
VELOCITIES
BASE TEST
SPRING TIDE

STATION

82

LEGEND

- PHYSICAL MODEL RESULTS
- DEPTH-AVERAGED NUMERICAL MODEL RESULTS



TIME IN HOURS AFTER MOON'S TRANSIT OF 116TH MERIDIAN
TEST CONDITIONS
TIDAL RANGE AT QUEENS DATE = 7.1 FT

VELOCITIES
BASE TEST
SPRING TIDE

STATION
9A

LEGEND

- PHYSICAL MODEL RESULTS
- DEPTH-AVERAGED NUMERICAL MODEL RESULTS

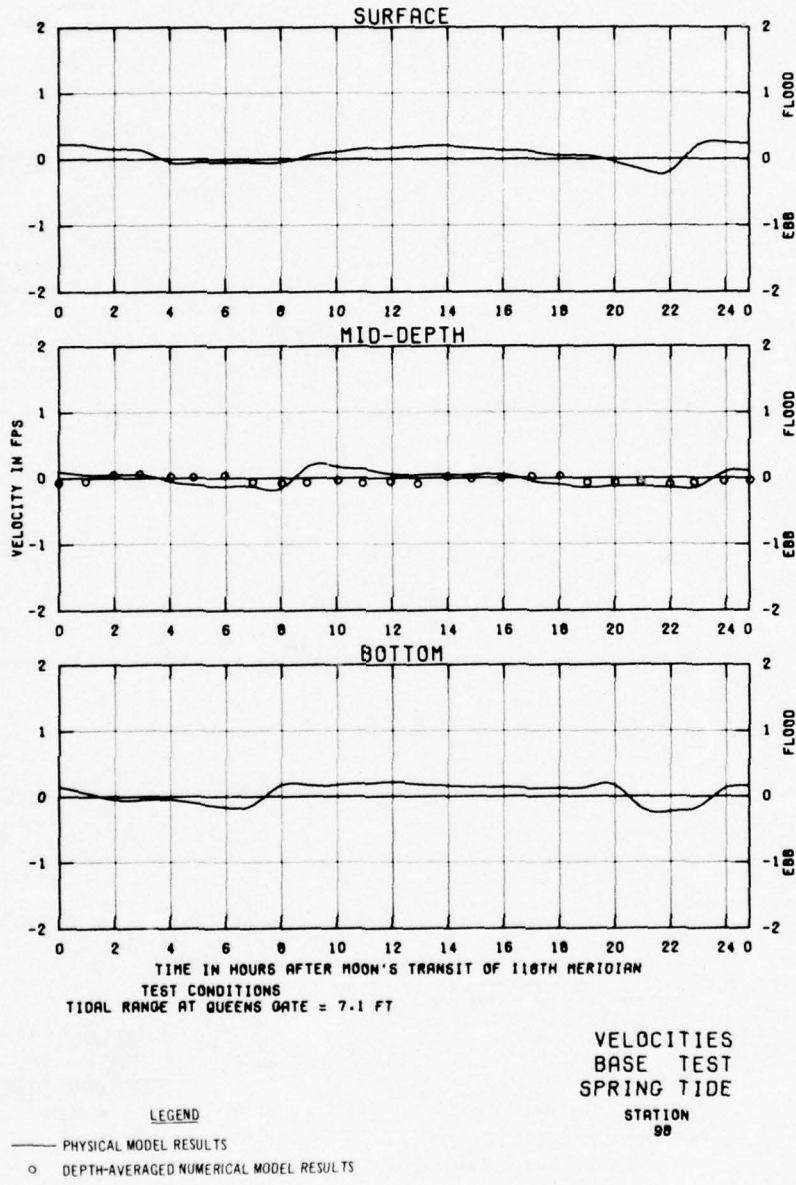
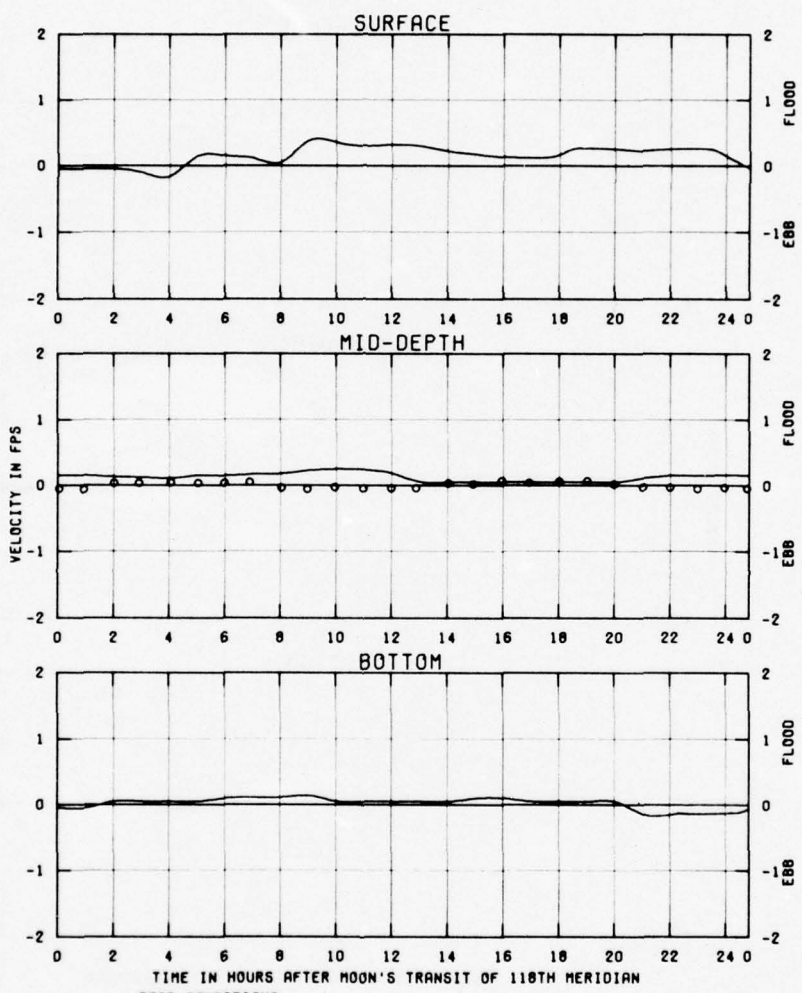


PLATE 22



TEST CONDITIONS
TIDAL RANGE AT QUEENS GATE = 7.1 FT

VELOCITIES
BASE TEST
SPRING TIDE

STATION
9C

LEGEND
— PHYSICAL MODEL RESULTS
○ DEPTH-AVERAGED NUMERICAL MODEL RESULTS

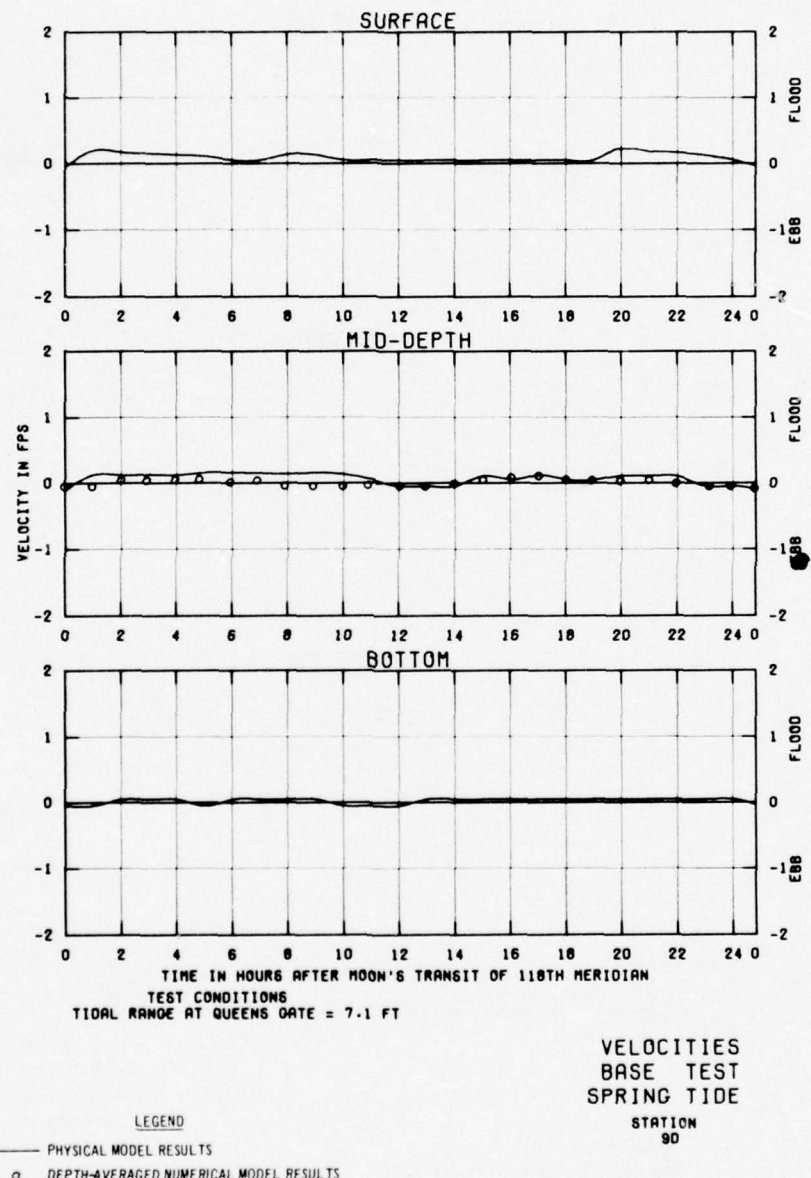
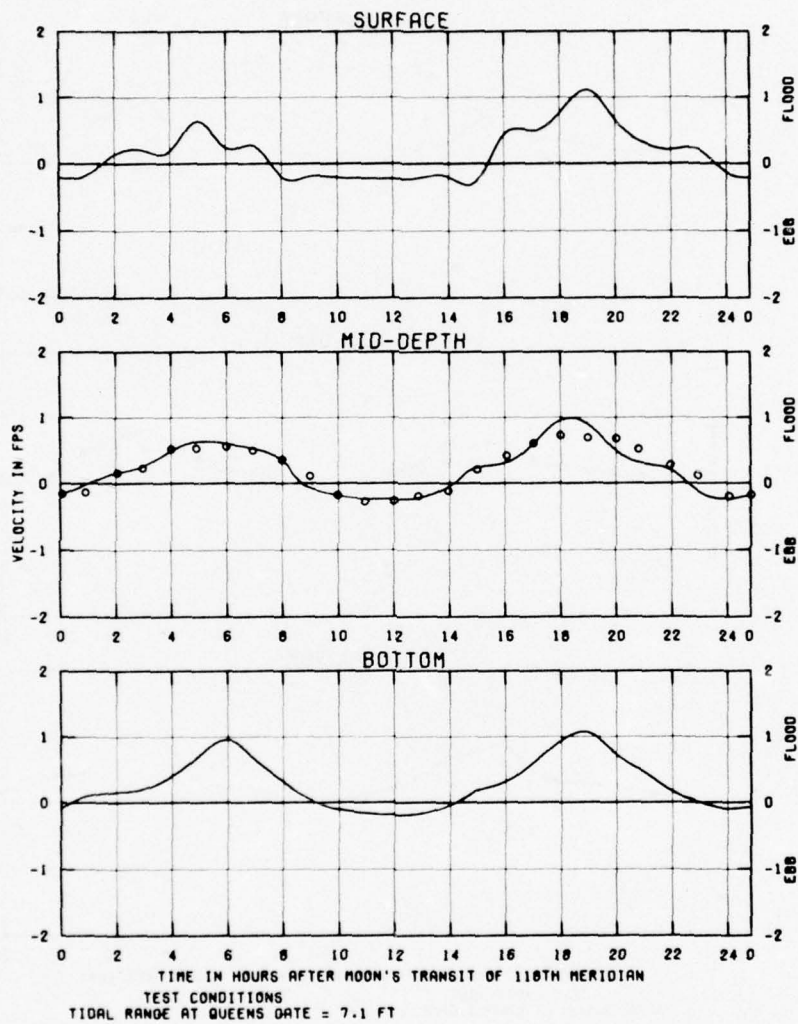


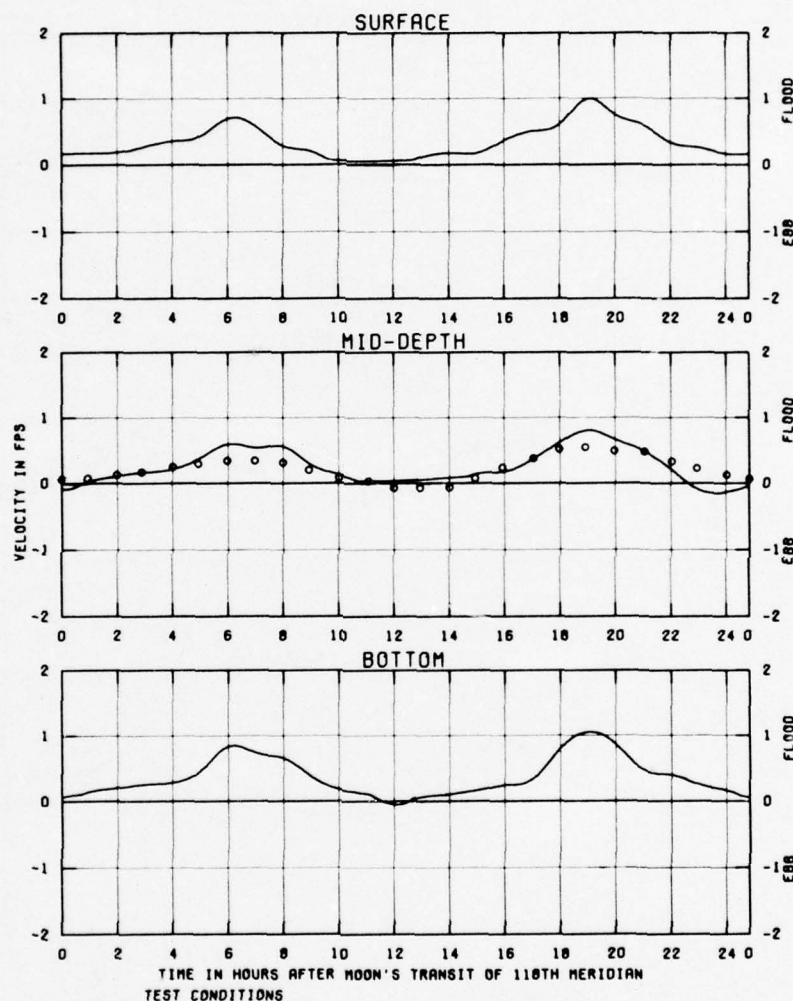
PLATE 24



LEGEND
 — PHYSICAL MODEL RESULTS
 ○ DEPTH-AVERAGED NUMERICAL MODEL RESULTS

VELOCITIES
BASE TEST
SPRING TIDE
STATION
10A

PLATE 25



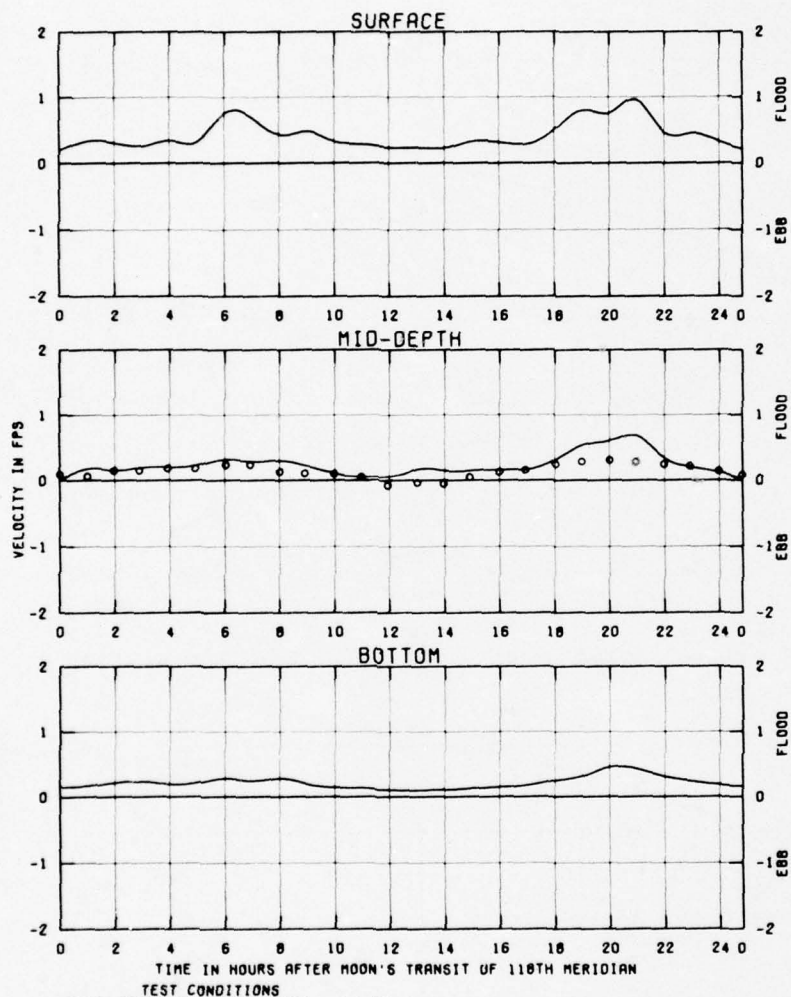
TEST CONDITIONS
TIDAL RANGE AT QUEENS DATE = 7.1 FT

VELOCITIES
BASE TEST
SPRING TIDE

STATION
108

LEGEND

- PHYSICAL MODEL RESULTS
- DEPTH-AVERAGED NUMERICAL MODEL RESULTS



TEST CONDITIONS
TIDAL RANGE AT QUEENS DATE = 7.1 FT

VELOCITIES
BASE TEST
SPRING TIDE

STATION
10C

LEGEND
— PHYSICAL MODEL RESULTS
○ DEPTH-AVERAGED NUMERICAL MODEL RESULTS

PLATE 27

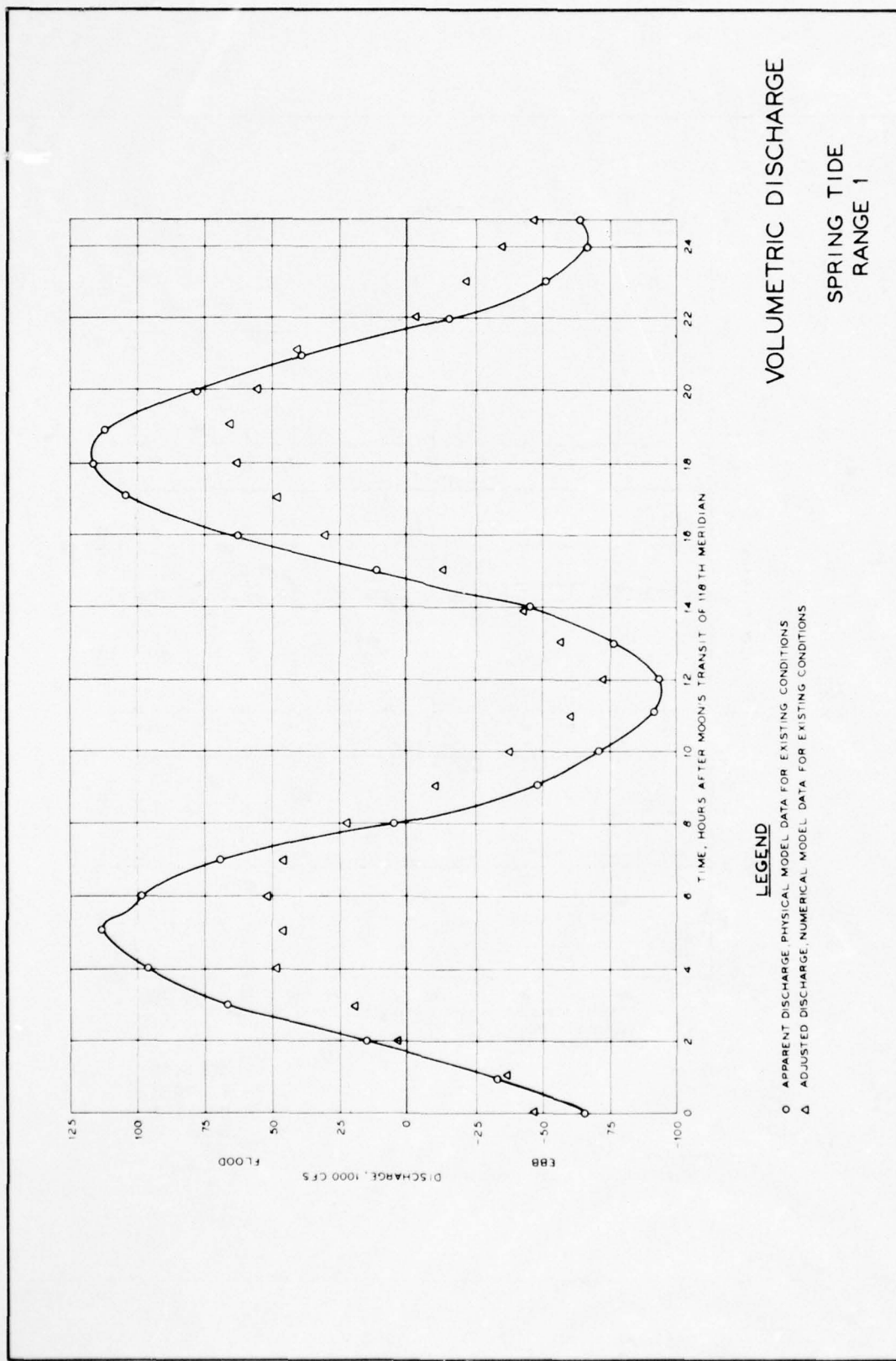
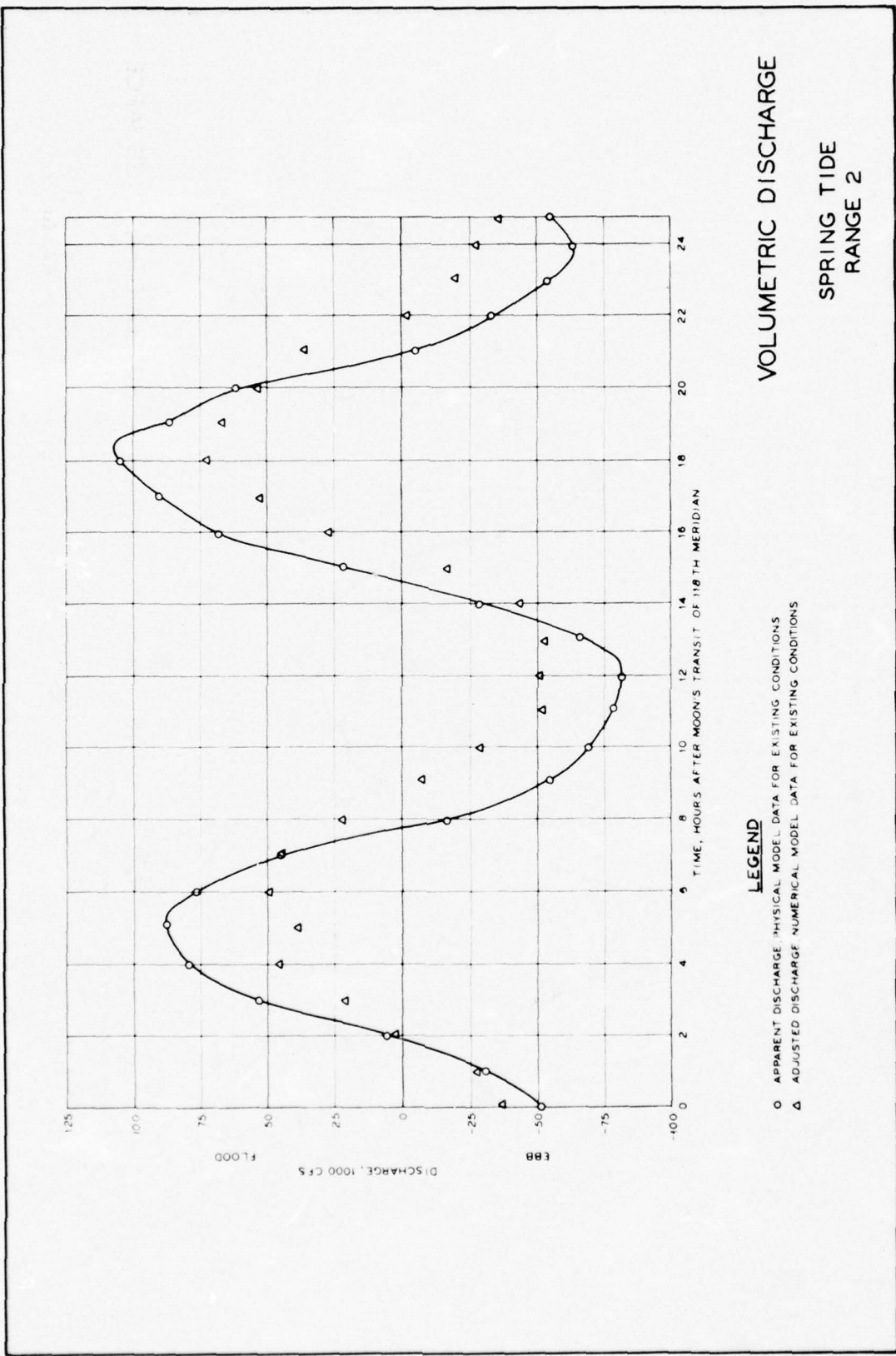


PLATE 28



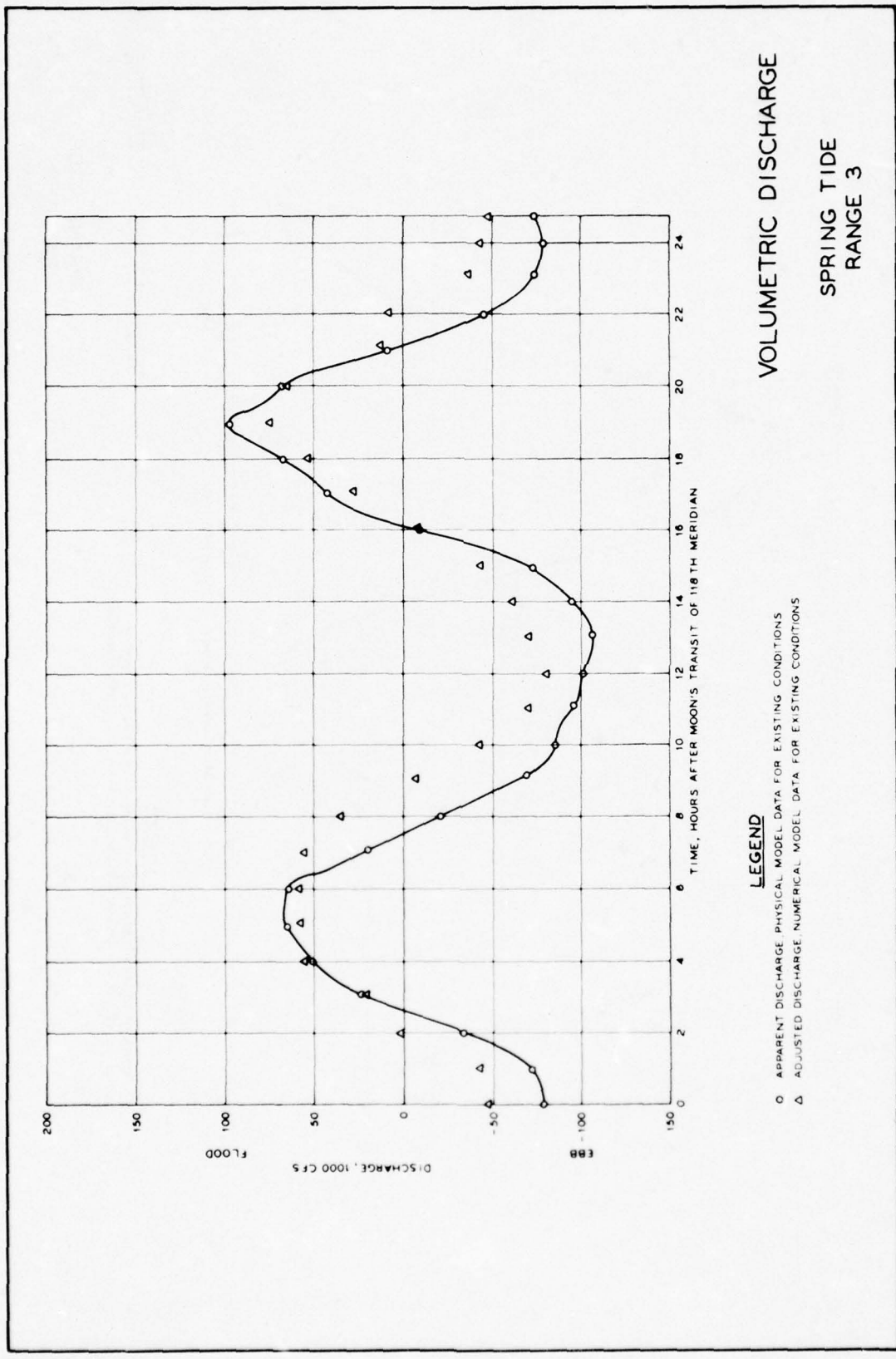
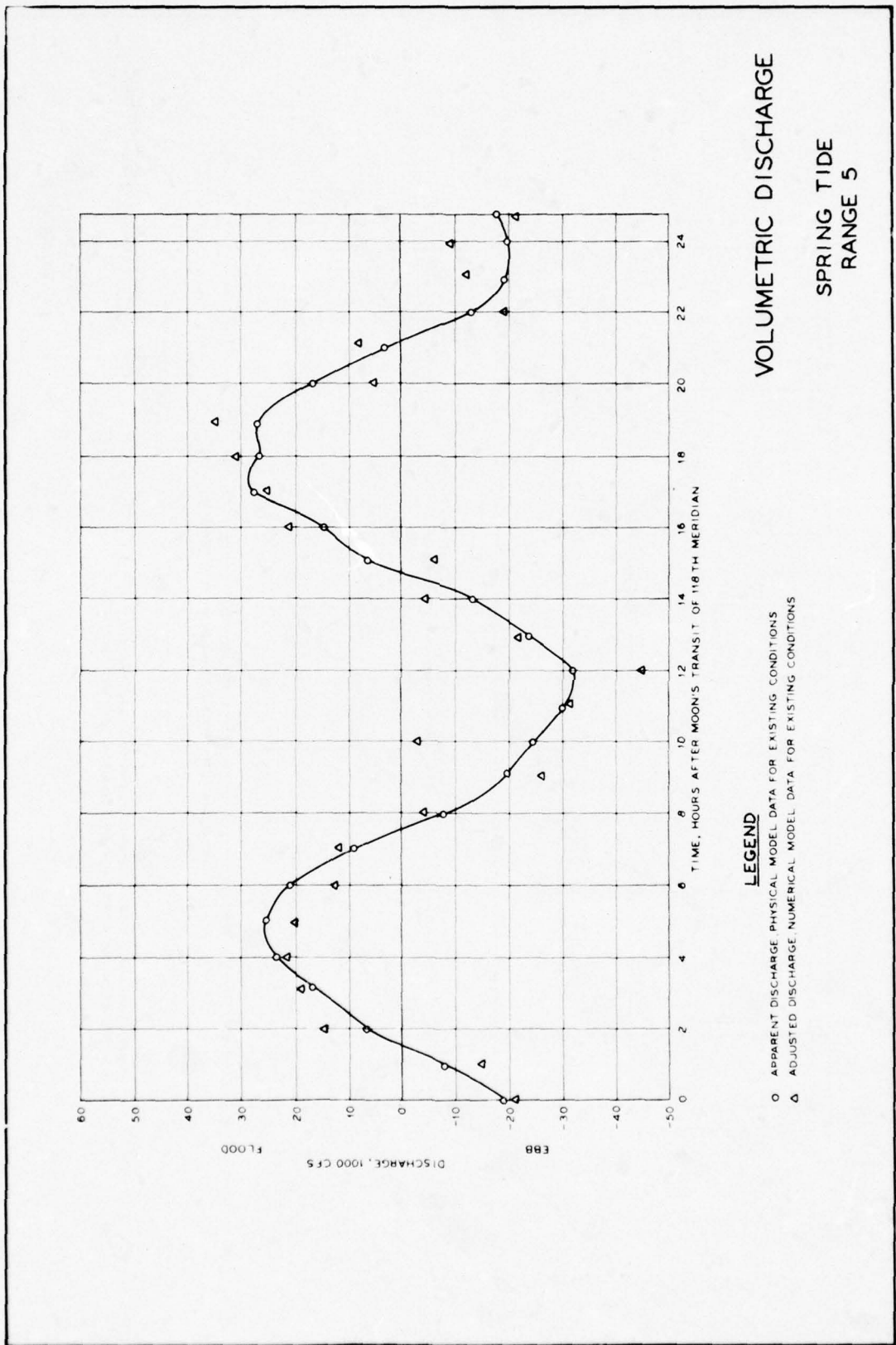


PLATE 30



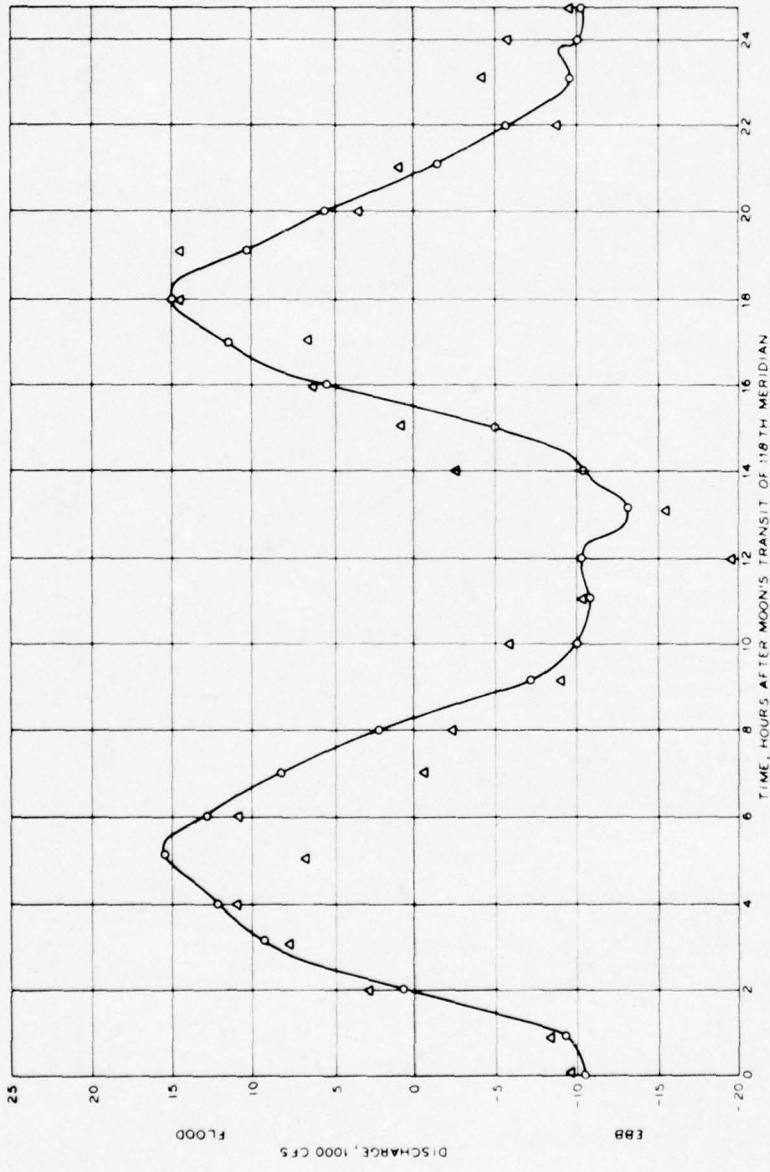
LEGEND

○ APPARENT DISCHARGE PHYSICAL MODEL DATA FOR EXISTING CONDITIONS

△ ADJUSTED DISCHARGE NUMERICAL MODEL DATA FOR EXISTING CONDITIONS

VOLUMETRIC DISCHARGE

SPRING TIDE
RANGE 5



VOLUMETRIC DISCHARGE
SPRING TIDE
RANGE 8

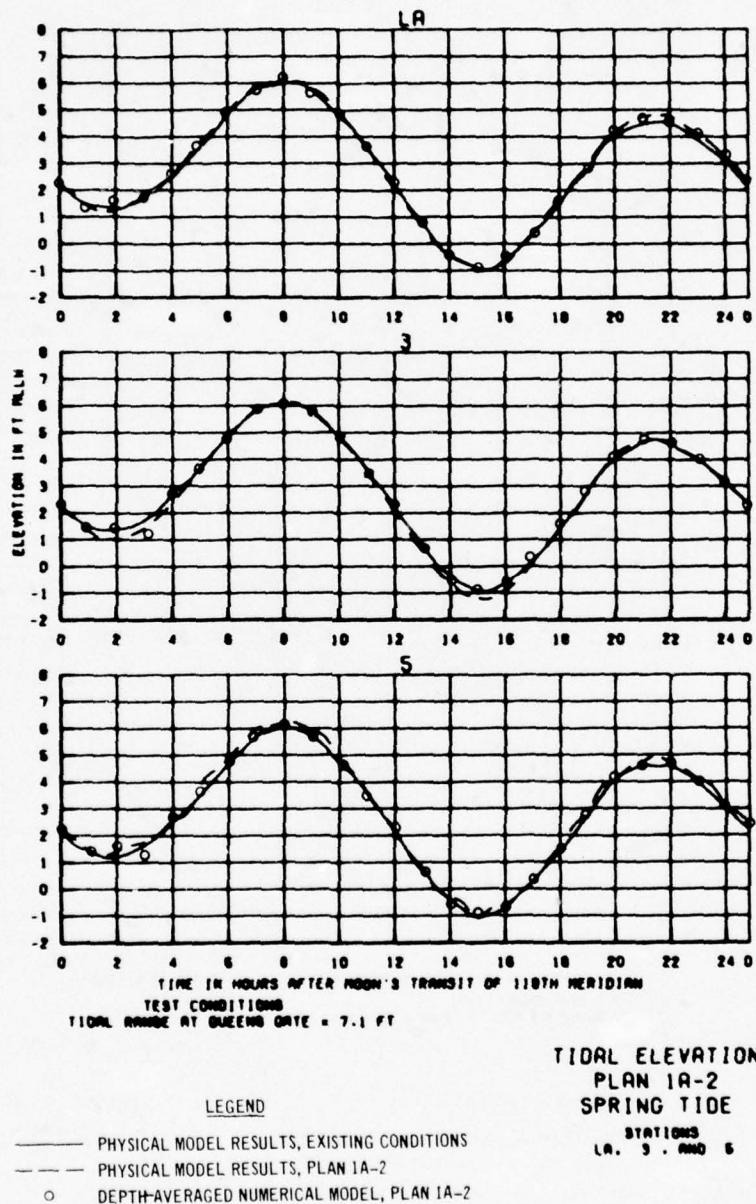
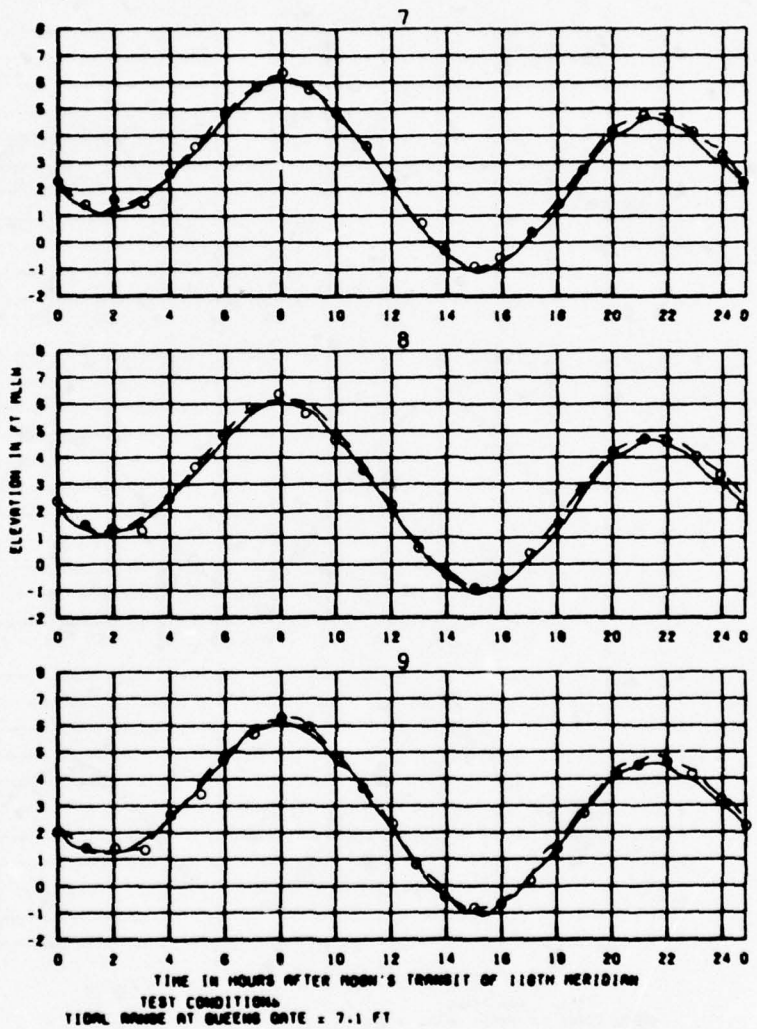


PLATE 33

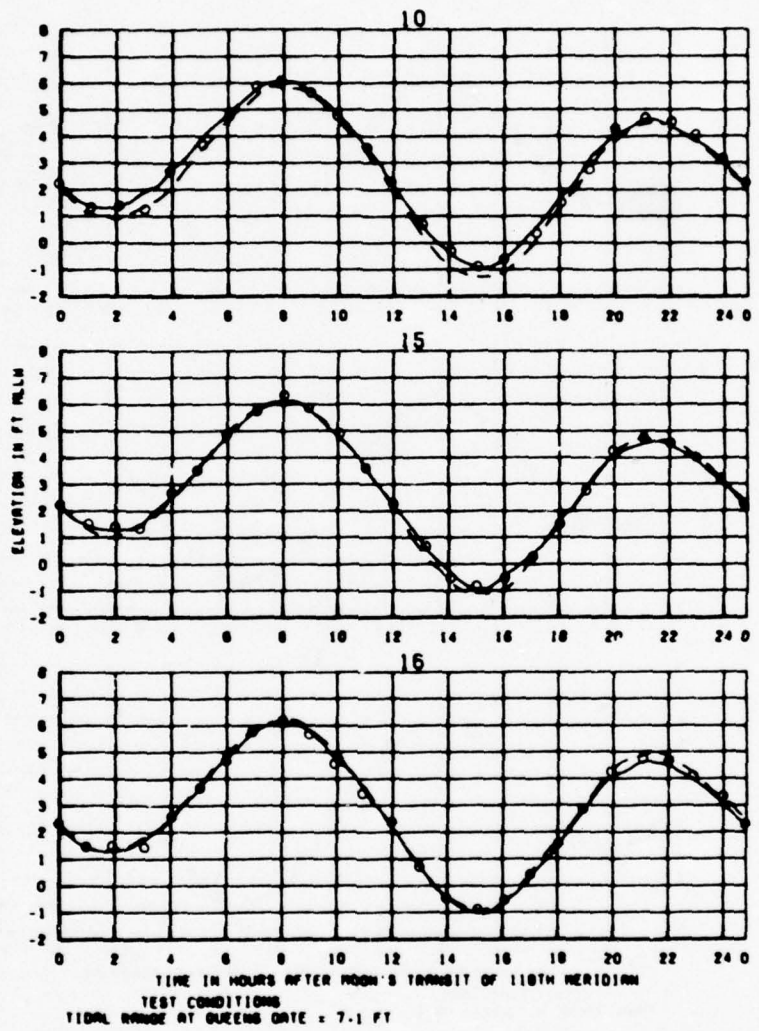


LEGEND

- PHYSICAL MODEL RESULTS, EXISTING CONDITIONS
- - - PHYSICAL MODEL RESULTS, PLAN 1A-2
- DEPTH-AVERAGED NUMERICAL MODEL, PLAN 1A-2

**TIDAL ELEVATIONS
PLAN 1A-2
SPRING TIDE**

STATIONS
7, 8 AND 9



TIDAL ELEVATIONS

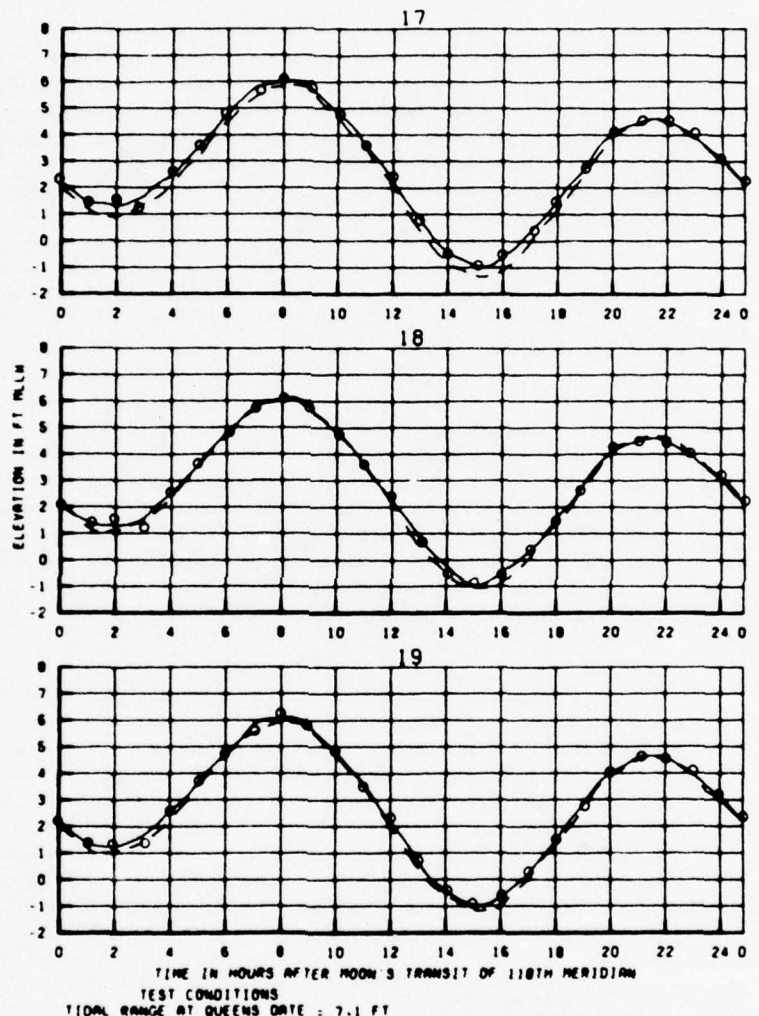
PLAN IA-2

SPRING TIDE

STATIONS

10, 15, AND 16

- LEGEND**
- PHYSICAL MODEL RESULTS, EXISTING CONDITIONS
 - - - PHYSICAL MODEL RESULTS, PLAN IA-2
 - DEPTH-AVERAGED NUMERICAL MODEL, PLAN IA-2

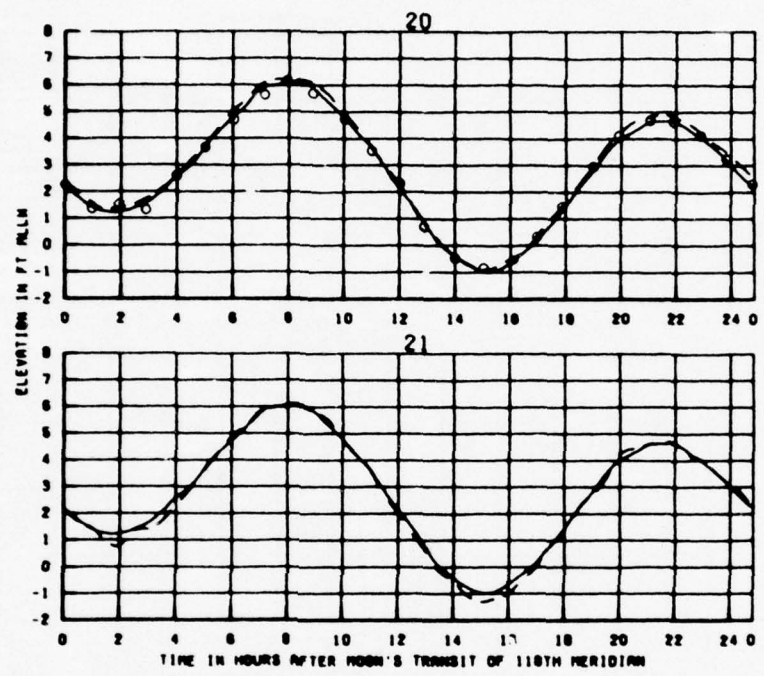


TIDAL ELEVATIONS
PLAN 1A-2
SPRING TIDE

LEGEND

- PHYSICAL MODEL RESULTS, EXISTING CONDITIONS
- — PHYSICAL MODEL RESULTS, PLAN 1A-2
- DEPTH-AVERAGED NUMERICAL MODEL, PLAN 1A-2

STATIONS
17, 18, AND 19



TEST CONDITIONS
TIDAL RANGE AT QUEENS DATE = 7.1 FT

TIDAL ELEVATIONS
PLAN 1A-2
SPRING TIDE

STATIONS
20 AND 21

- LEGEND
- PHYSICAL MODEL RESULTS, EXISTING CONDITIONS
 - PHYSICAL MODEL RESULTS, PLAN 1A-2
 - DEPTH-AVERAGED NUMERICAL MODEL, PLAN 1A-2

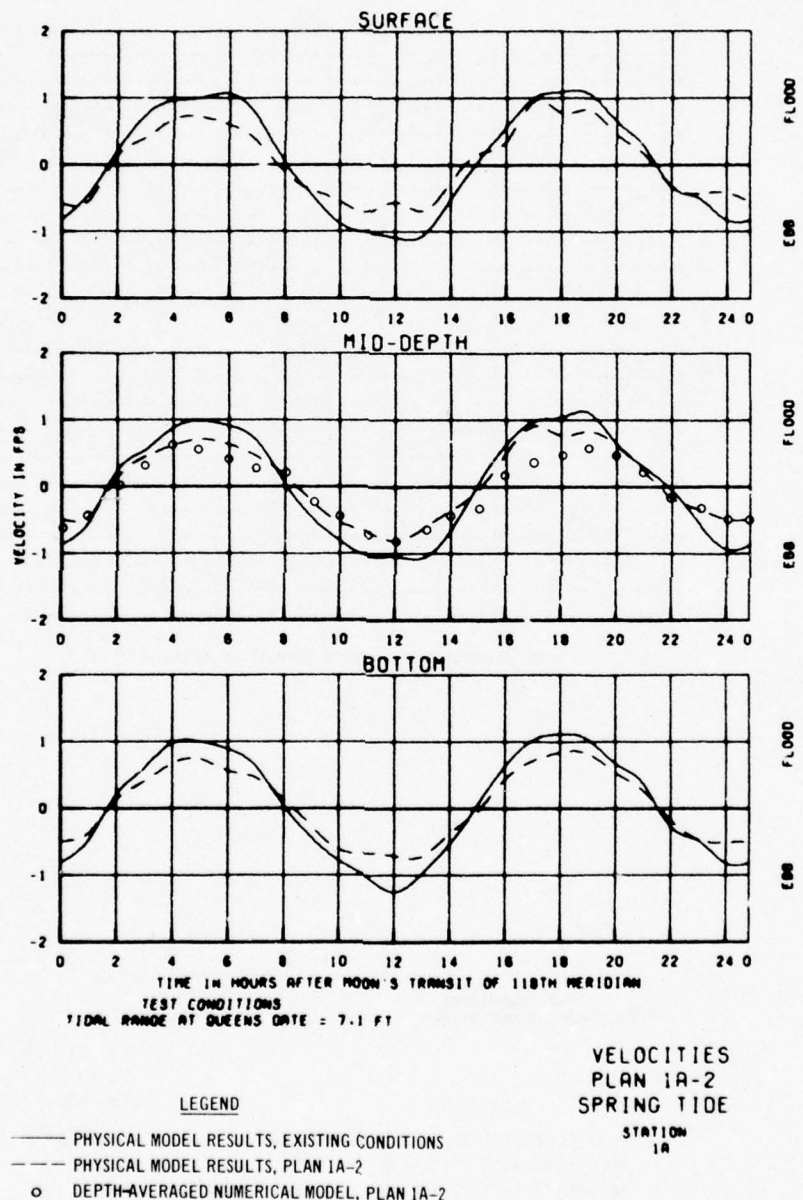
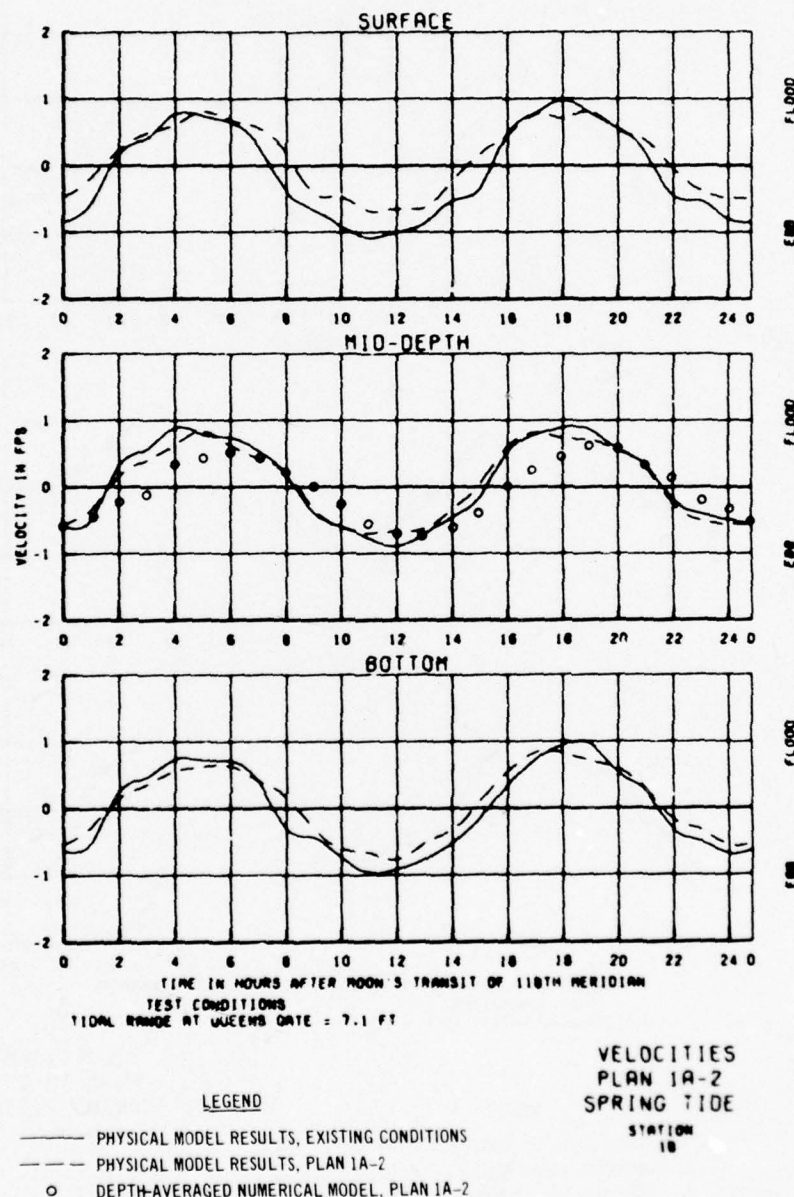


PLATE 38



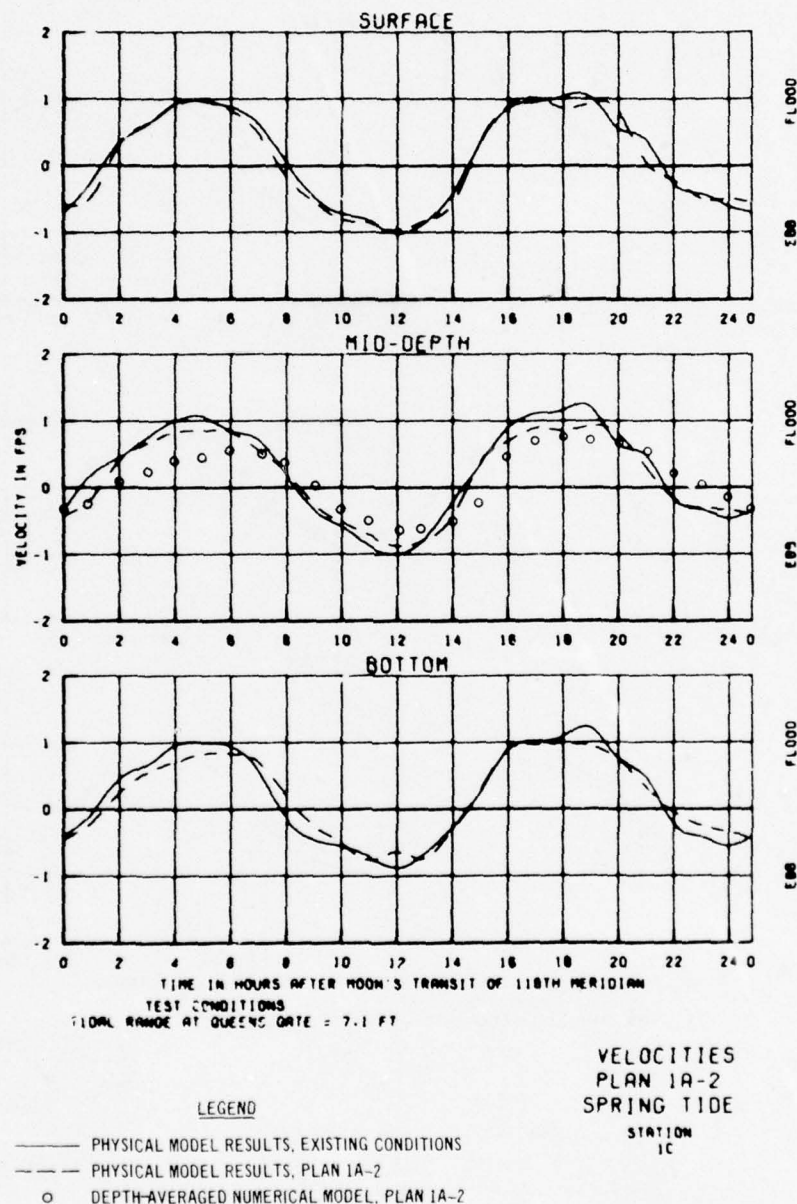
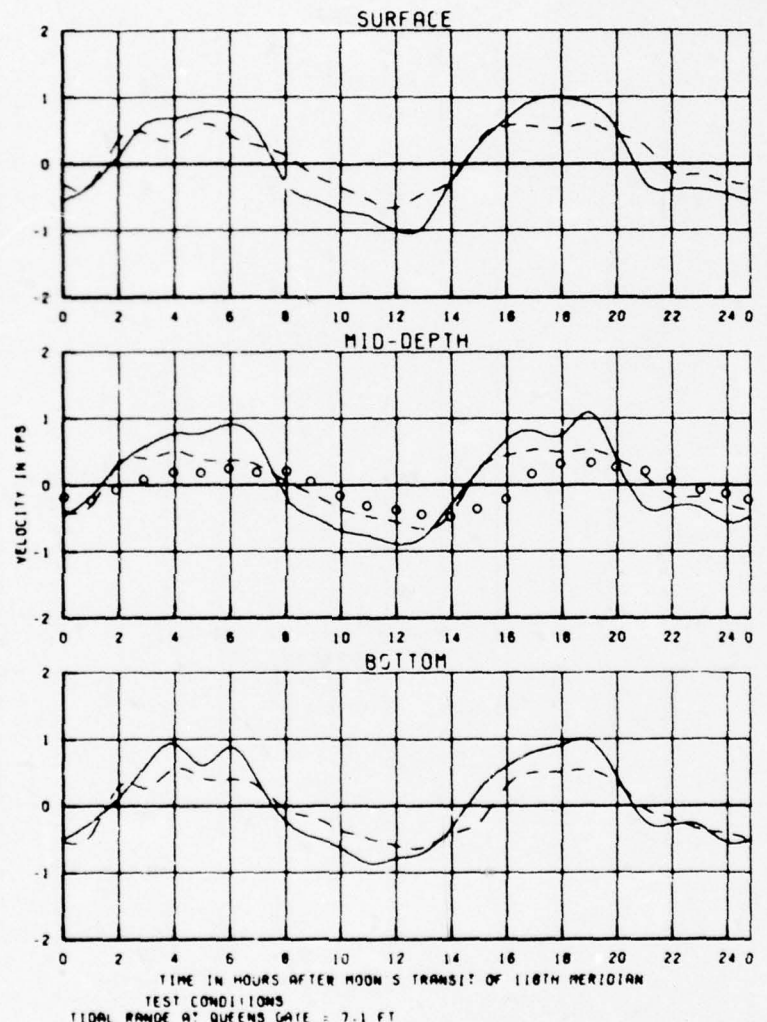


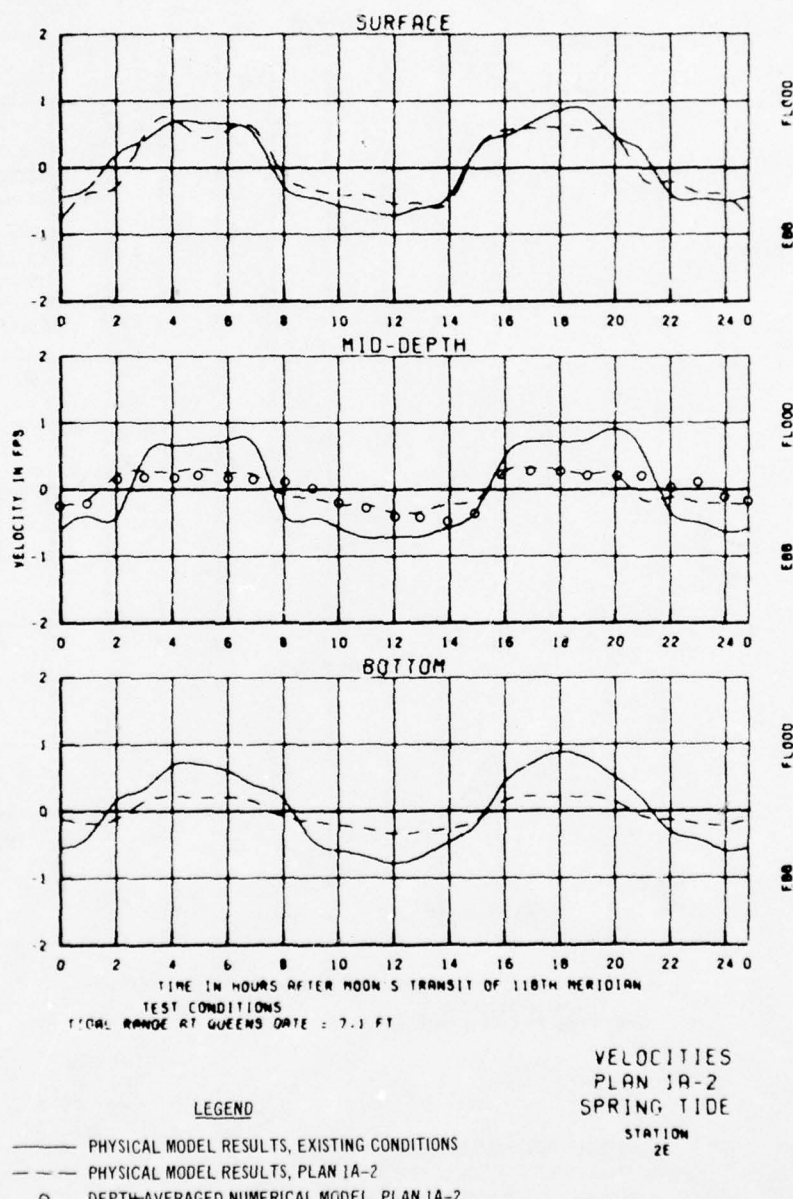
PLATE 40

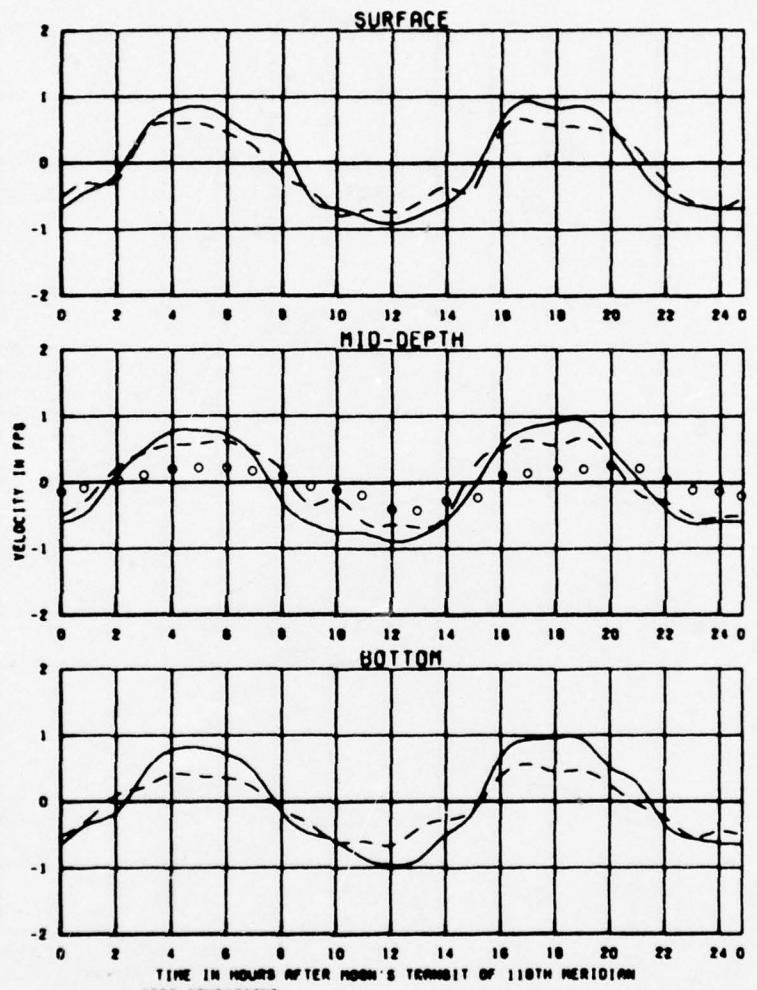


TEST CONDITIONS
TIDAL RANGE AT QUEENS GATE = 7.1 FT

VELOCITIES
PLAN 1A-2
SPRING TIDE
STATION
20

LEGEND
— PHYSICAL MODEL RESULTS, EXISTING CONDITIONS
- - - PHYSICAL MODEL RESULTS, PLAN 1A-2
○ DEPTH-AVERAGED NUMERICAL MODEL, PLAN 1A-2





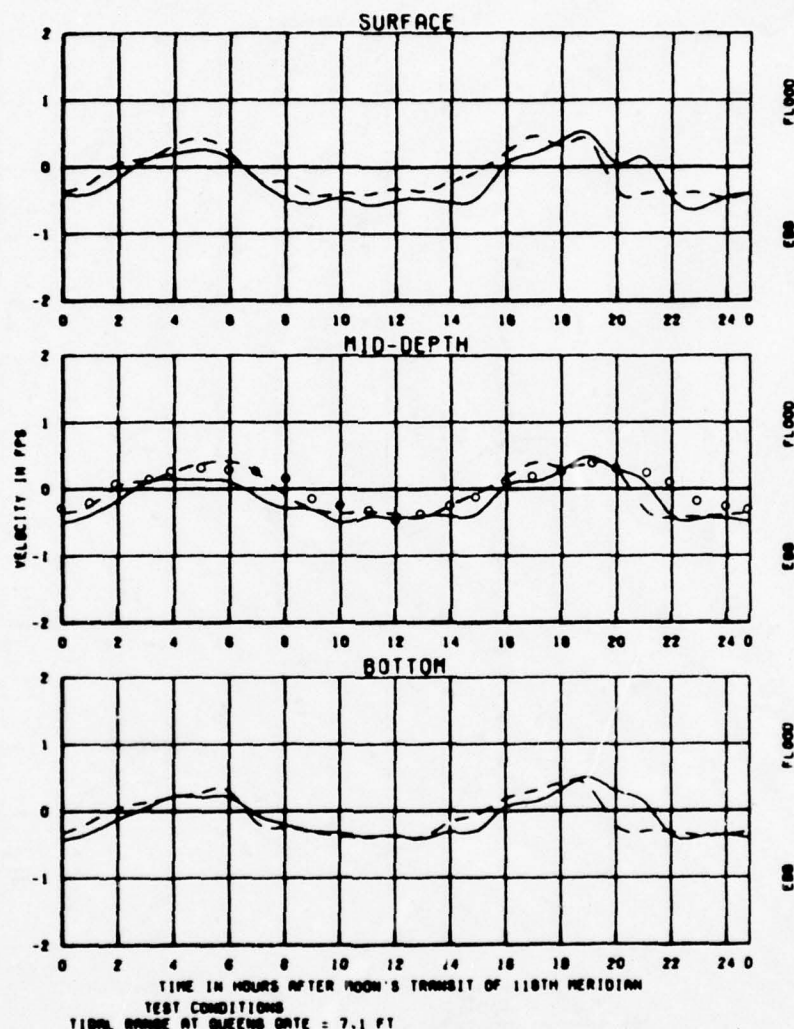
TEST CONDITIONS
TIDAL RANGE AT QUEENS DATE = 7.1 FT

VELOCITIES
PLAN 1A-2
SPRING TIDE

STATION
27

LEGEND

- PHYSICAL MODEL RESULTS, EXISTING CONDITIONS
- - PHYSICAL MODEL RESULTS, PLAN 1A-2
- DEPTH-AVERAGED NUMERICAL MODEL, PLAN 1A-2

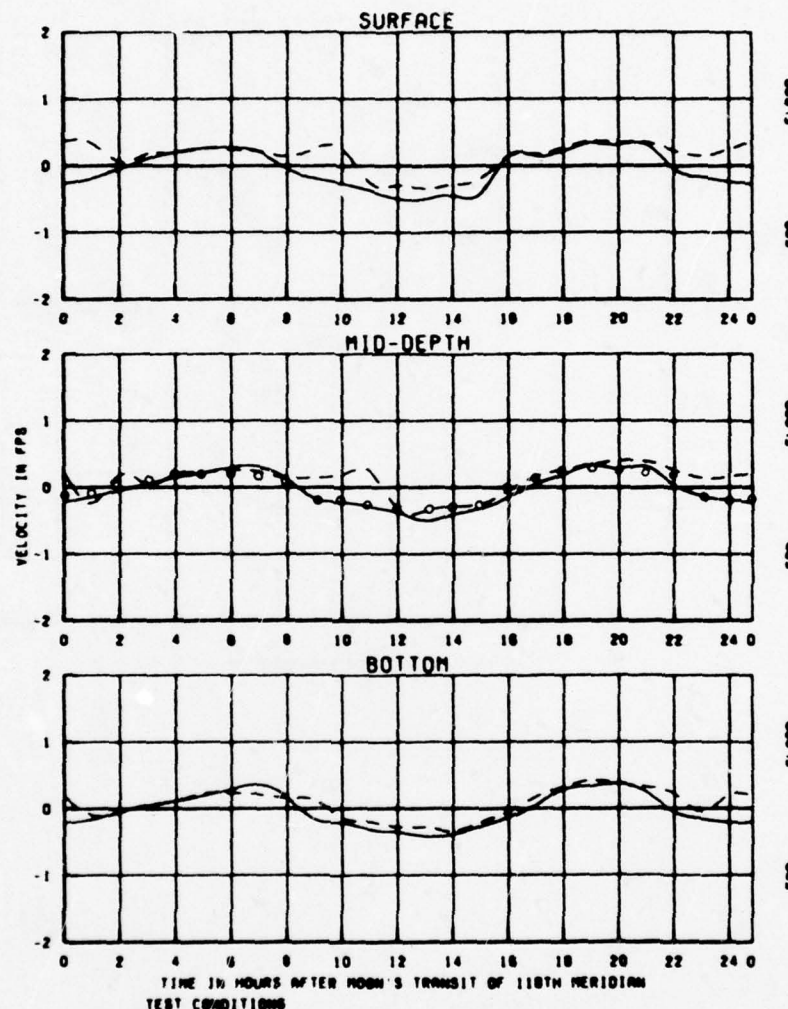


VELOCITIES
PLAN 1A-2
SPRING TIDE

STATION
30

LEGEND

- PHYSICAL MODEL RESULTS, EXISTING CONDITIONS
- PHYSICAL MODEL RESULTS, PLAN 1A-2
- DEPTH-AVERAGED NUMERICAL MODEL, PLAN 1A-2



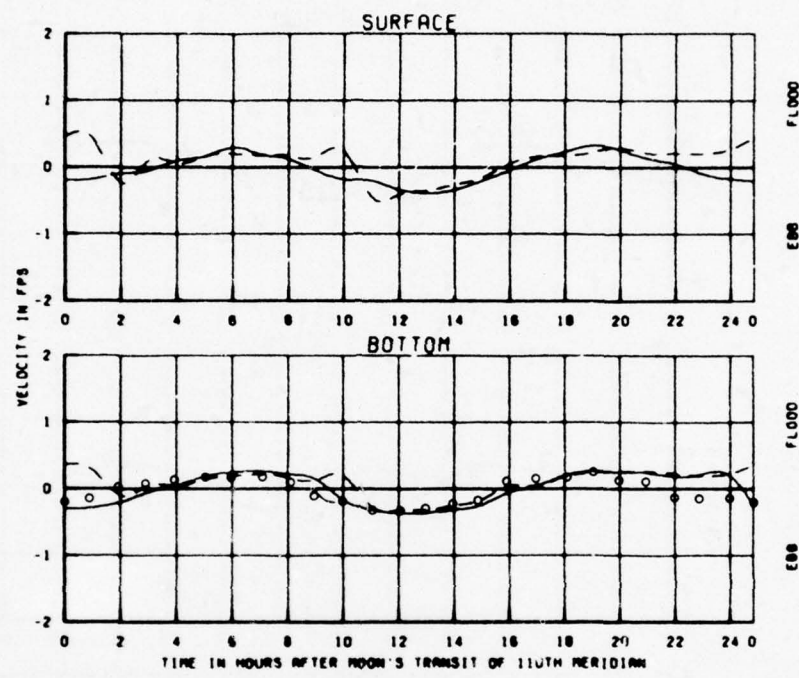
TEST CONDITIONS
TIDAL RANGE AT QUEENS BAYE = 7.1 FT

VELOCITIES
PLAN 1A-2
SPRING TIDE

STATION
3M

LEGEND

- PHYSICAL MODEL RESULTS, EXISTING CONDITIONS
- - - PHYSICAL MODEL RESULTS, PLAN 1A-2
- DEPTH-AVERAGED NUMERICAL MODEL, PLAN 1A-2



TEST CONDITIONS
TIDAL RANGE AT QUEENS DATE = 7.1 FT

LEGEND

- PHYSICAL MODEL RESULTS, EXISTING CONDITIONS
- PHYSICAL MODEL RESULTS, PLAN IA-2
- DEPTH-AVERAGED NUMERICAL MODEL, PLAN IA-2

VELOCITIES
PLAN IA-2
SPRING TIDE

STATION
31

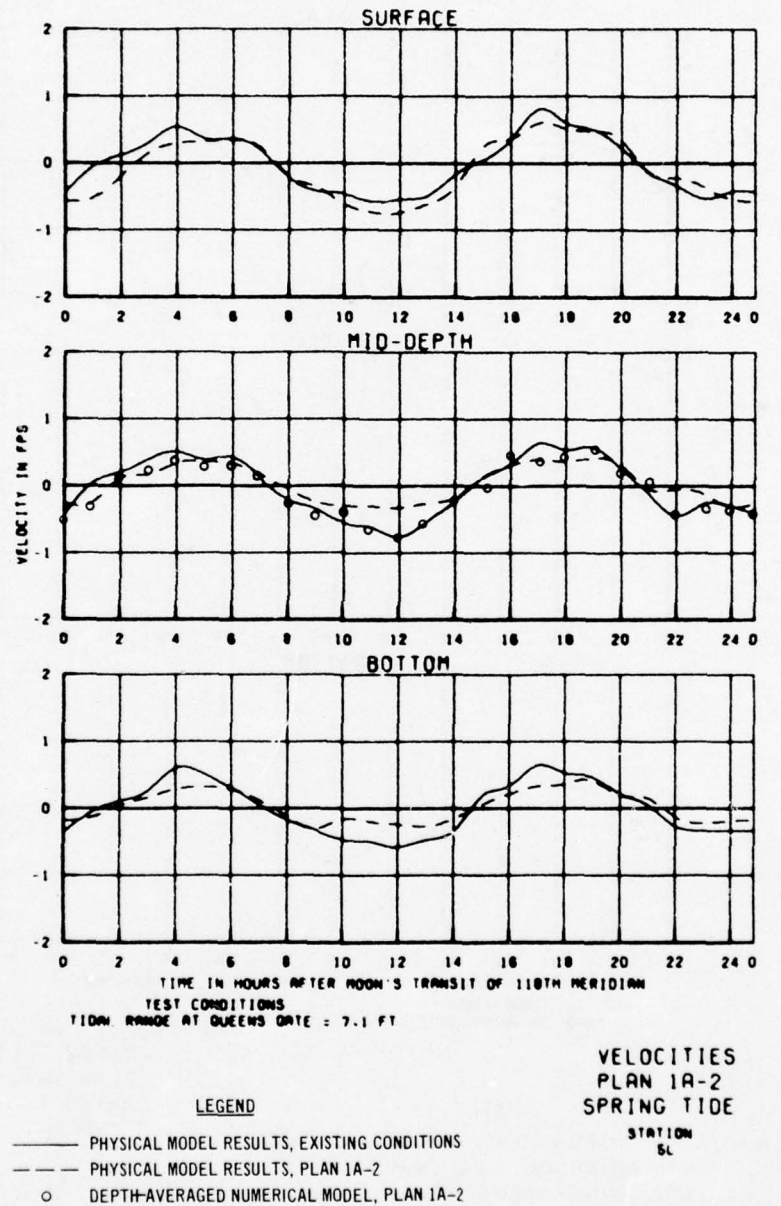


PLATE 47

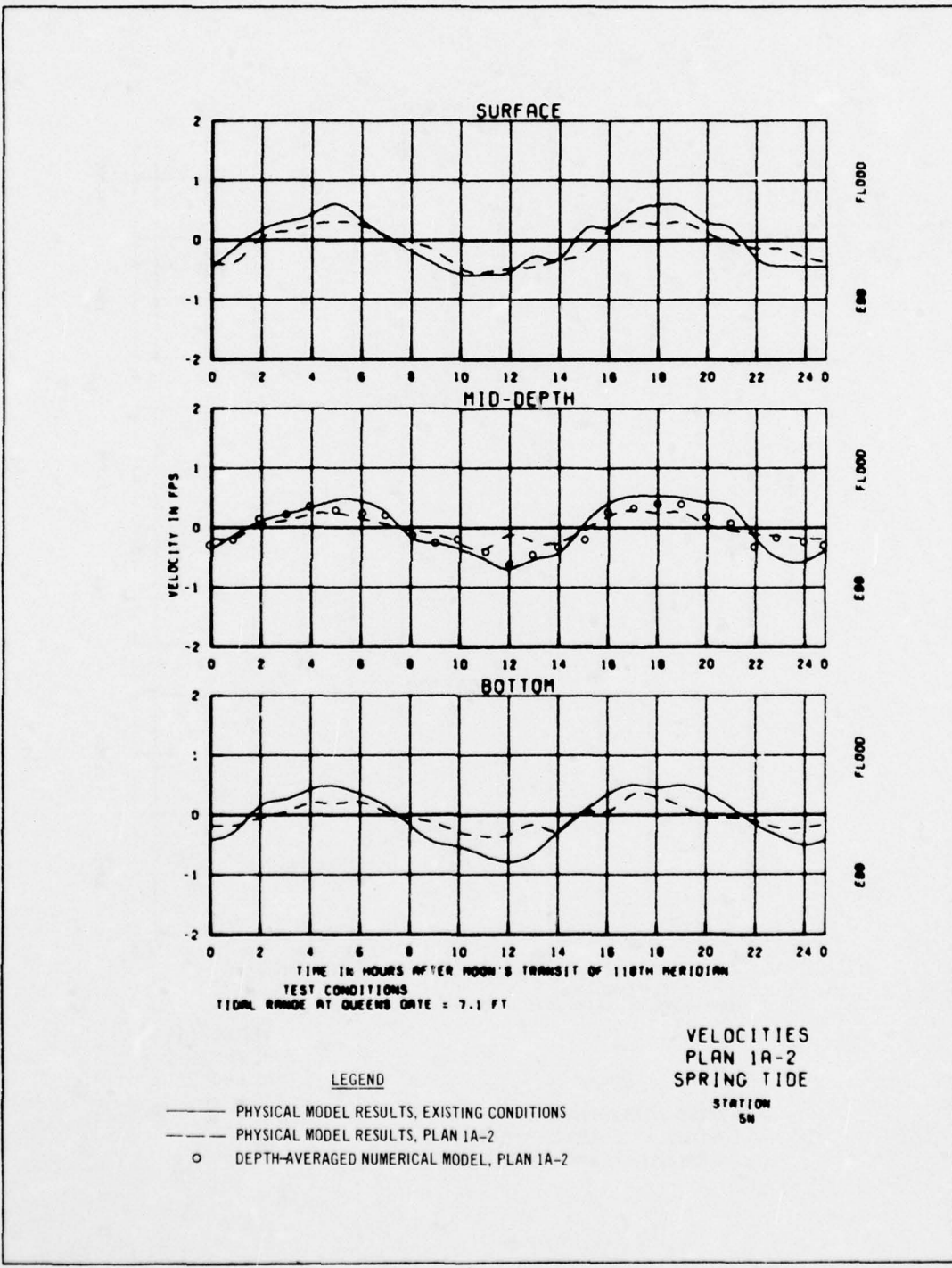
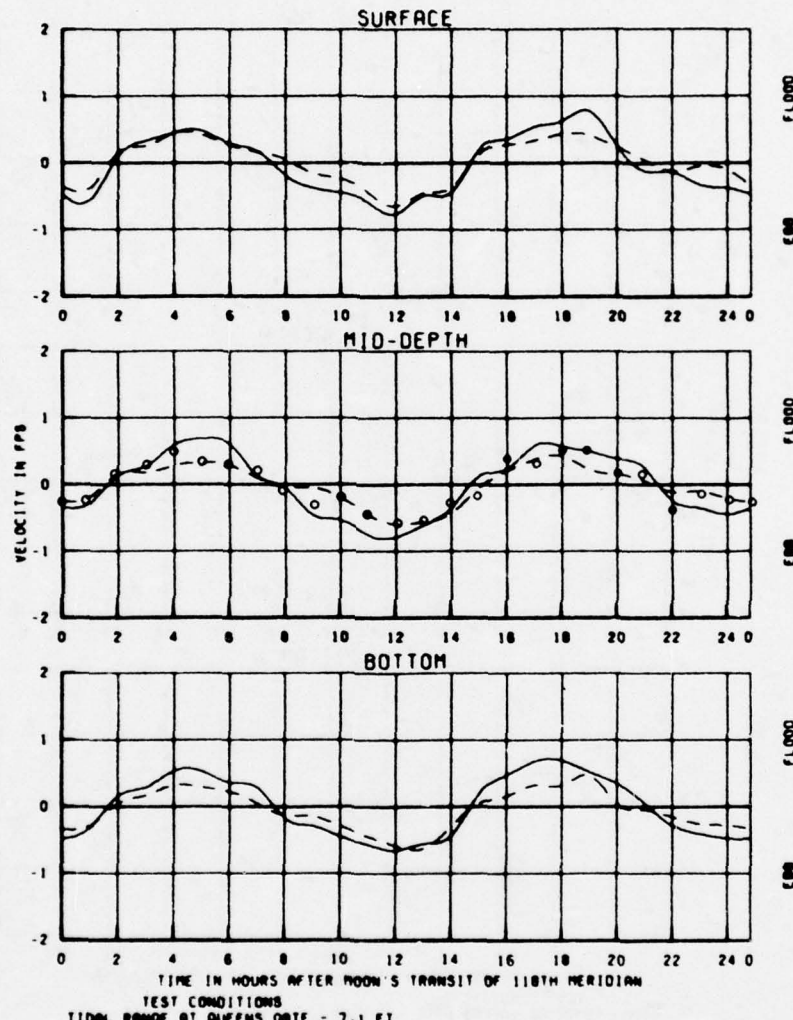


PLATE 48



LEGEND

- PHYSICAL MODEL RESULTS, EXISTING CONDITIONS
- - PHYSICAL MODEL RESULTS, PLAN 1A-2
- DEPTH-AVERAGED NUMERICAL MODEL, PLAN 1A-2

VELOCITIES
PLAN 1A-2
SPRING TIDE
STATION
6M

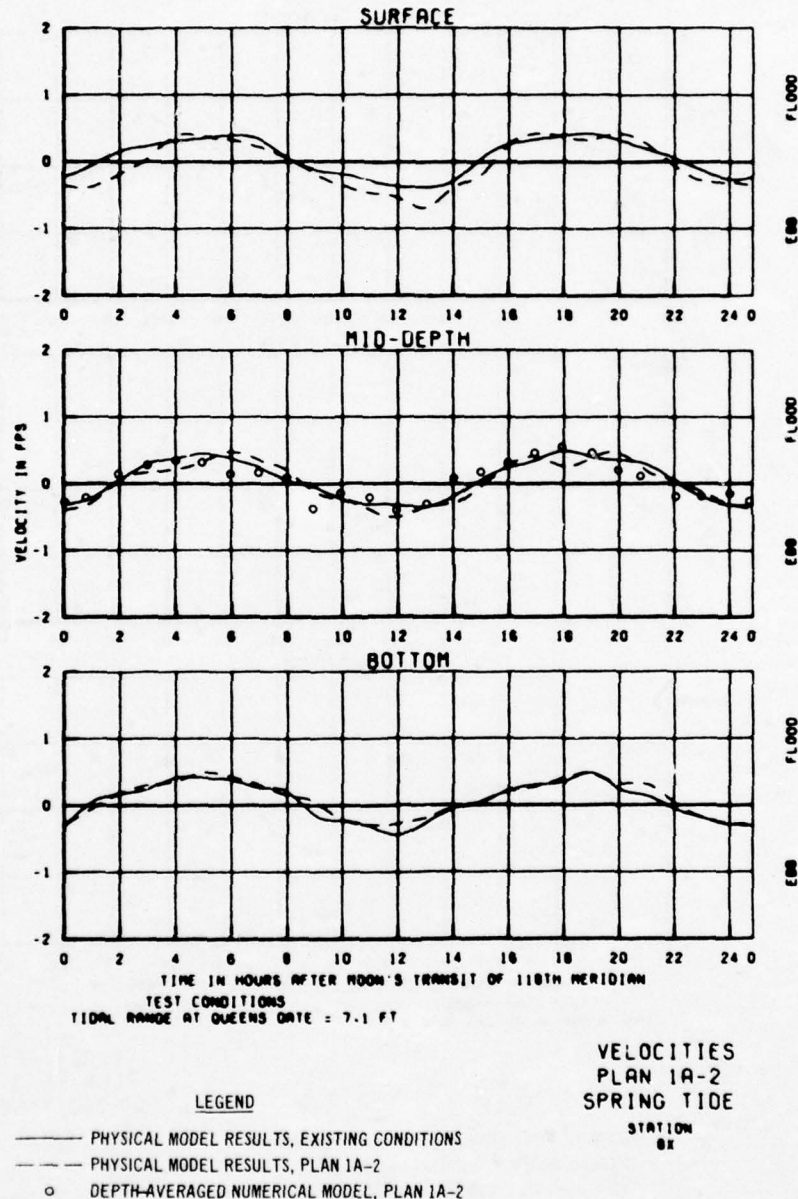
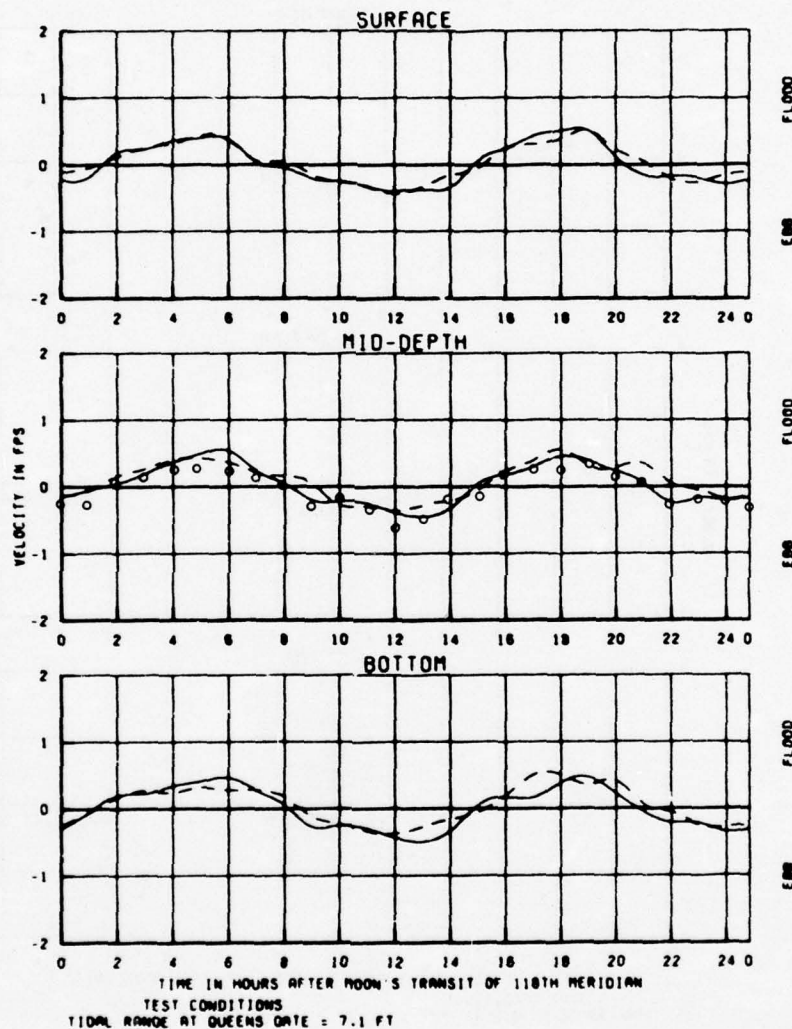


PLATE 50



TIME IN HOURS AFTER MOON'S TRANSIT OF 110TH MERIDIAN
TEST CONDITIONS
TIDAL RANGE AT QUEENS DATE = 7.1 FT

VELOCITIES
PLAN 1A-2
SPRING TIDE
STATION
8Y

LEGEND
 — PHYSICAL MODEL RESULTS, EXISTING CONDITIONS
 - - - PHYSICAL MODEL RESULTS, PLAN 1A-2
 ○ DEPTH-AVERAGED NUMERICAL MODEL, PLAN 1A-2

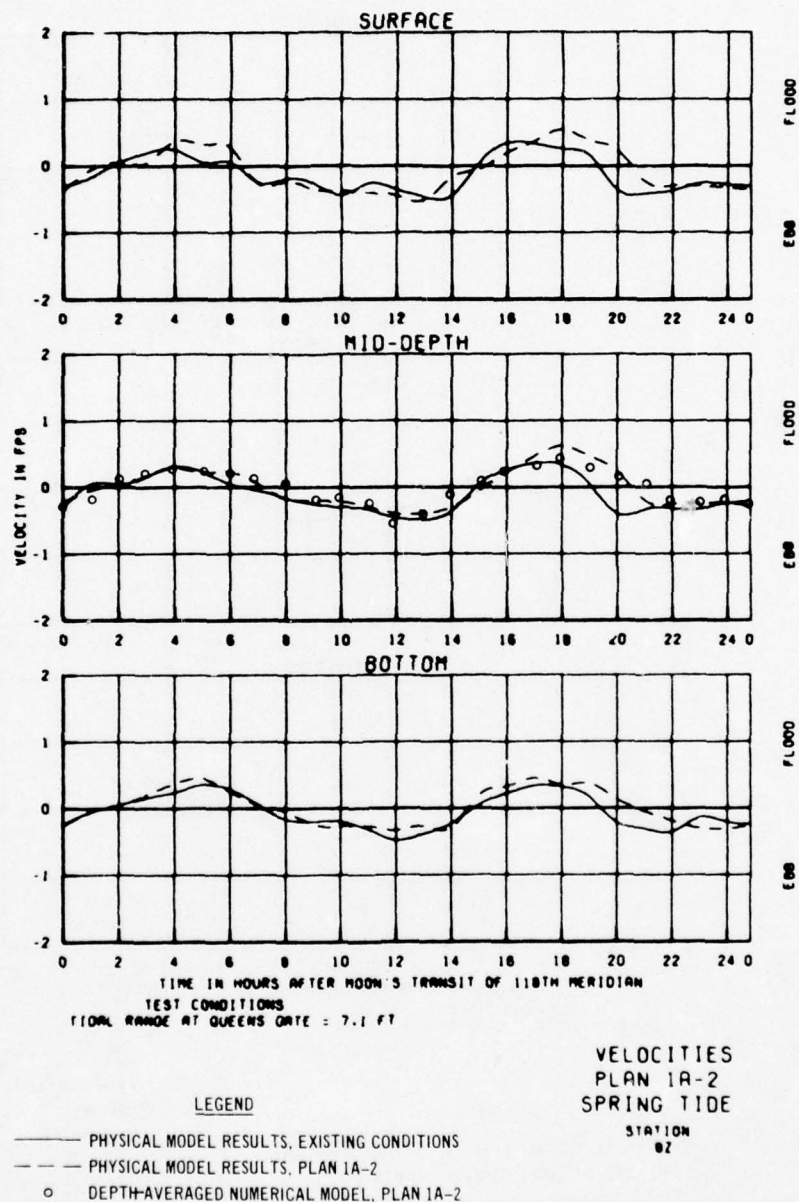
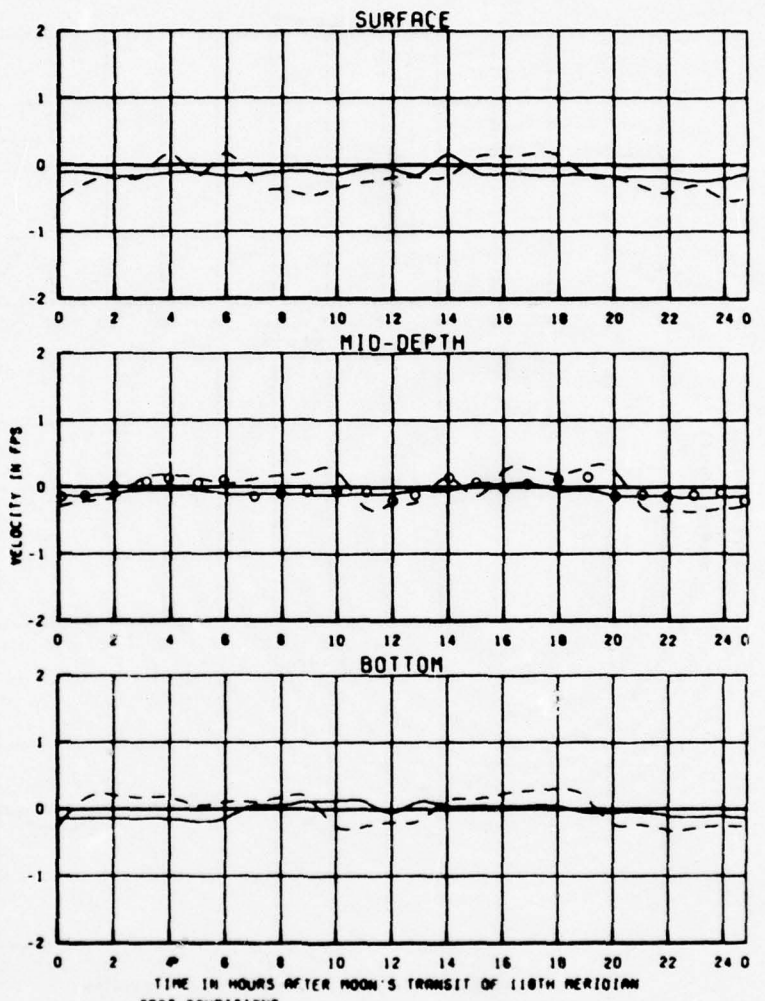


PLATE 52



TIME IN HOURS AFTER MOON'S TRANSIT OF 116TH MERIDIANT

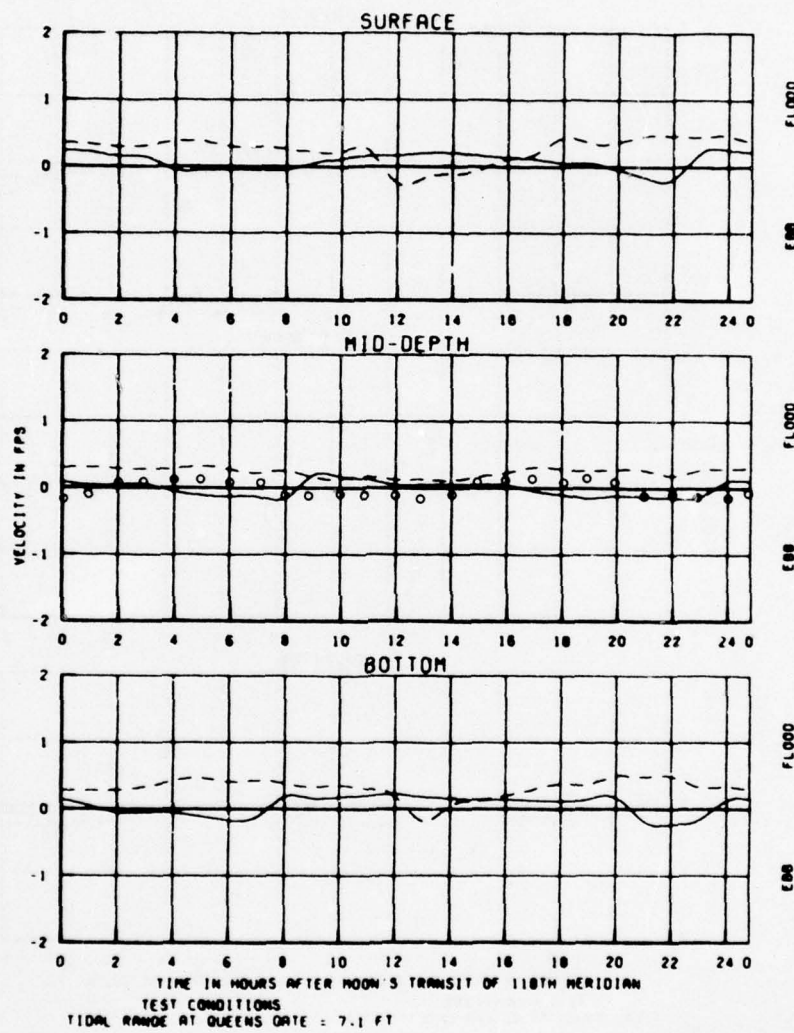
TEST CONDITIONS
TIDAL RANGE AT QUEENS DATE = 7.1 FT

VELOCITIES
PLAN 1A-2
SPRING TIDE

STATION
88

LEGEND

- PHYSICAL MODEL RESULTS, EXISTING CONDITIONS
- — PHYSICAL MODEL RESULTS, PLAN 1A-2
- DEPTH-AVERAGED NUMERICAL MODEL, PLAN 1A-2

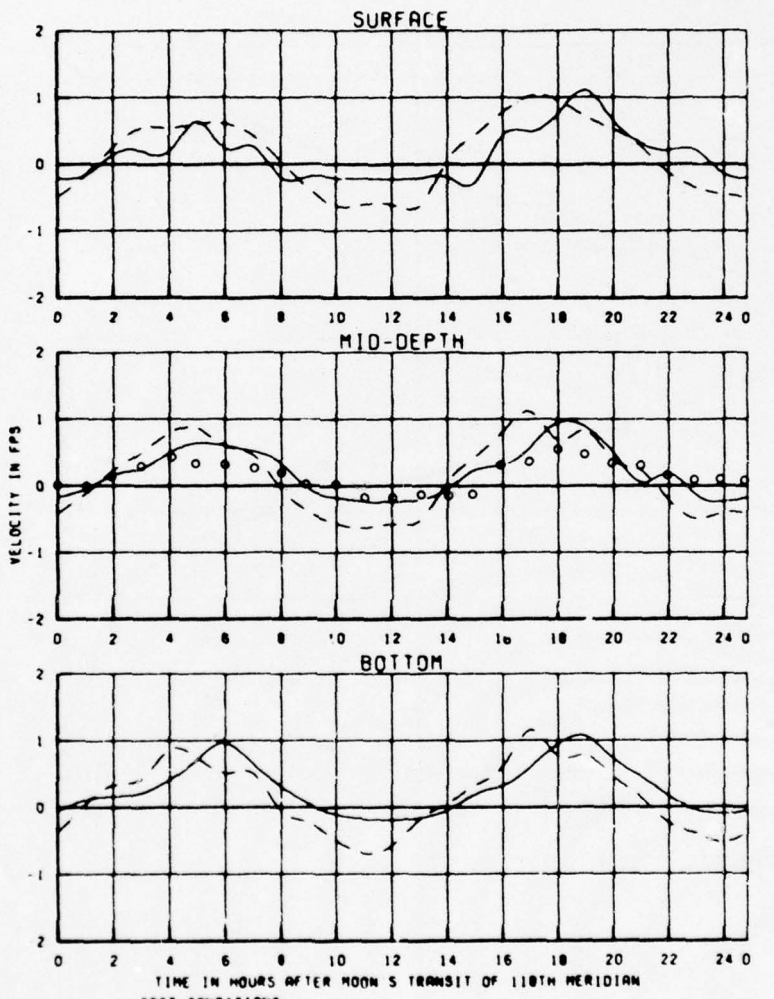


LEGEND

- PHYSICAL MODEL RESULTS, EXISTING CONDITIONS
- - - PHYSICAL MODEL RESULTS, PLAN IA-2
- DEPTH-AVERAGED NUMERICAL MODEL, PLAN IA-2

VELOCITIES
PLAN IA-2
SPRING TIDE

STATION
98



TIME IN HOURS AFTER MOON'S TRANSIT OF 118TH MERIDIAN

TEST CONDITIONS

TIDAL RANGE AT QUEENS DATE = 7.1 FT

VELOCITIES
PLAN 1A-2
SPRING TIDE
STATION
10A

LEGEND

- PHYSICAL MODEL RESULTS, EXISTING CONDITIONS
- - PHYSICAL MODEL RESULTS, PLAN 1A-2
- DEPTH-AVERAGED NUMERICAL MODEL, PLAN 1A-2

AD-A031 178

ARMY ENGINEER WATERWAYS EXPERIMENT STATION VICKSBURG MISS F/G 8/3
NUMERICAL ANALYSIS OF TIDAL CIRCULATION FOR LONG BEACH HARBOR. --ETC(U)
SEP 76 D C RANEY

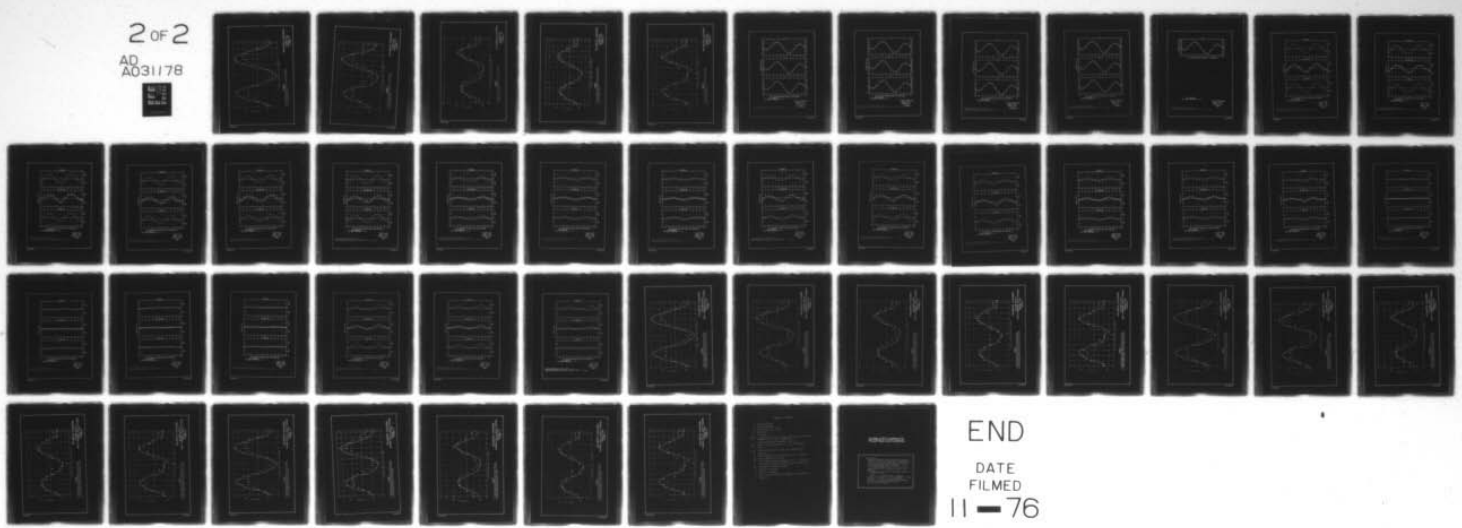
UNCLASSIFIED

WES-MP-H-76-4-3

NL

2 OF 2

AD A031178
EE FILM



END

DATE
FILMED
11 - 76

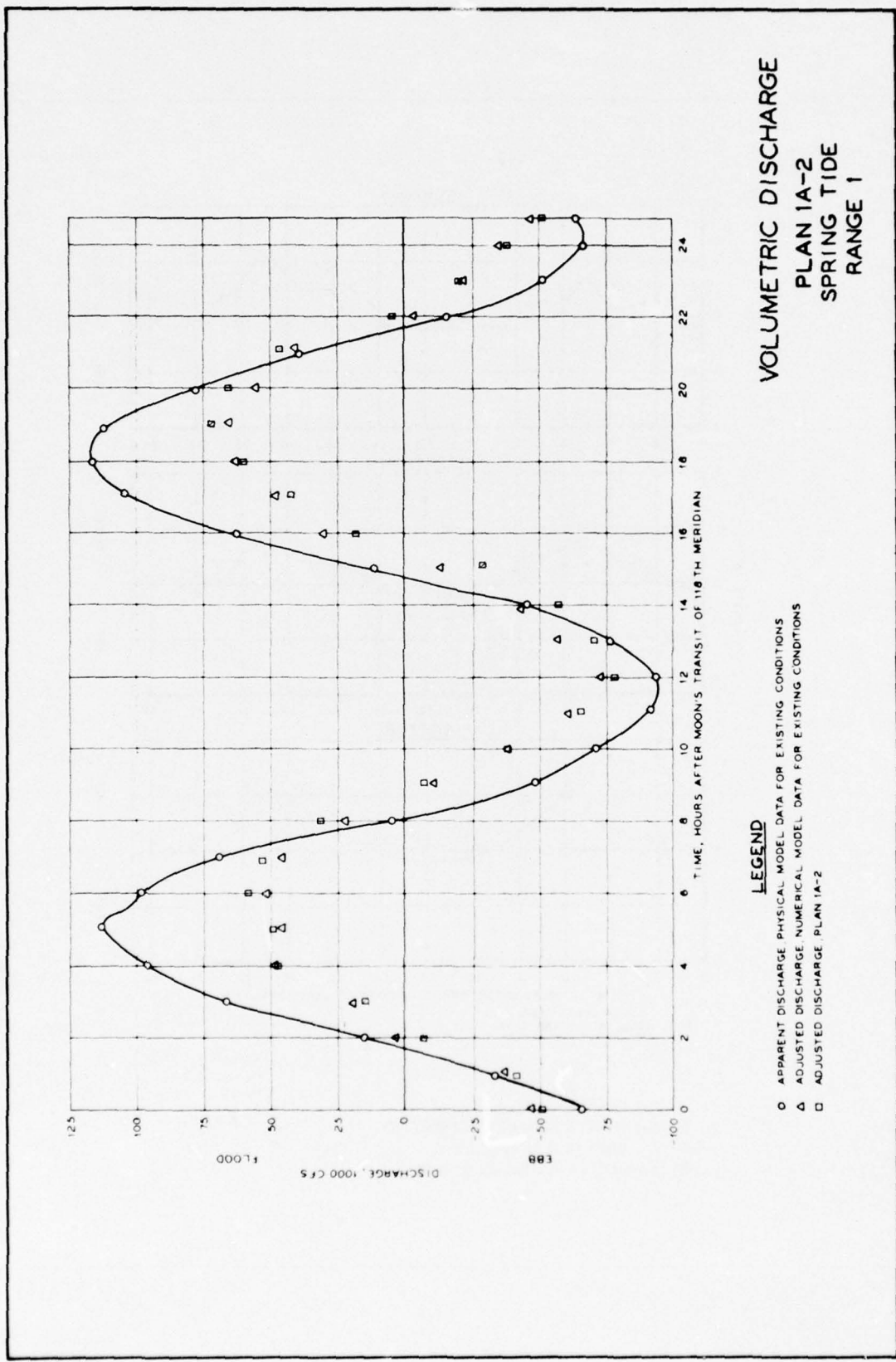
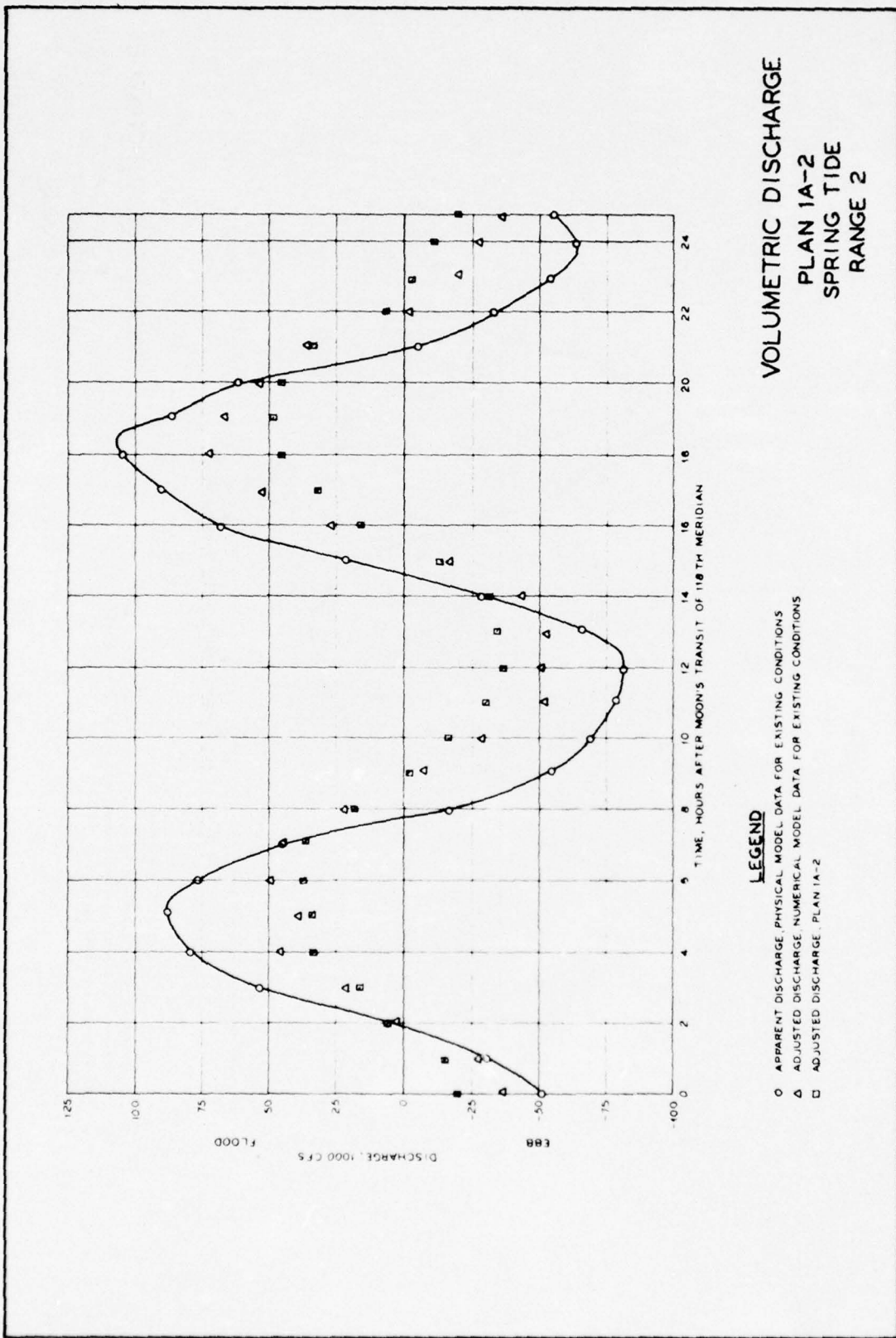
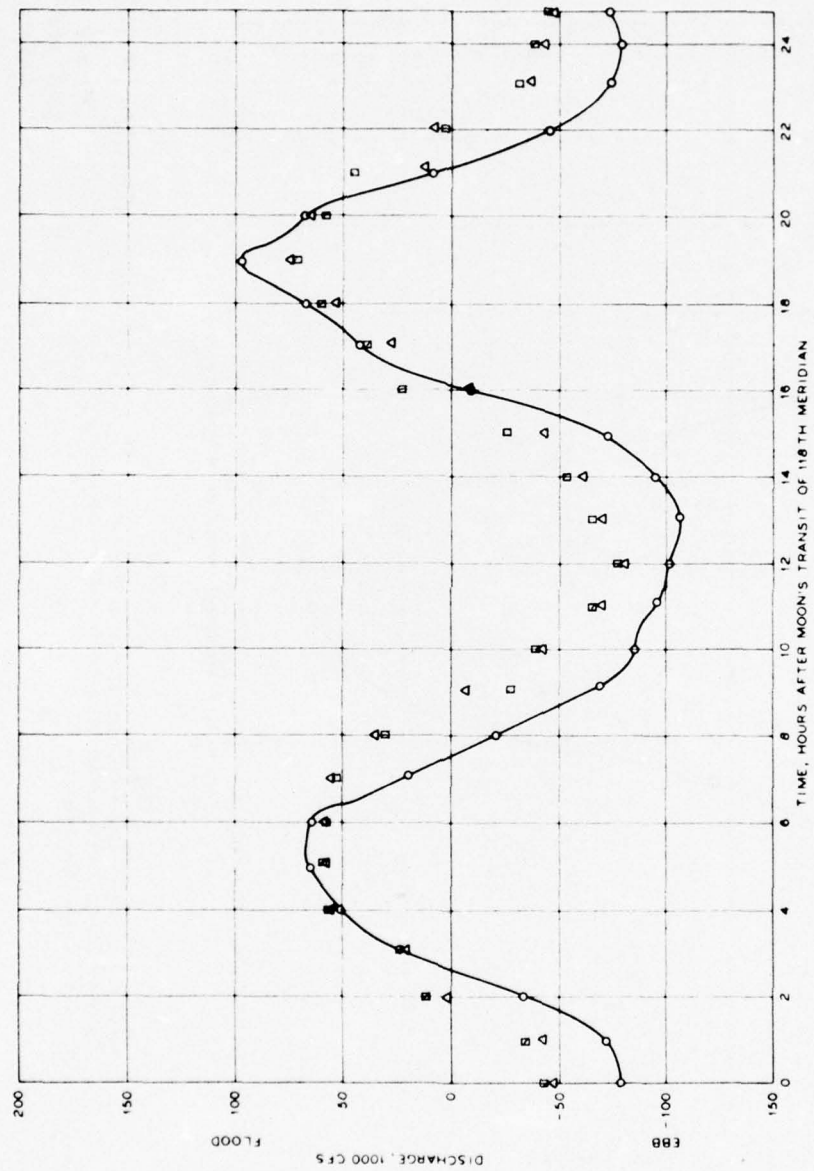


PLATE 56

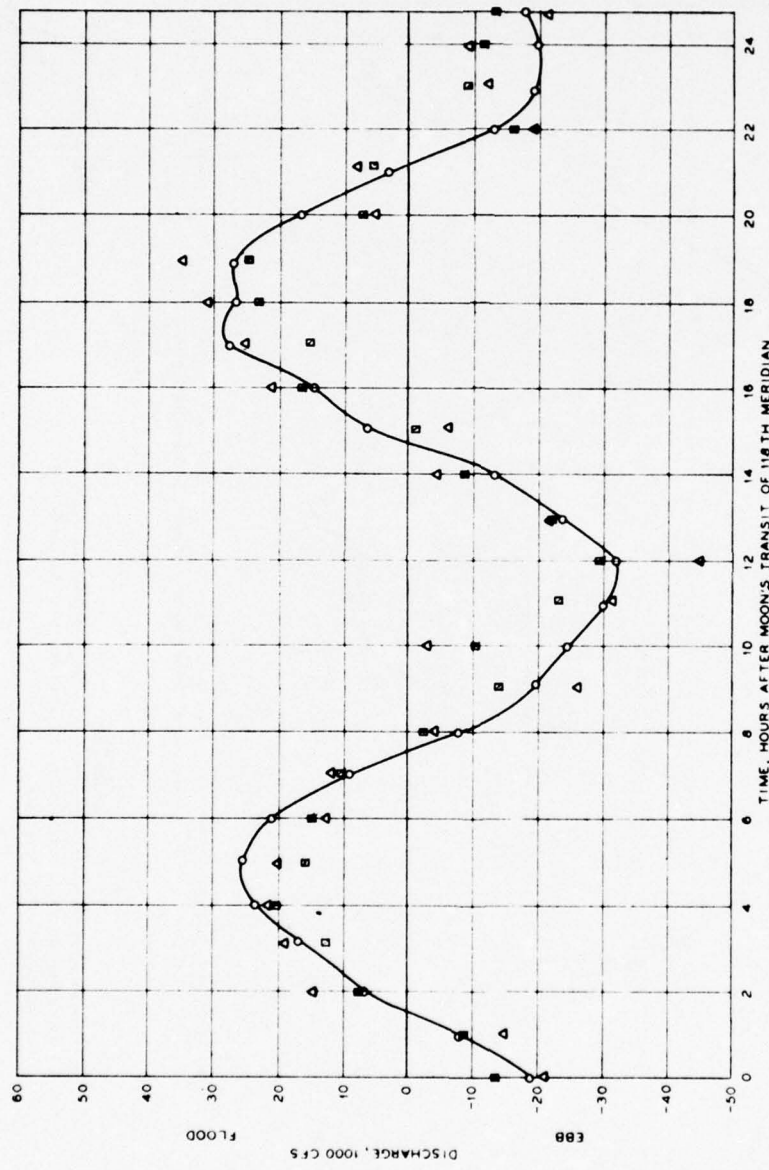


VOLUMETRIC DISCHARGE
PLAN IA-2
SPRING TIDE
RANGE 3



LEGEND

- APPARENT DISCHARGE, PHYSICAL MODEL DATA FOR EXISTING CONDITIONS
- △ ADJUSTED DISCHARGE, NUMERICAL MODEL DATA FOR EXISTING CONDITIONS
- ADJUSTED DISCHARGE, PLAN IA-2



VOLUMETRIC DISCHARGE
PLAN 1A-2
SPRING TIDE
RANGE 5

LEGEND

- APPARENT DISCHARGE (PHYSICAL MODEL DATA FOR EXISTING CONDITIONS)
- △ ADJUSTED DISCHARGE (NUMERICAL MODEL DATA FOR EXISTING CONDITIONS)
- ADJUSTED DISCHARGE, PLAN 1A-2

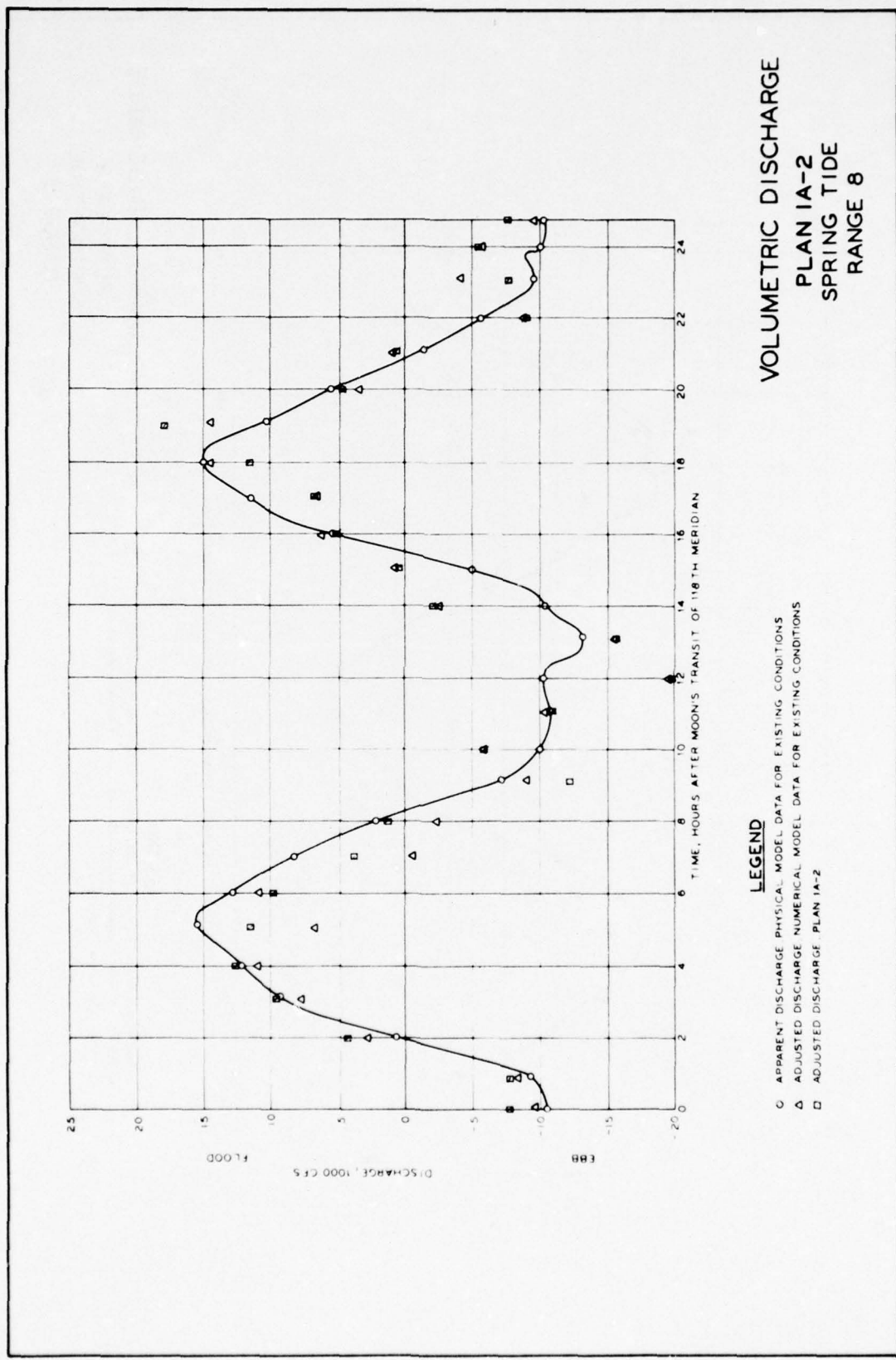
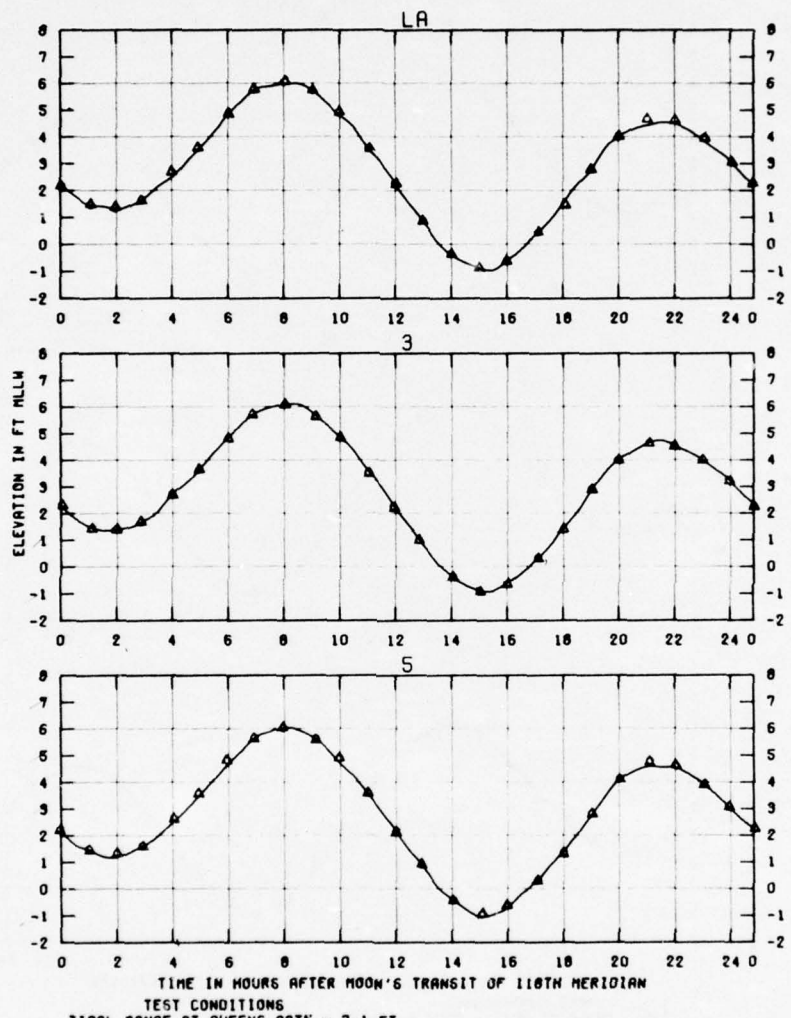


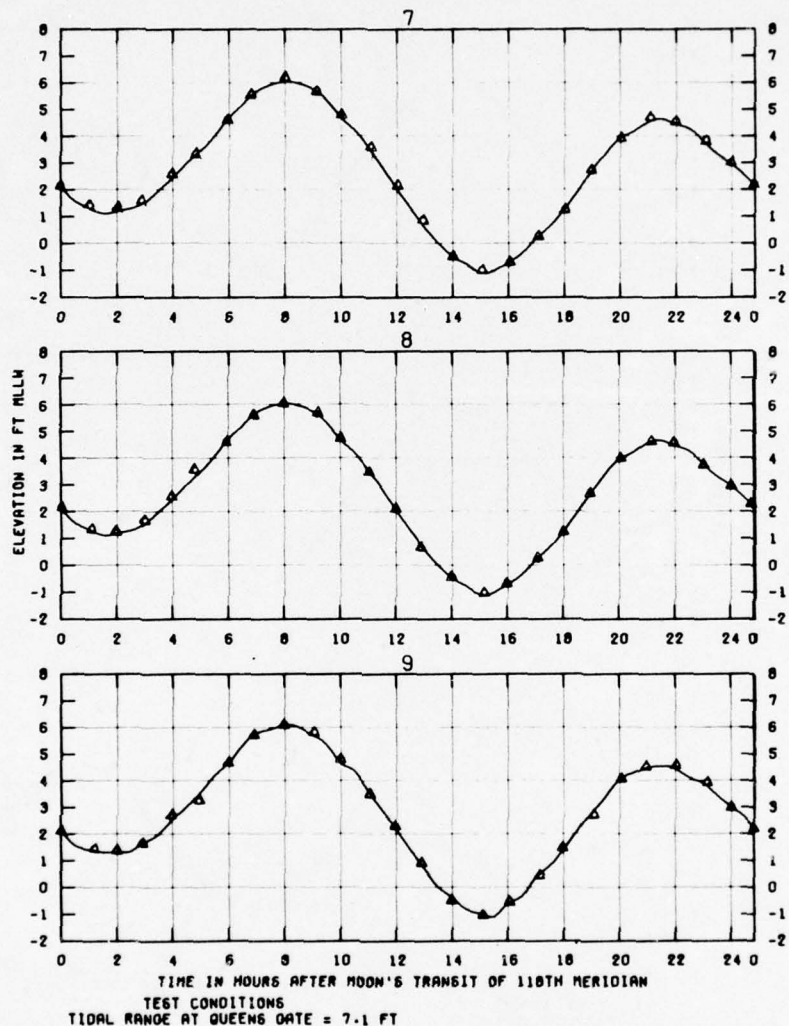
PLATE 60



TIDAL ELEVATIONS
BASE TEST
SPRING TIDE

STATIONS
LA. 3 AND 5

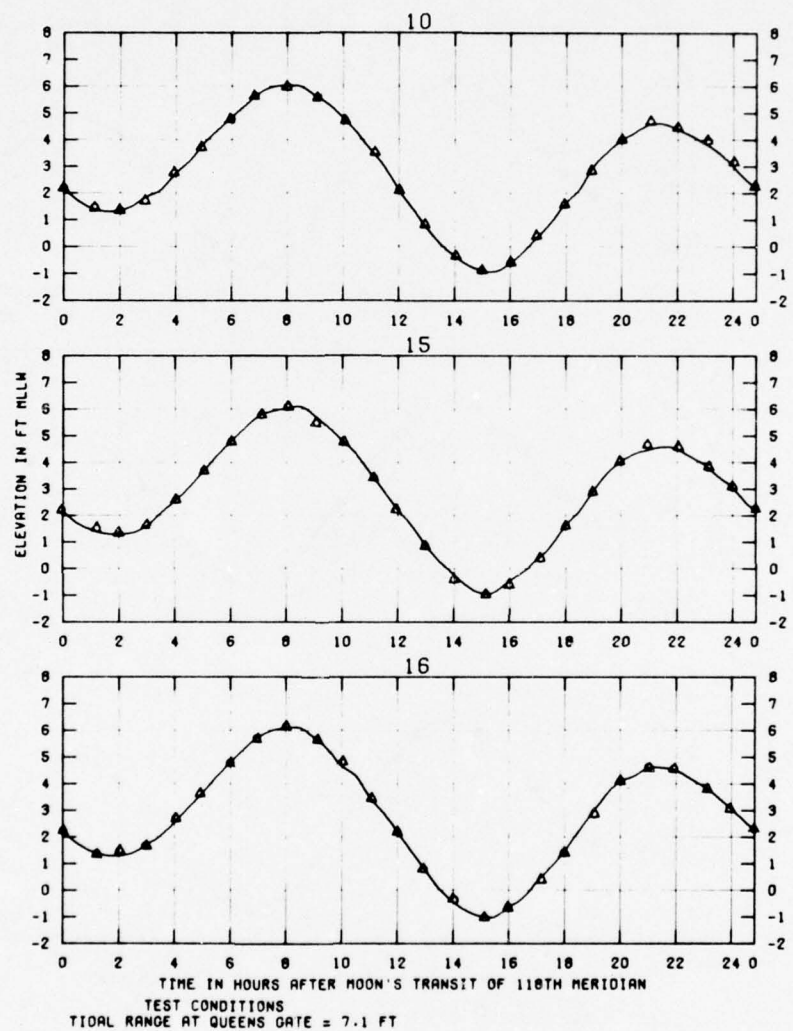
—PHYSICAL MODEL RESULTS, EXISTING CONDITIONS
○DEPTH-AVERAGED NUMERICAL MODEL RESULTS, EXISTING CONDITIONS
△DEPTH-AVERAGED NUMERICAL MODEL RESULTS, SCHEME STFP 2 (600, -82 ft CHANNEL)



TIDAL ELEVATIONS
BASE TEST
SPRING TIDE

STATIONS
7, 8, AND 9

—PHYSICAL MODEL RESULTS, EXISTING CONDITIONS
○DEPTH-AVERAGED NUMERICAL MODEL RESULTS, EXISTING CONDITIONS
△DEPTH-AVERAGED NUMERICAL MODEL RESULTS, SCHEME STPP 2 (600, -82 ft CHANNEL)



TIDAL ELEVATIONS
BASE TEST
SPRING TIDE

STATIONS
10, 15, AND 16

- PHYSICAL MODEL RESULTS, EXISTING CONDITIONS
 ○ DEPTH-AVERAGED NUMERICAL MODEL RESULTS, EXISTING CONDITIONS
 ▲ DEPTH-AVERAGED NUMERICAL MODEL RESULTS, SCHEME STFP 2 (600, -82 ft CHANNEL)

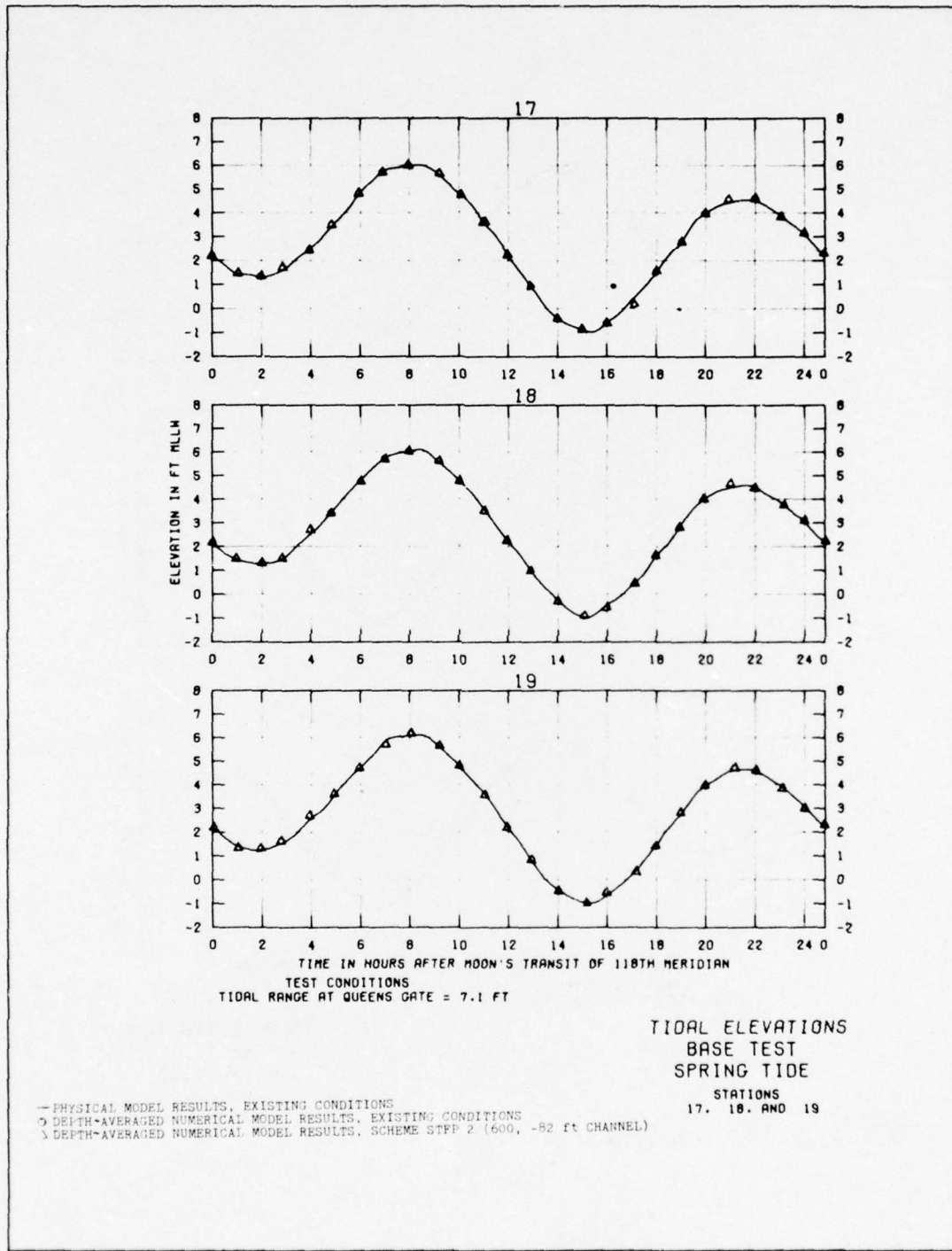
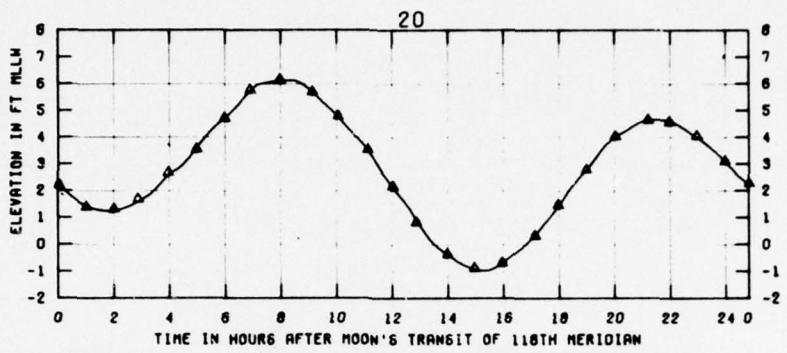


PLATE 64



TEST CONDITIONS
TIDAL RANGE AT QUEENS DATE = 7.1 FT

TIDAL ELEVATIONS
BASE TEST
SPRING TIDE
STATION
20

— PHYSICAL MODEL RESULTS, EXISTING CONDITIONS
○ DEPTH-AVERAGED NUMERICAL MODEL RESULTS, EXISTING CONDITIONS
△ DEPTH-AVERAGED NUMERICAL MODEL RESULTS, SCHEME STPP 2 (600, -52 ft CHANNEL)

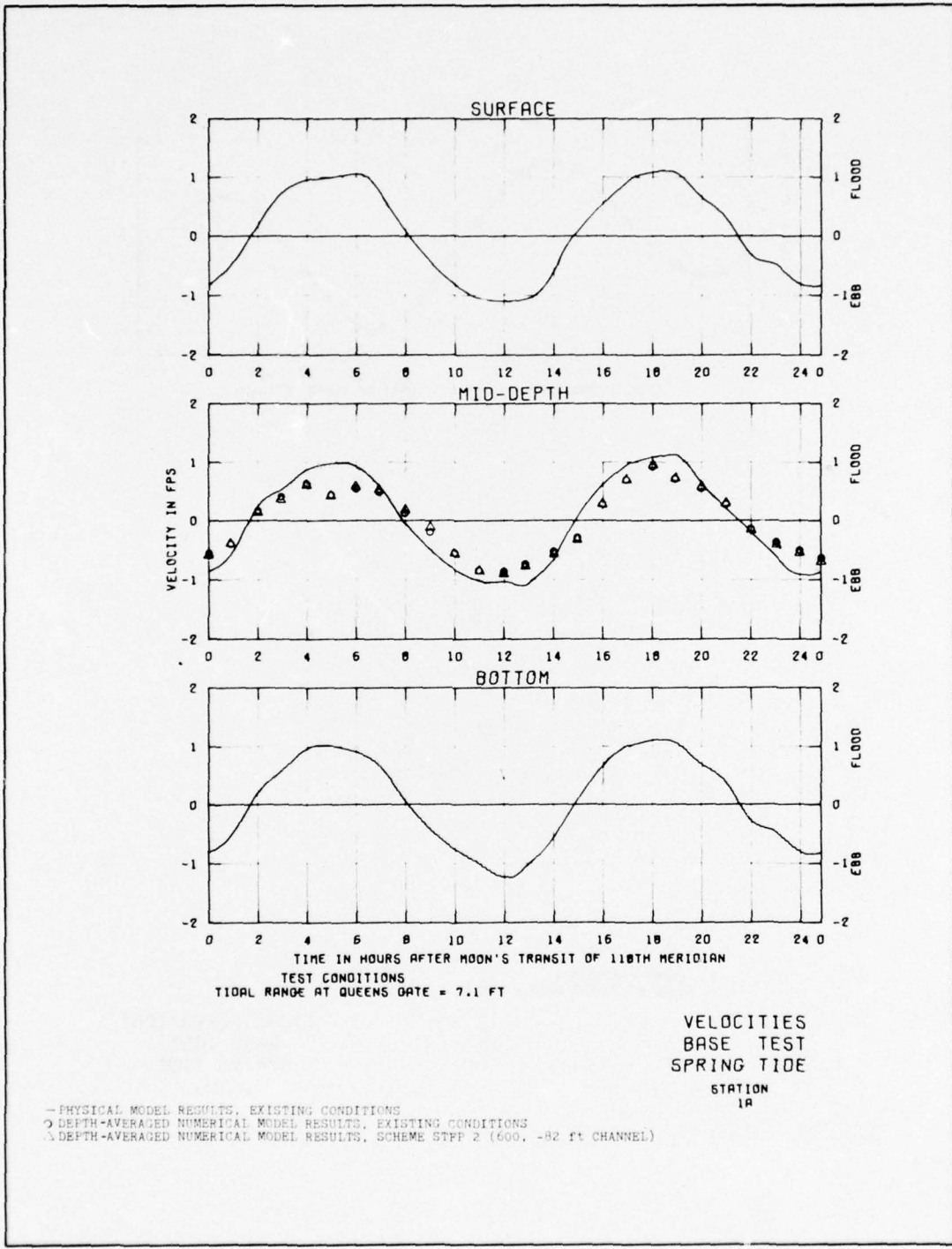
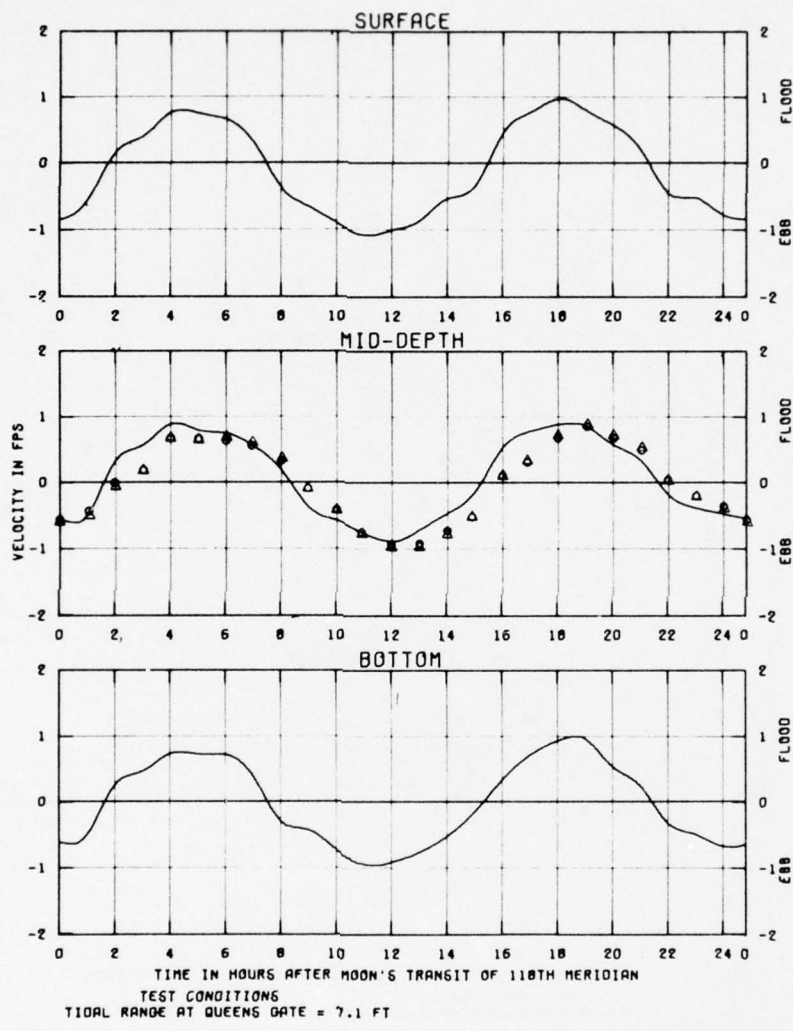


PLATE 66

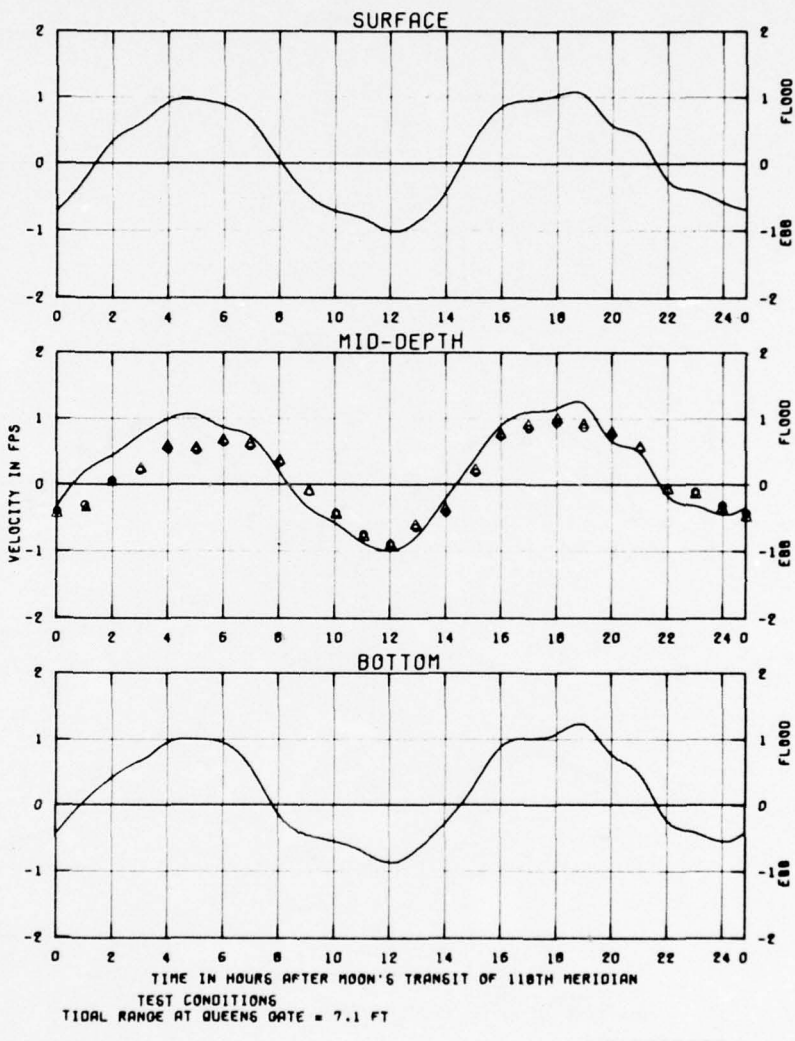


TEST CONDITIONS
TIDAL RANGE AT QUEENS DATE = 7.1 FT

VELOCITIES
BASE TEST
SPRING TIDE

STATION
10

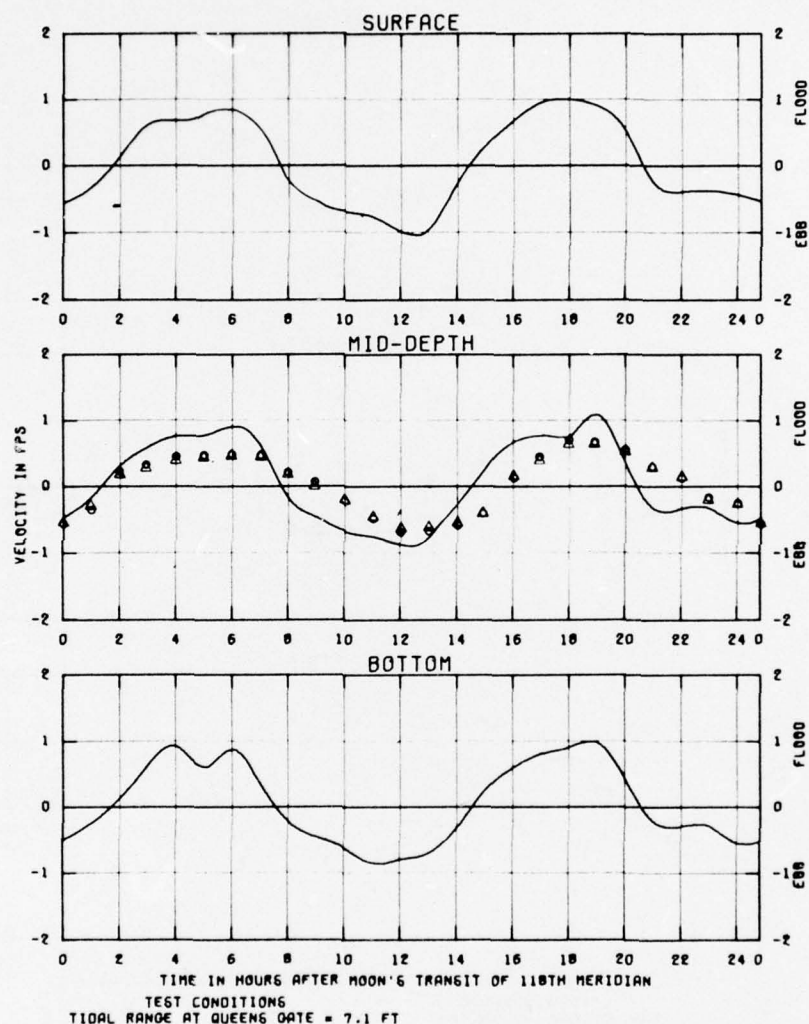
—PHYSICAL MODEL RESULTS, EXISTING CONDITIONS
○DEPTH-AVERAGED NUMERICAL MODEL RESULTS, EXISTING CONDITIONS
△DEPTH-AVERAGED NUMERICAL MODEL RESULTS, SCHEME STPP 2 (600, -82 ft CHANNEL)



VELOCITIES
BASE TEST
SPRING TIDE

STATION
IC

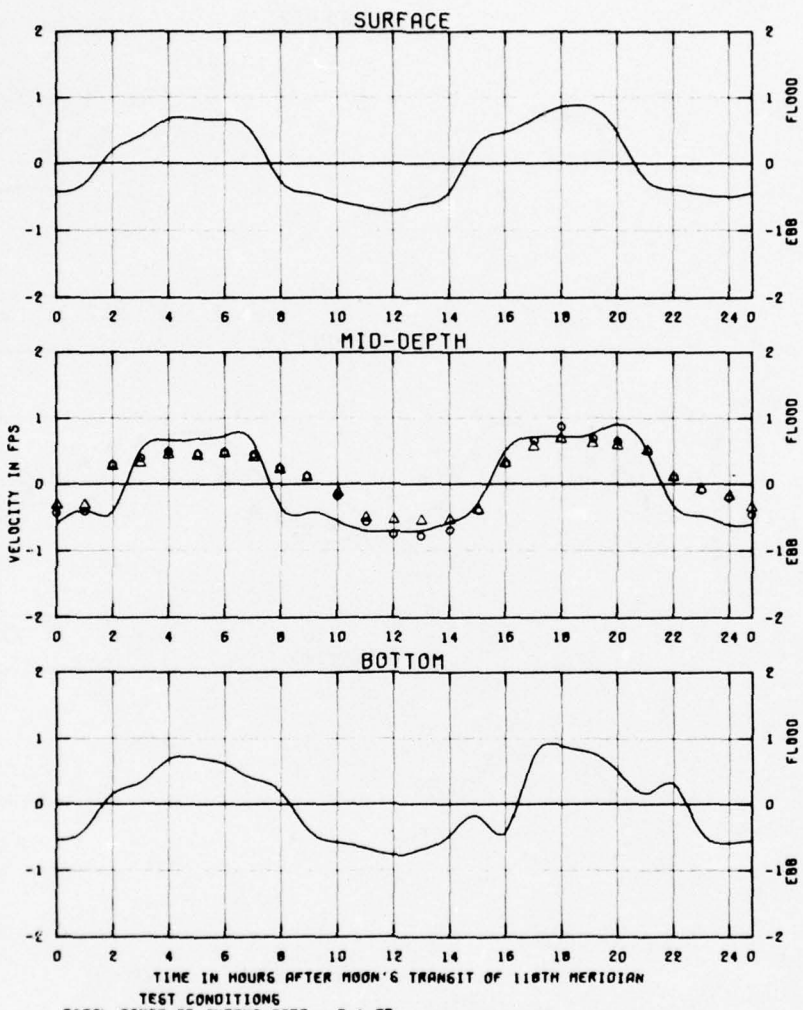
—PHYSICAL MODEL RESULTS, EXISTING CONDITIONS
○ DEPTH-AVERAGED NUMERICAL MODEL RESULTS, EXISTING CONDITIONS
△ DEPTH-AVERAGED NUMERICAL MODEL RESULTS, SCHEME STPP 2 (600, -82 ft CHANNEL)



VELOCITIES
BASE TEST
SPRING TIDE

STATION
20

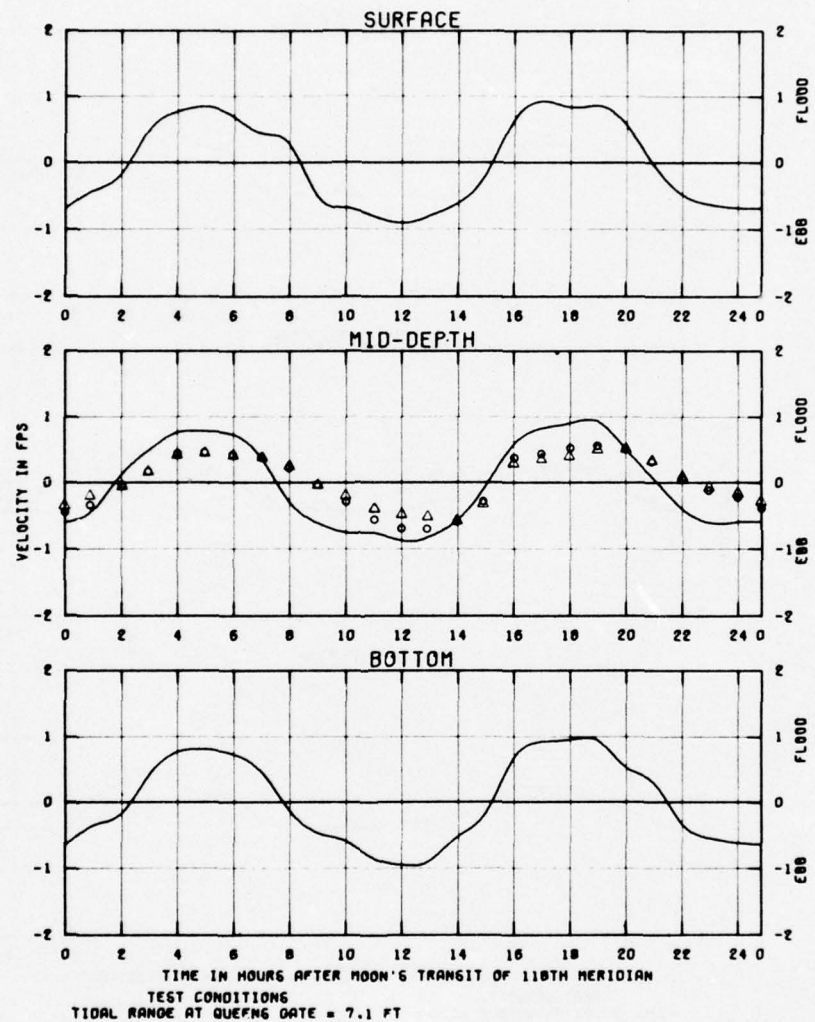
— PHYSICAL MODEL RESULTS, EXISTING CONDITIONS
 ○ DEPTH-AVERAGED NUMERICAL MODEL RESULTS, EXISTING CONDITIONS
 △ DEPTH-AVERAGED NUMERICAL MODEL RESULTS, SCHEME STPP 2 (600, -82 ft CHANNEL)



VELOCITIES
BASE TEST
SPRING TIDE

STATION
2E

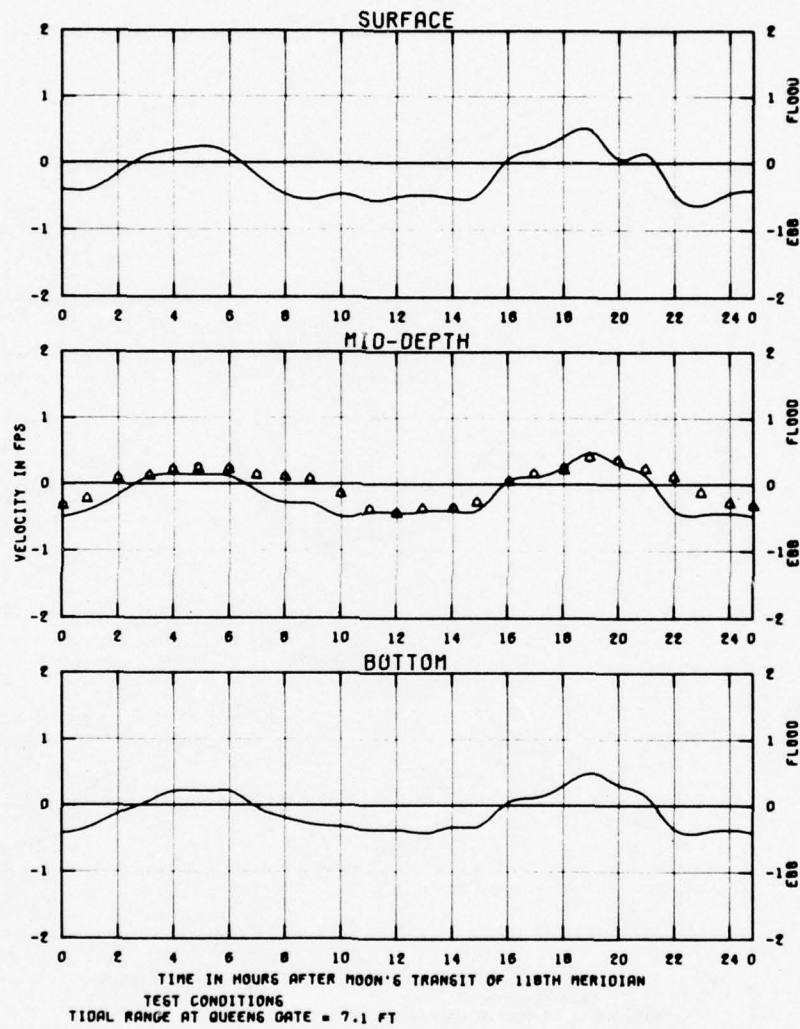
— PHYSICAL MODEL RESULTS, EXISTING CONDITIONS
○ DEPTH-AVERAGED NUMERICAL MODEL RESULTS, EXISTING CONDITIONS
△ DEPTH-AVERAGED NUMERICAL MODEL RESULTS, SCHEME STPP 2 (600, -82 ft CHANNEL)



VELOCITIES
BASE TEST
SPRING TIDE

STATION
2F

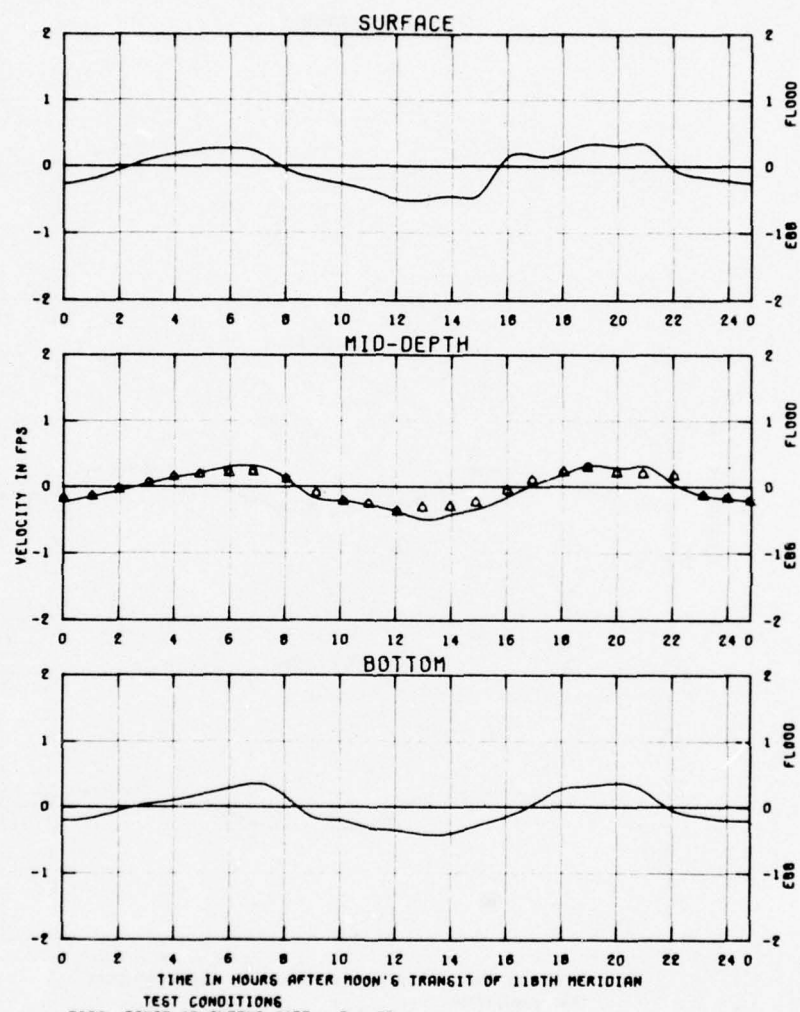
—PHYSICAL MODEL RESULTS, EXISTING CONDITIONS
○ DEPTH-AVERAGED NUMERICAL MODEL RESULTS, EXISTING CONDITIONS
△ DEPTH-AVERAGED NUMERICAL MODEL RESULTS, SCHEME STPP 2 (600, -82 ft CHANNEL)



VELOCITIES
BASE TEST
SPRING TIDE

STATION
30

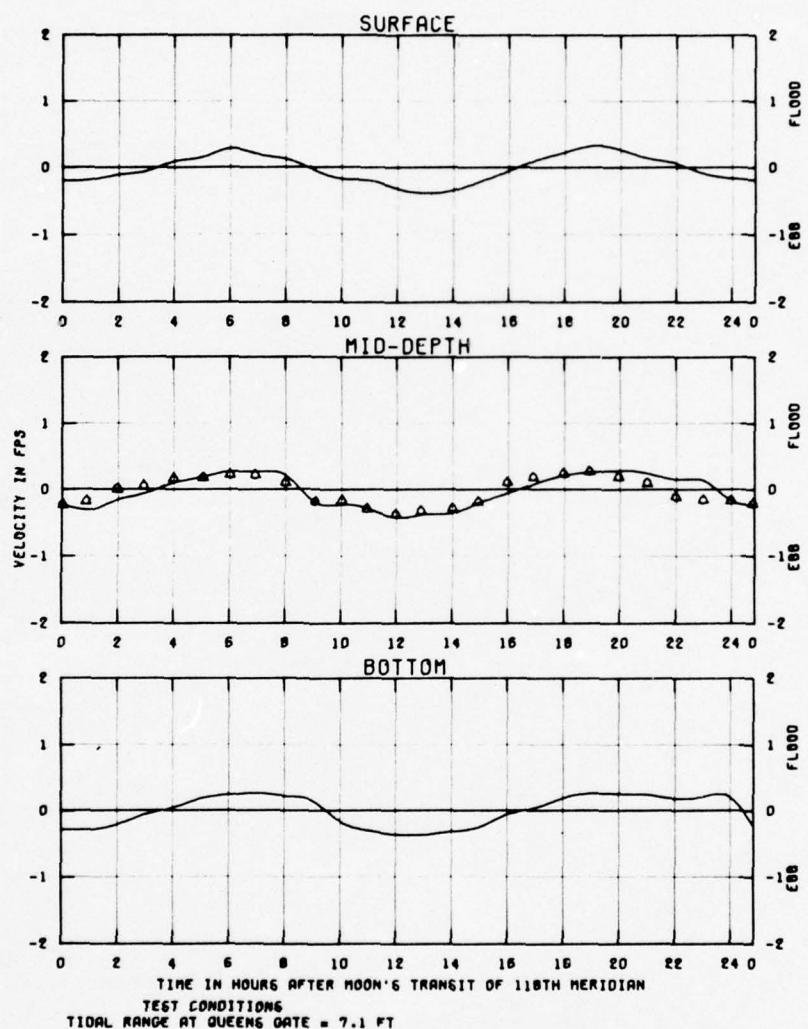
— PHYSICAL MODEL RESULTS, EXISTING CONDITIONS
○ DEPTH-AVERAGED NUMERICAL MODEL RESULTS, EXISTING CONDITIONS
△ DEPTH-AVERAGED NUMERICAL MODEL RESULTS, SCHEME STFP 2 (600, -82 ft CHANNEL)



VELOCITIES
BASE TEST
SPRING TIDE

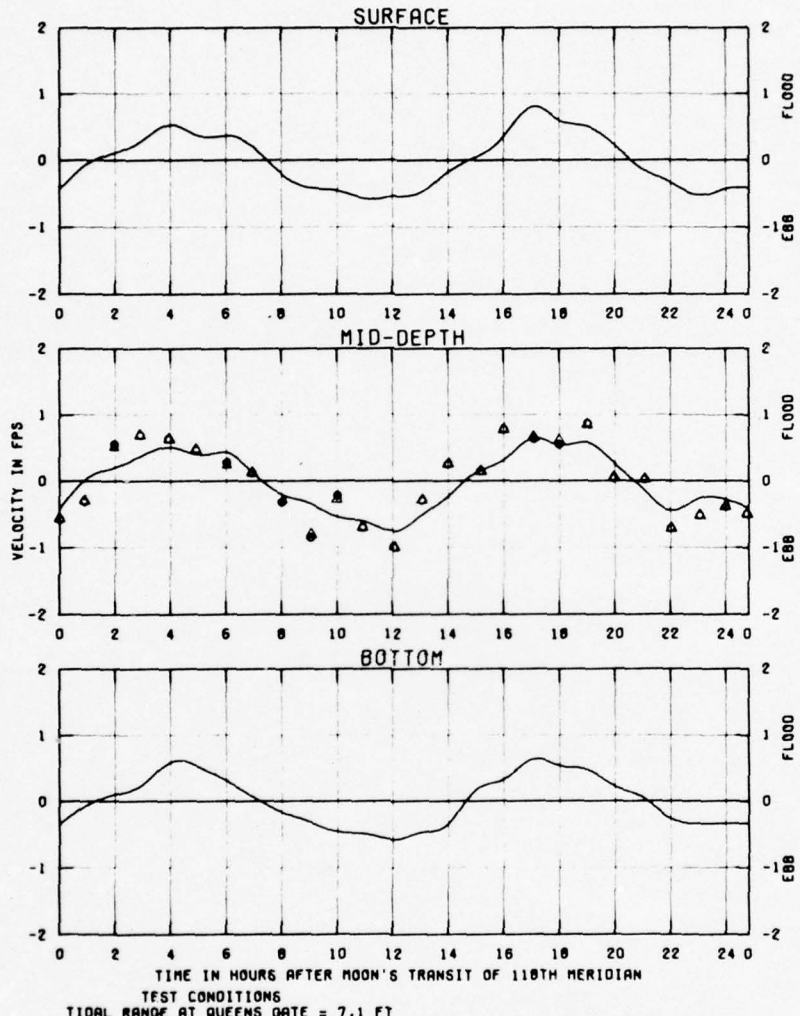
STATION
3M

— PHYSICAL MODEL RESULTS, EXISTING CONDITIONS
◊ DEPTH-AVERAGED NUMERICAL MODEL RESULTS, EXISTING CONDITIONS
× DEPTH-AVERAGED NUMERICAL MODEL RESULTS, SCHEME STPP 2 (600, -82 ft CHANNEL)



VELOCITIES
BASE TEST
SPRING TIDE
STATION
31

- PHYSICAL MODEL RESULTS, EXISTING CONDITIONS
○ DEPTH-AVERAGED NUMERICAL MODEL RESULTS, EXISTING CONDITIONS
△ DEPTH-AVERAGED NUMERICAL MODEL RESULTS, SCHEME STPP 2 (600, -82 ft CHANNEL)



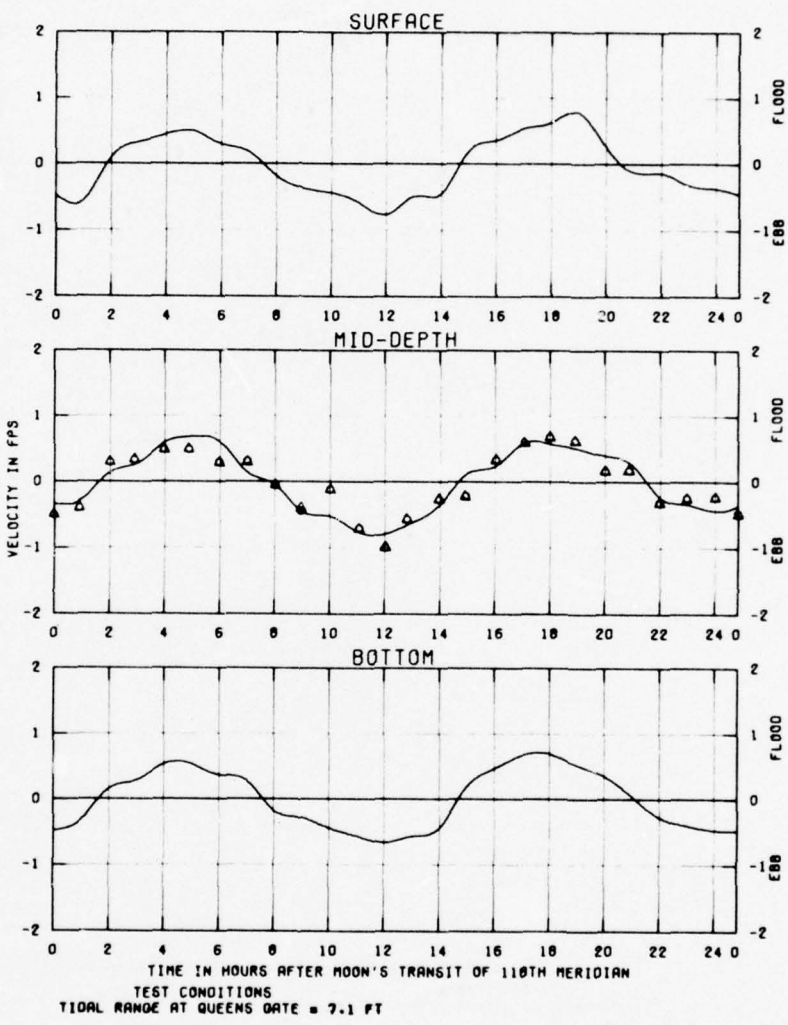
TEST CONDITIONS
TIDAL RANGE AT QUEENS GATE = 7.1 FT

VELOCITIES
BASE TEST
SPRING TIDE

STATION
SL

— PHYSICAL MODEL RESULTS, EXISTING CONDITIONS
○ DEPTH-AVERAGED NUMERICAL MODEL RESULTS, EXISTING CONDITIONS
△ DEPTH-AVERAGED NUMERICAL MODEL RESULTS, SCHEME STFP 2 (600, -82 ft CHANNEL)

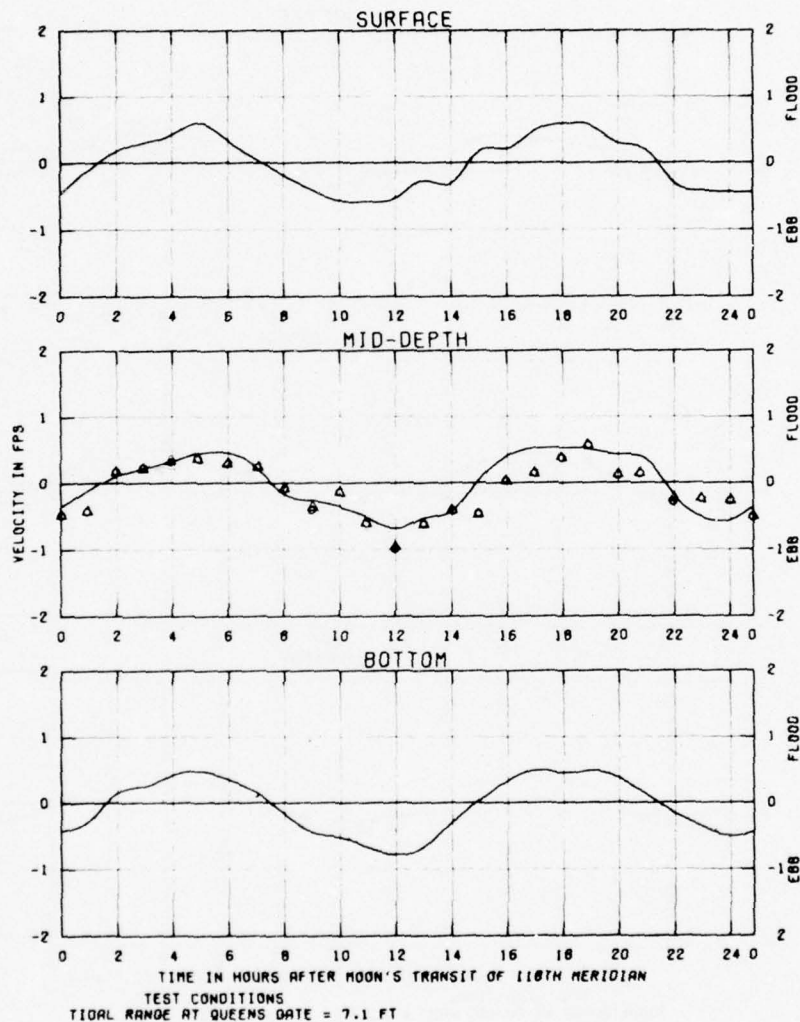
PLATE 75



VELOCITIES
BASE TEST
SPRING TIDE

STATION
SM

— PHYSICAL MODEL RESULTS, EXISTING CONDITIONS
○ DEPTH-AVERAGED NUMERICAL MODEL RESULTS, EXISTING CONDITIONS
△ DEPTH-AVERAGED NUMERICAL MODEL RESULTS, SCHEME STPP 2 (600, -82 ft CHANNEL)

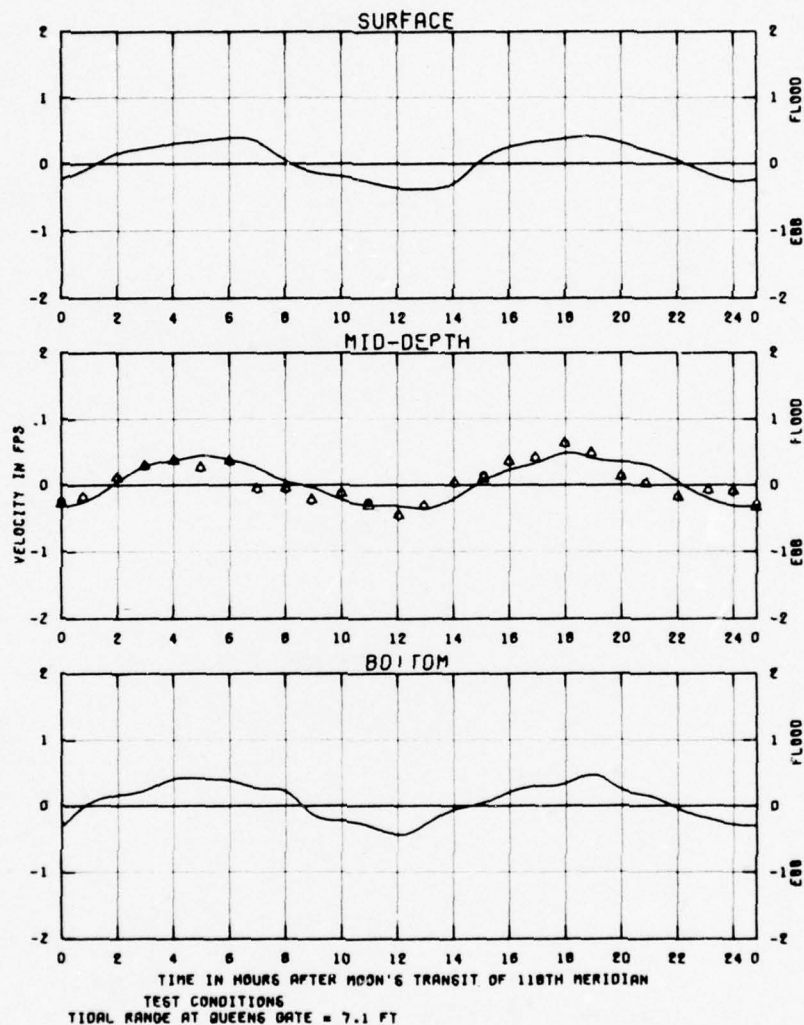


TEST CONDITIONS
TIDAL RANGE AT QUEENS DATE = 7.1 FT

VELOCITIES
BASE TEST
SPRING TIDE

STATION
SM

— PHYSICAL MODEL RESULTS, EXISTING CONDITIONS
○ DEPTH-AVERAGED NUMERICAL MODEL RESULTS, EXISTING CONDITIONS
△ DEPTH-AVERAGED NUMERICAL MODEL RESULTS, SCHEWE STEP 2 (600, -82 ft CHANNEL)



VELOCITIES
BASE TEST
SPRING TIDE
STATION
BX

— PHYSICAL MODEL RESULTS, EXISTING CONDITIONS
 ○ DEPTH-AVERAGED NUMERICAL MODEL RESULTS, EXISTING CONDITIONS
 △ DEPTH-AVERAGED NUMERICAL MODEL RESULTS, SCHEME STPP 2 (600, -82 ft CHANNEL)

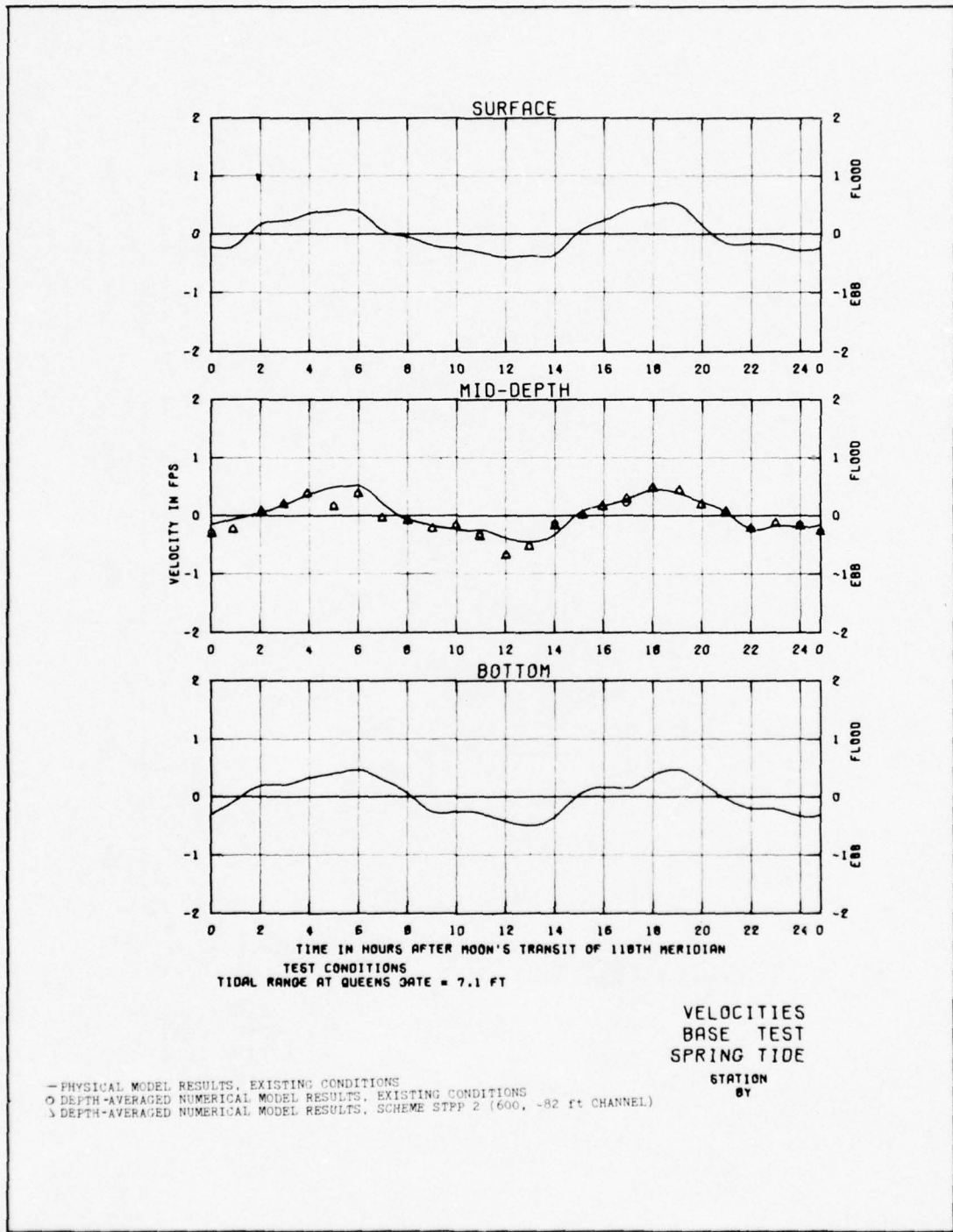
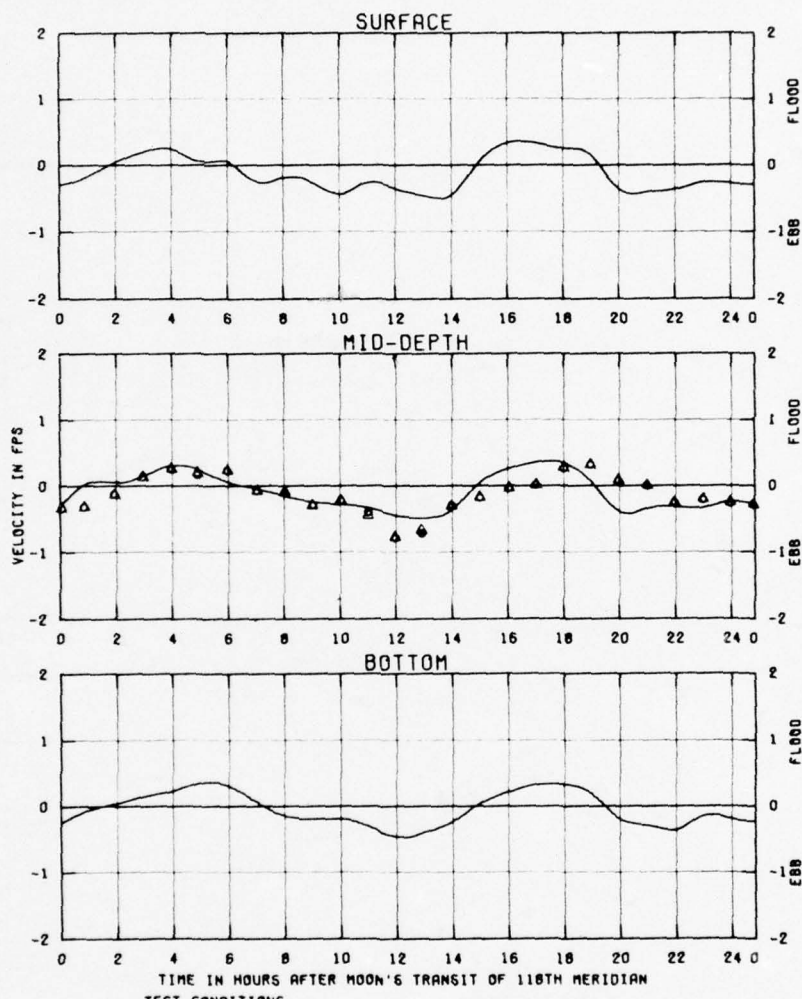


PLATE 79



TEST CONDITIONS
TIDAL RANGE AT QUEENS GATE = 7.1 FT

VELOCITIES
BASE TEST
SPRING TIDE

STATION
BZ

- PHYSICAL MODEL RESULTS, EXISTING CONDITIONS
○ DEPTH-AVERAGED NUMERICAL MODEL RESULTS, EXISTING CONDITIONS
△ DEPTH-AVERAGED NUMERICAL MODEL RESULTS, SCHEME STFF 2 (600, -82 ft CHANNEL)

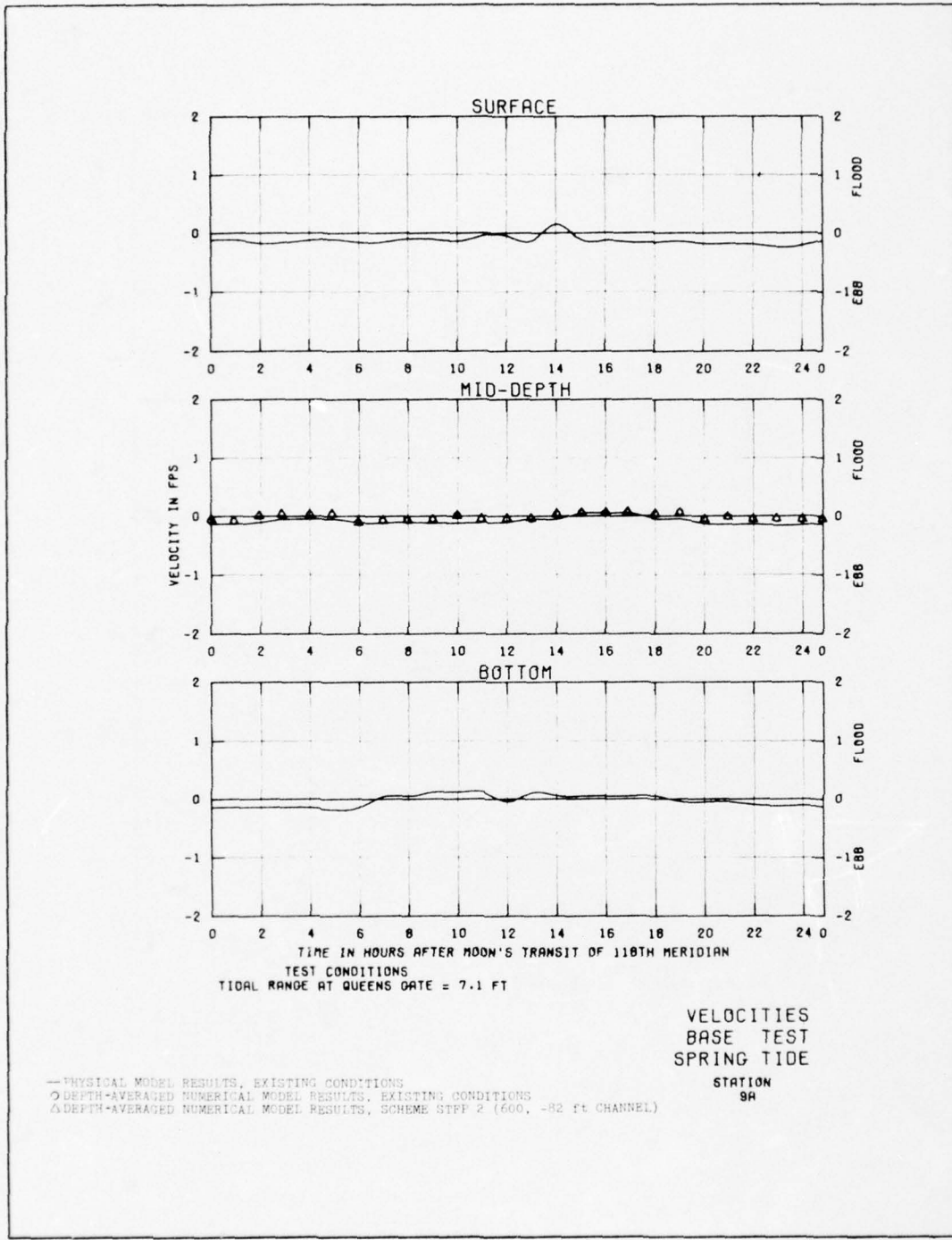
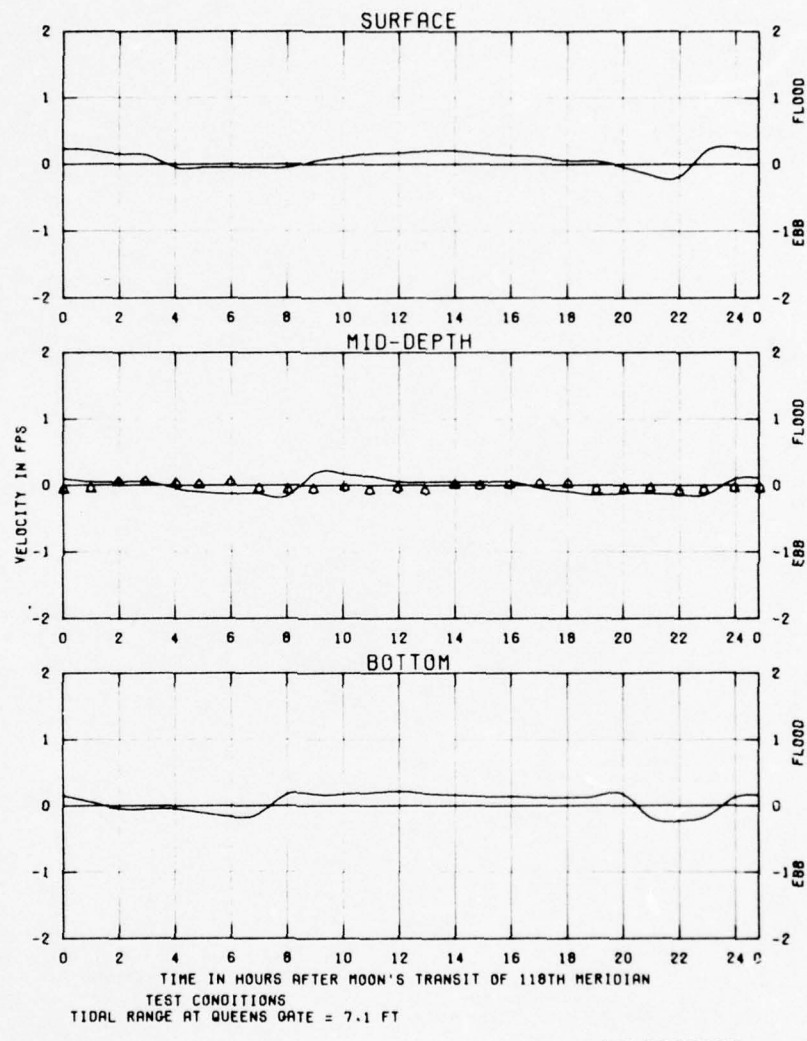


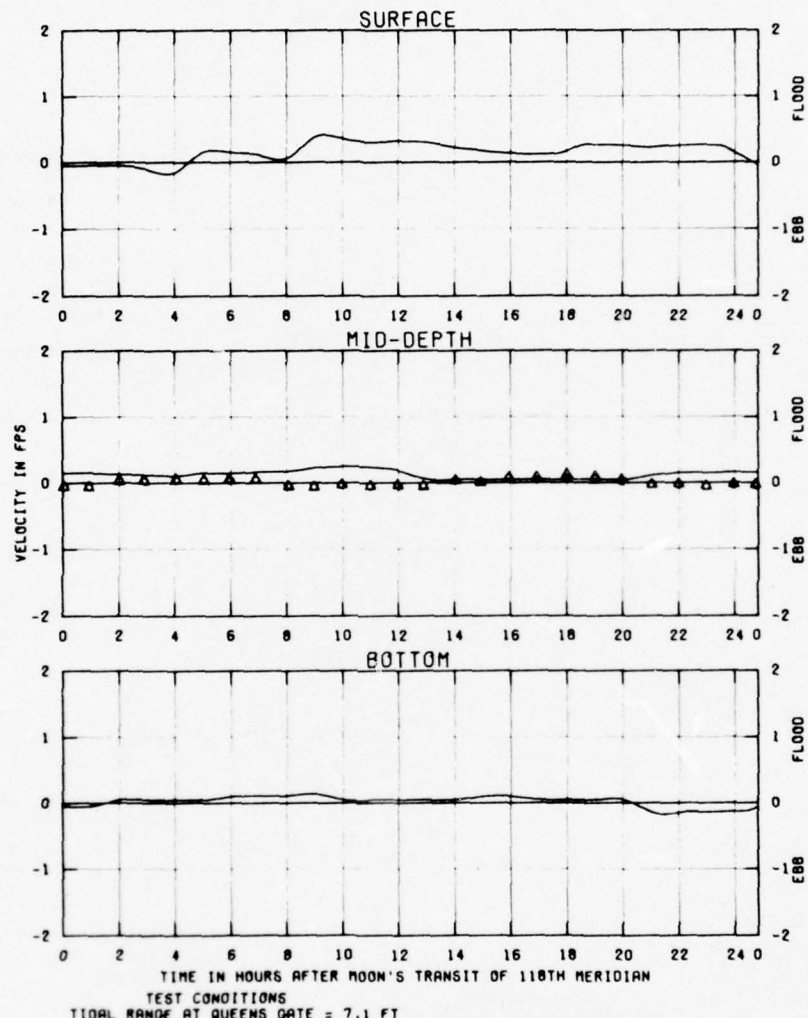
PLATE 81



VELOCITIES
BASE TEST
SPRING TIDE

STATION
98

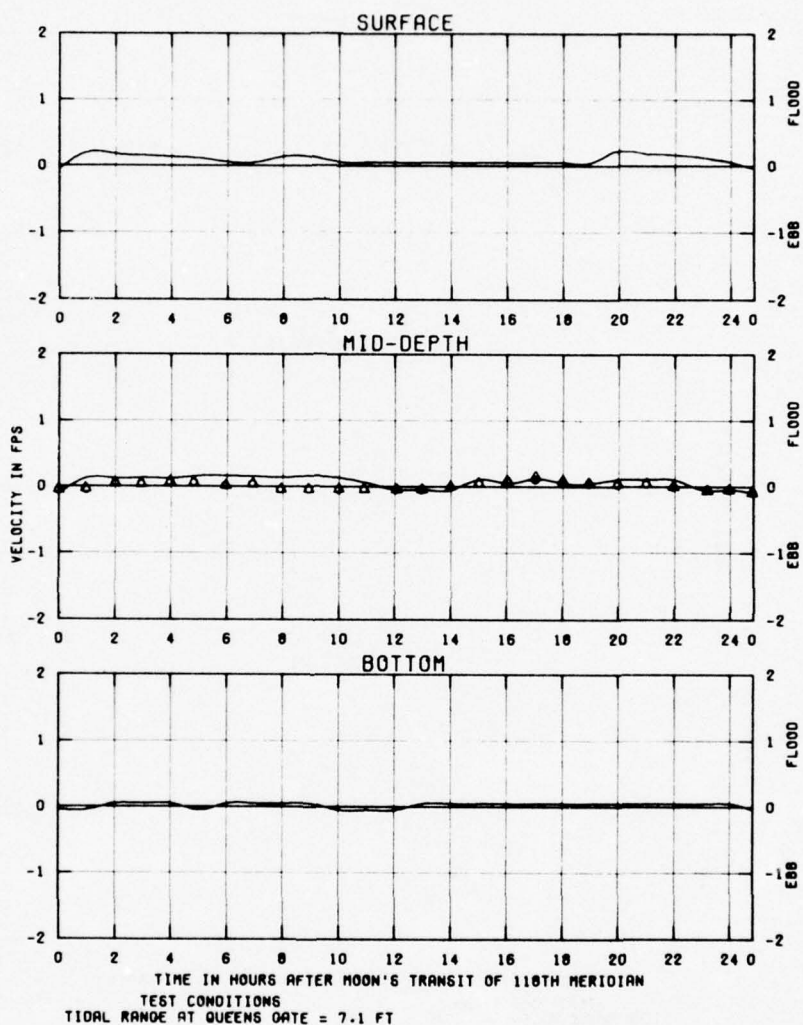
— PHYSICAL MODEL RESULTS, EXISTING CONDITIONS
 ○ DEPTH-AVERAGED NUMERICAL MODEL RESULTS, EXISTING CONDITIONS
 ▲ DEPTH-AVERAGED NUMERICAL MODEL RESULTS, SCHEME STPP 2 (600, -82 ft CHANNEL)



VELOCITIES
BASE TEST
SPRING TIDE

STATION
9C

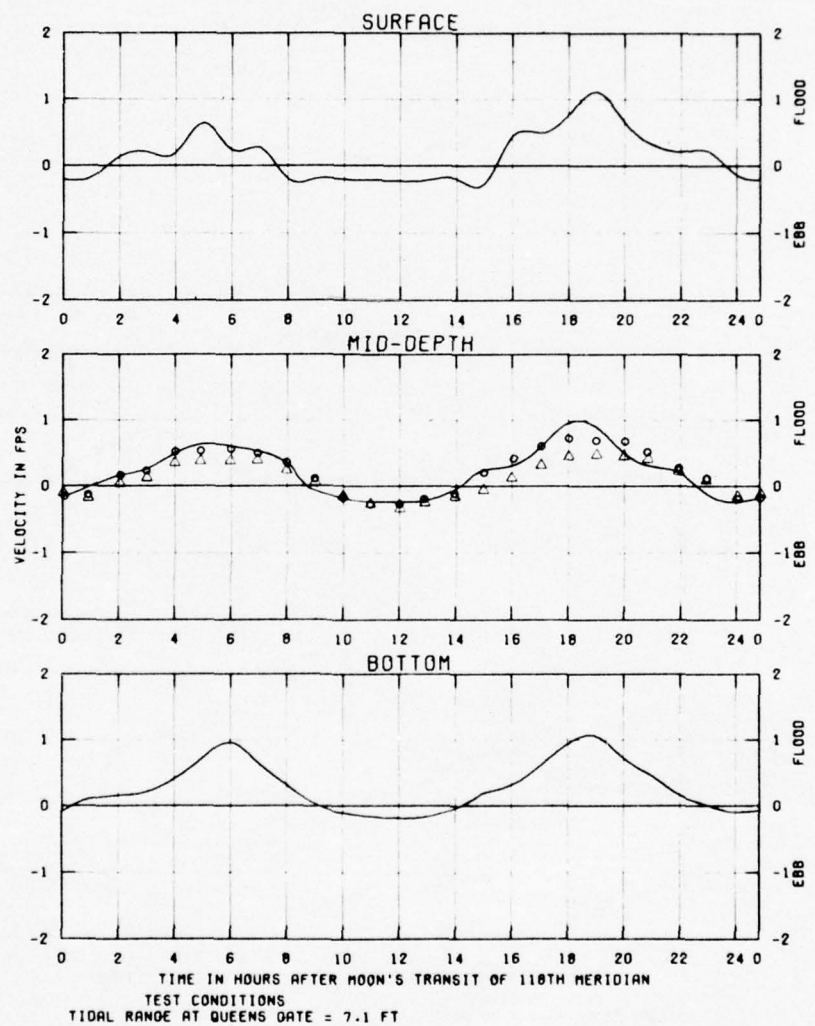
— PHYSICAL MODEL RESULTS, EXISTING CONDITIONS
○ DEPTH-AVERAGED NUMERICAL MODEL RESULTS, EXISTING CONDITIONS
△ DEPTH-AVERAGED NUMERICAL MODEL RESULTS, SCHEME STEP 2 (600, -82 ft CHANNEL)



VELOCITIES
BASE TEST
SPRING TIDE

STATION
90

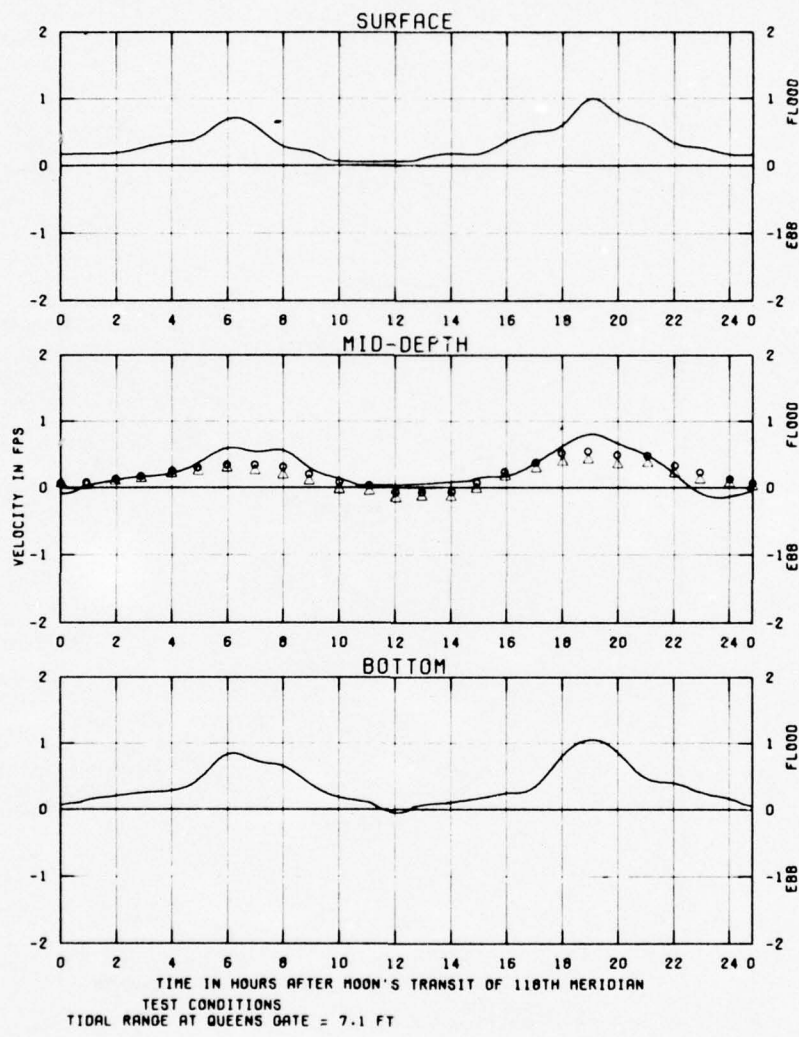
—PHYSICAL MODEL RESULTS, EXISTING CONDITIONS
○ DEPTH-AVERAGED NUMERICAL MODEL RESULTS, EXISTING CONDITIONS
△ DEPTH-AVERAGED NUMERICAL MODEL RESULTS, SCHEME STEF 2 (600, -82 ft CHANNEL)



VELOCITIES
BASE TEST
SPRING TIDE

STATION
10R

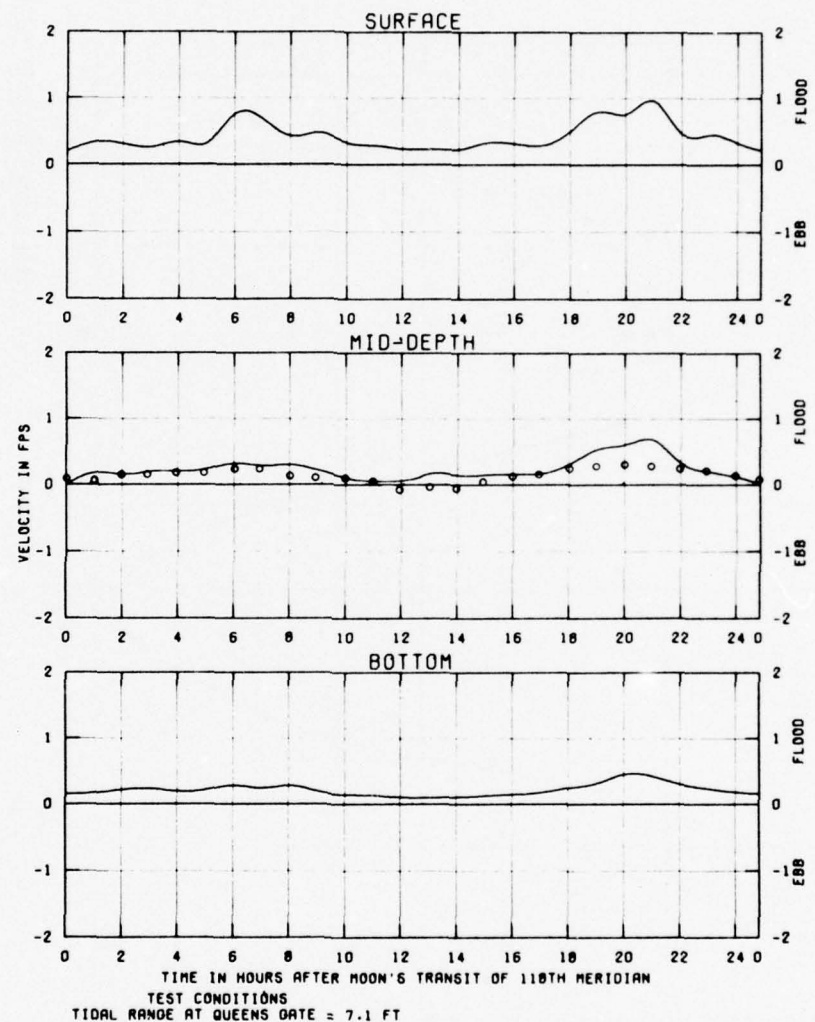
— PHYSICAL MODEL RESULTS, EXISTING CONDITIONS
○ DEPTH-AVERAGED NUMERICAL MODEL RESULTS, EXISTING CONDITIONS
△ DEPTH-AVERAGED NUMERICAL MODEL RESULTS, SCHEME STPP 2 (600, -82 ft CHANNEL)



VELOCITIES
BASE TEST
SPRING TIDE

STATION
108

— PHYSICAL MODEL RESULTS, EXISTING CONDITIONS
○ DEPTH-AVERAGED NUMERICAL MODEL RESULTS, EXISTING CONDITIONS
△ DEPTH-AVERAGED NUMERICAL MODEL RESULTS, SCHEME STPP 2 (600, -82 ft CHANNEL)



VELOCITIES
BASE TEST
SPRING TIDE

STATION
10C

— PHYSICAL MODEL RESULTS, EXISTING CONDITIONS
 ○ DEPTH-AVERAGED NUMERICAL MODEL RESULTS, EXISTING CONDITIONS
 △ DEPTH-AVERAGED NUMERICAL MODEL RESULTS, SCHEME STPP 2 (600, -82 ft CHANNEL)

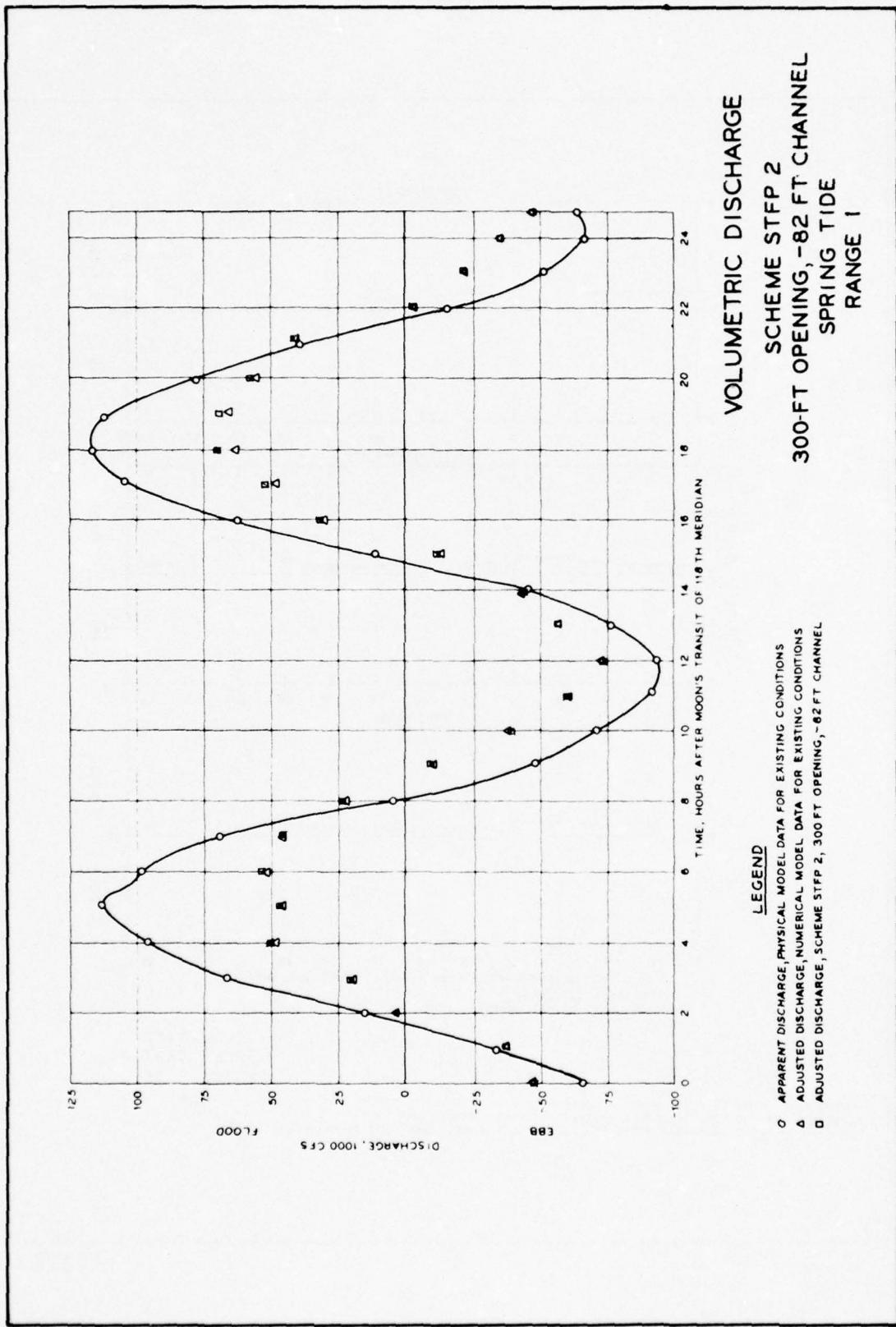
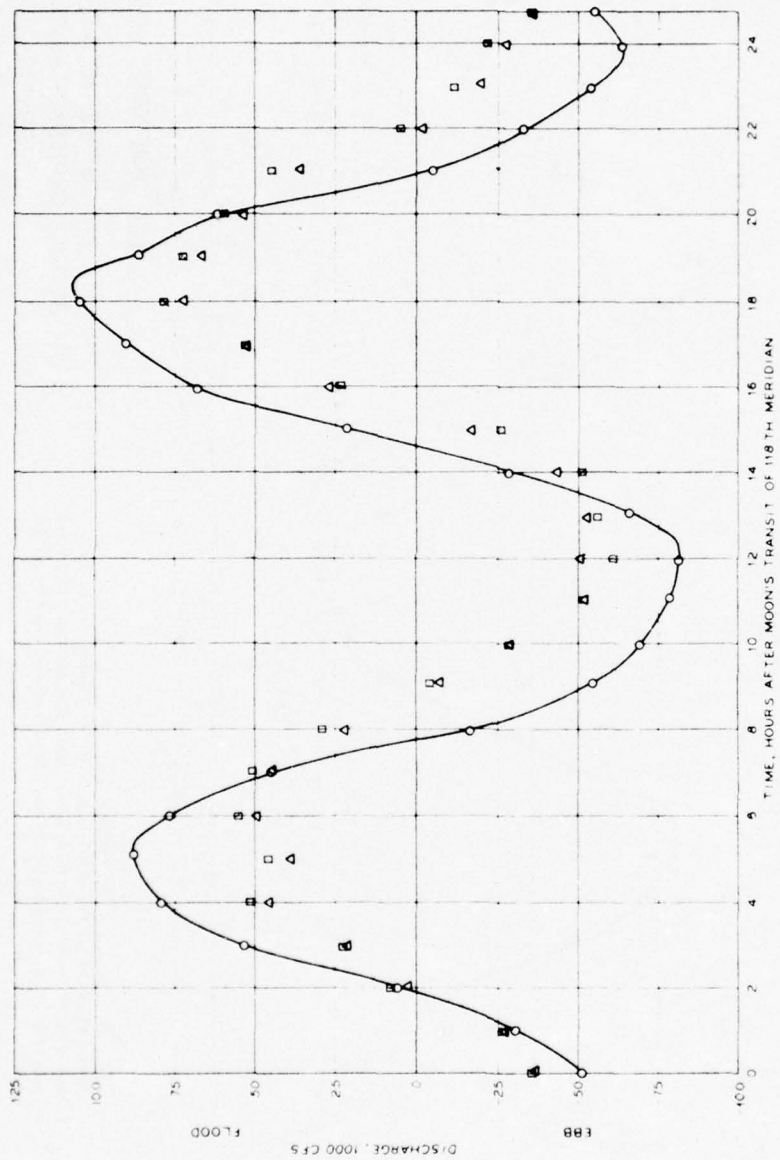


PLATE 88



VOLUMETRIC DISCHARGE

SCHEME STFP 2
300-FT OPENING, -82 FT CHANNEL
SPRING TIDE
RANGE 2

LEGEND

- APPARENT DISCHARGE, PHYSICAL MODEL DATA FOR EXISTING CONDITIONS
- △ ADJUSTED DISCHARGE, NUMERICAL MODEL DATA FOR EXISTING CONDITIONS
- ADJUSTED DISCHARGE, SCHEME STFP 2, 300 FT OPENING, -82 FT CHANNEL

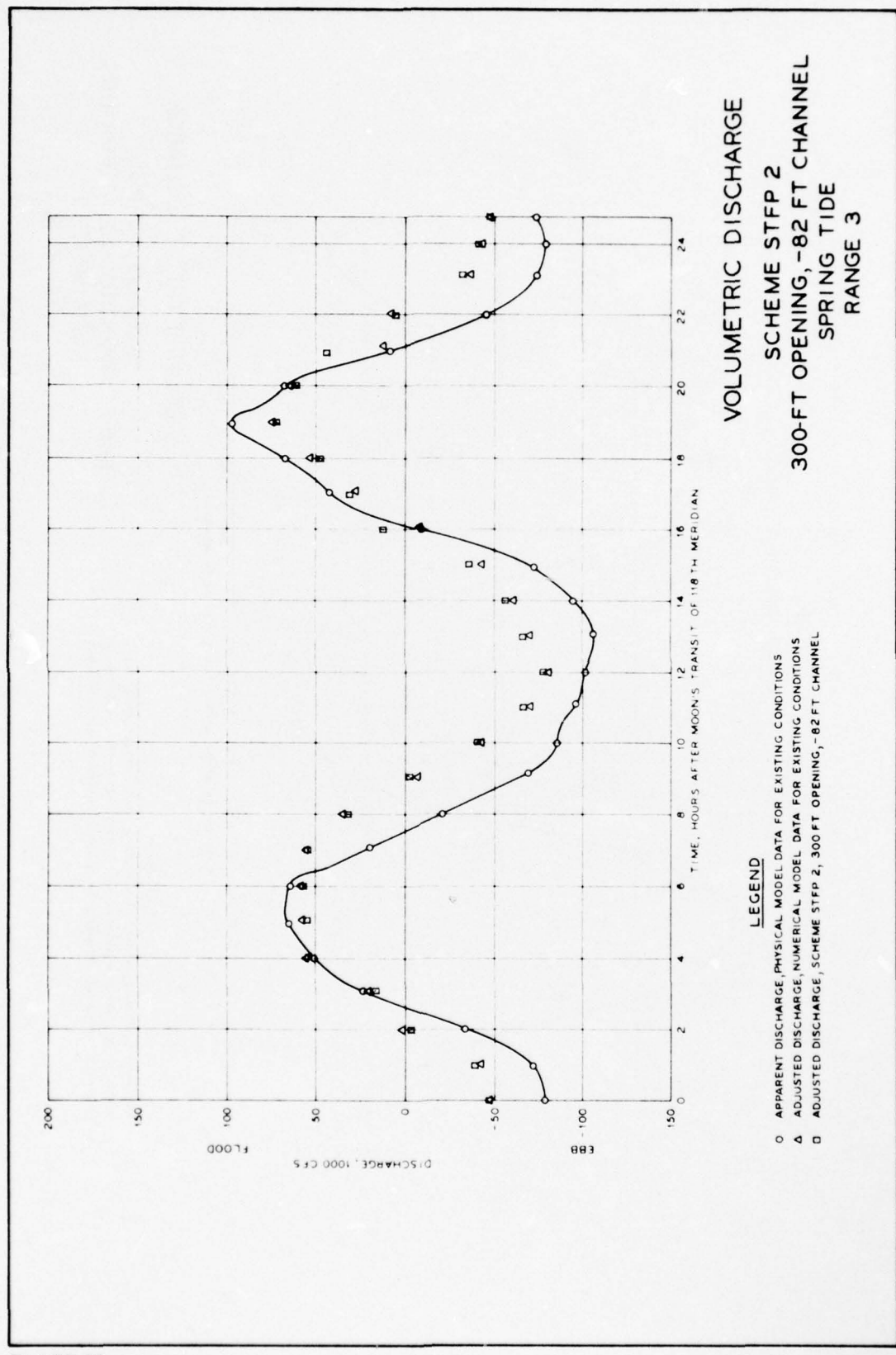
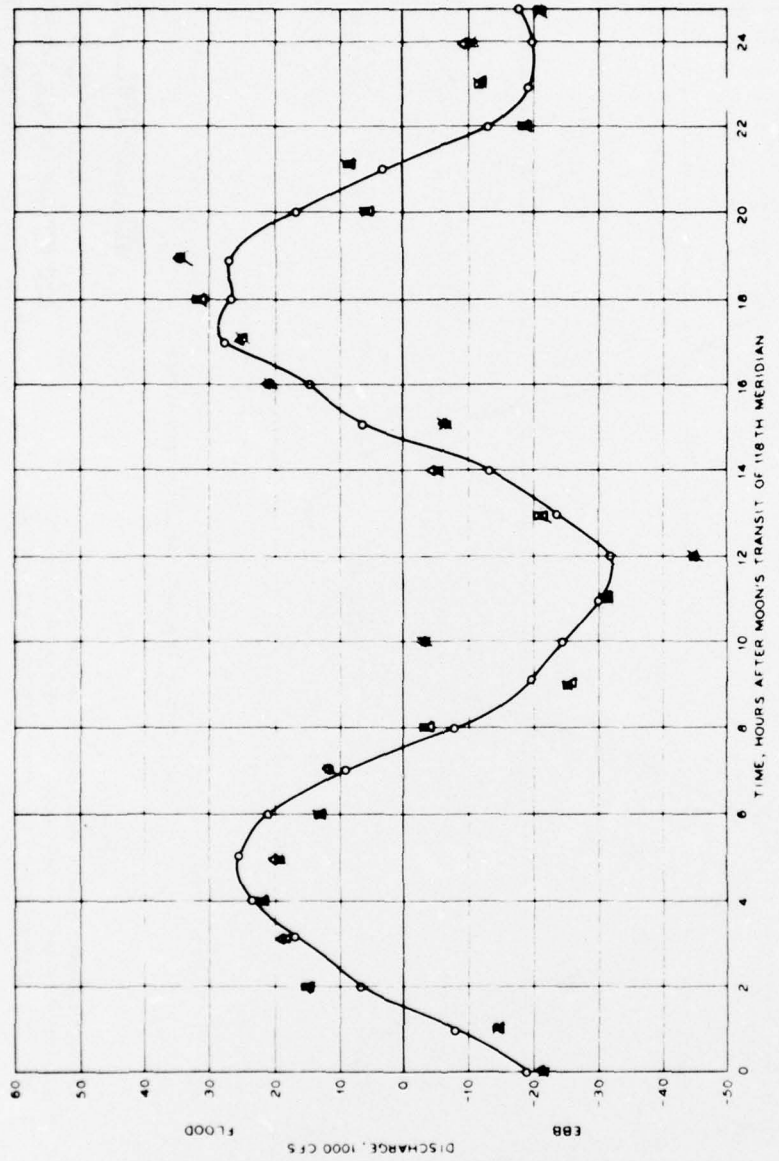


PLATE 90



VOLUMETRIC DISCHARGE

SCHEME STFP 2
300-FT OPENING, -82 FT CHANNEL
SPRING TIDE
RANGE 5

LEGEND

- APPARENT DISCHARGE, PHYSICAL MODEL DATA FOR EXISTING CONDITIONS
- ▲ ADJUSTED DISCHARGE, NUMERICAL MODEL DATA FOR EXISTING CONDITIONS
- ADJUSTED DISCHARGE, SCHEME STFP 2, 300 FT OPENING, -82 FT CHANNEL

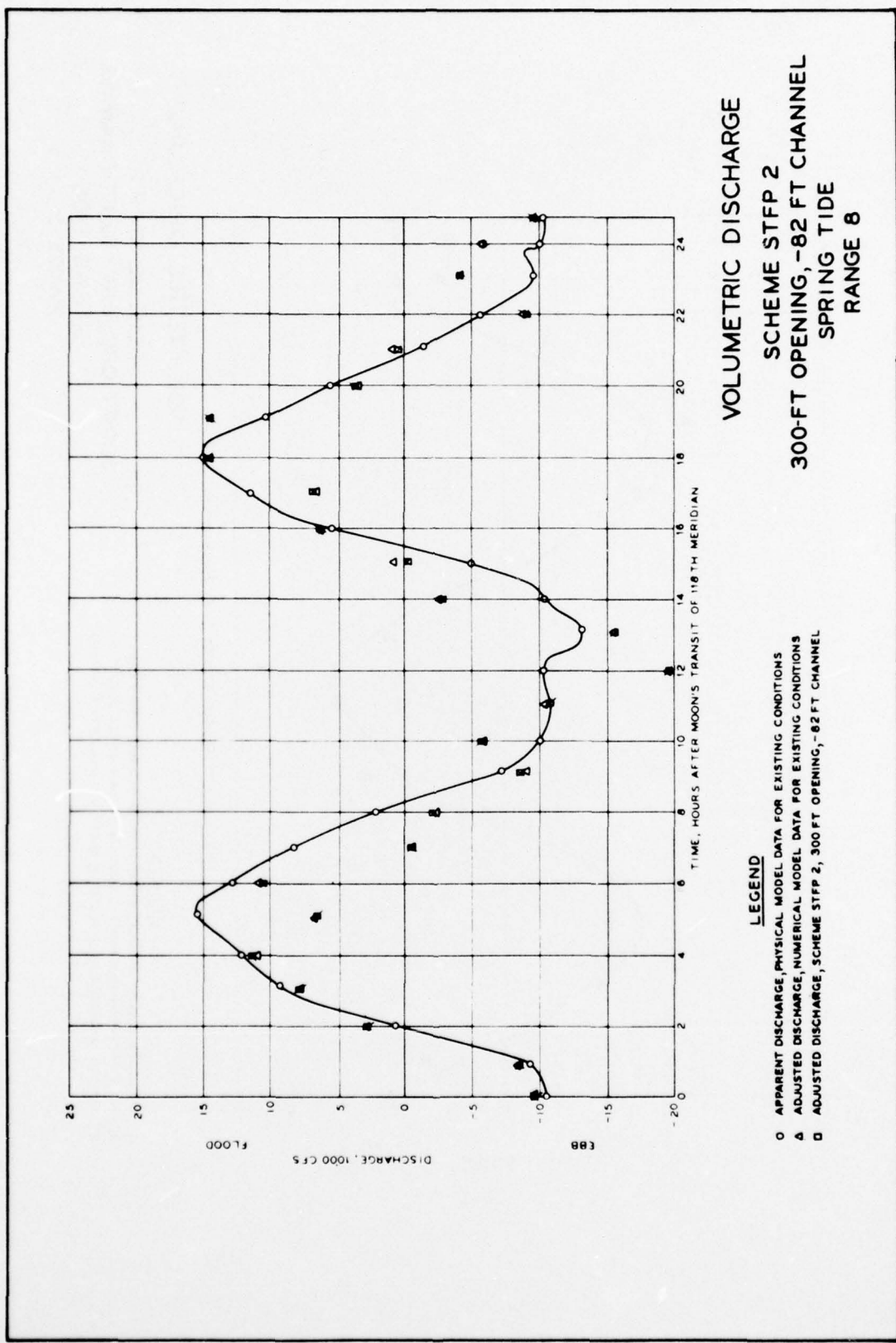
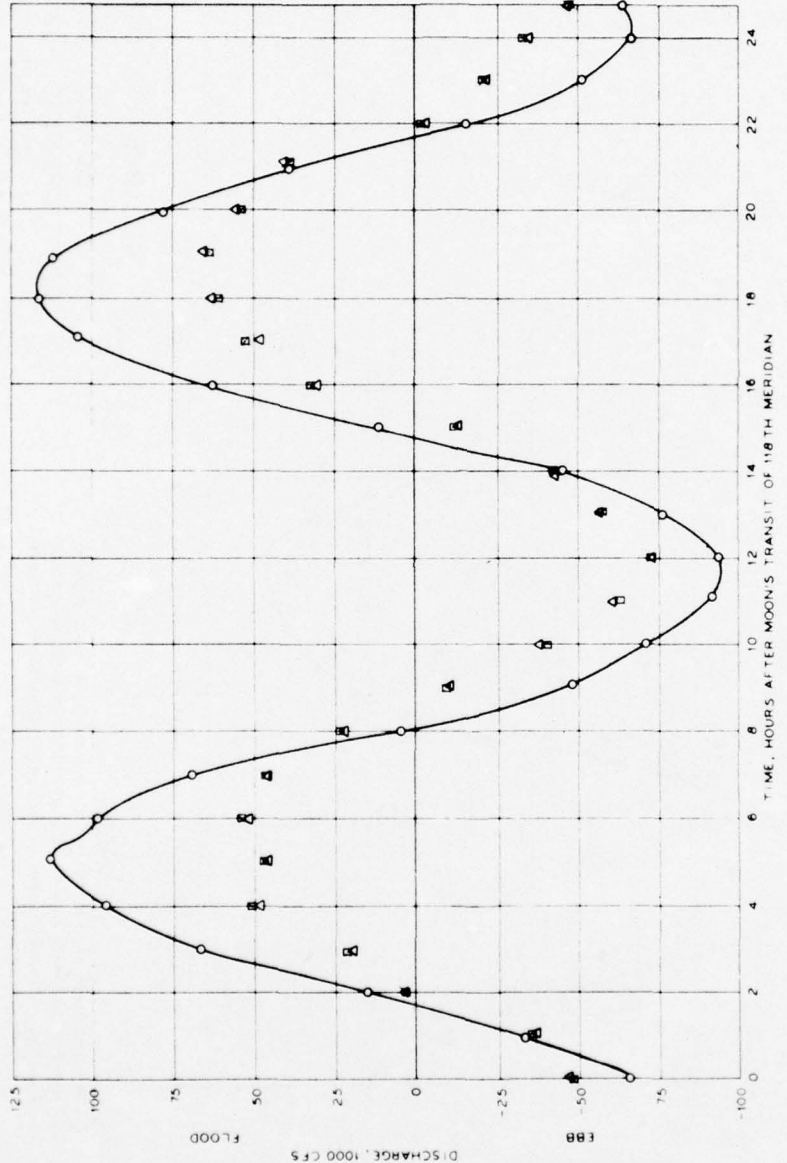


PLATE 92



VOLUMETRIC DISCHARGE
SCHEME STFP 2
-FT OPENING, -82 FT CHANNEL
SPRING TIDE
RANGE 1

LEGEND

- APPARENT DISCHARGE, PHYSICAL MODEL DATA FOR EXISTING CONDITIONS
 - ADJUSTED DISCHARGE, NUMERICAL MODEL DATA FOR EXISTING CONDITIONS
 - ADJUSTED DISCHARGE, SCHEME STEP 2, 600 FT OPENING, -82 FT CHANNEL

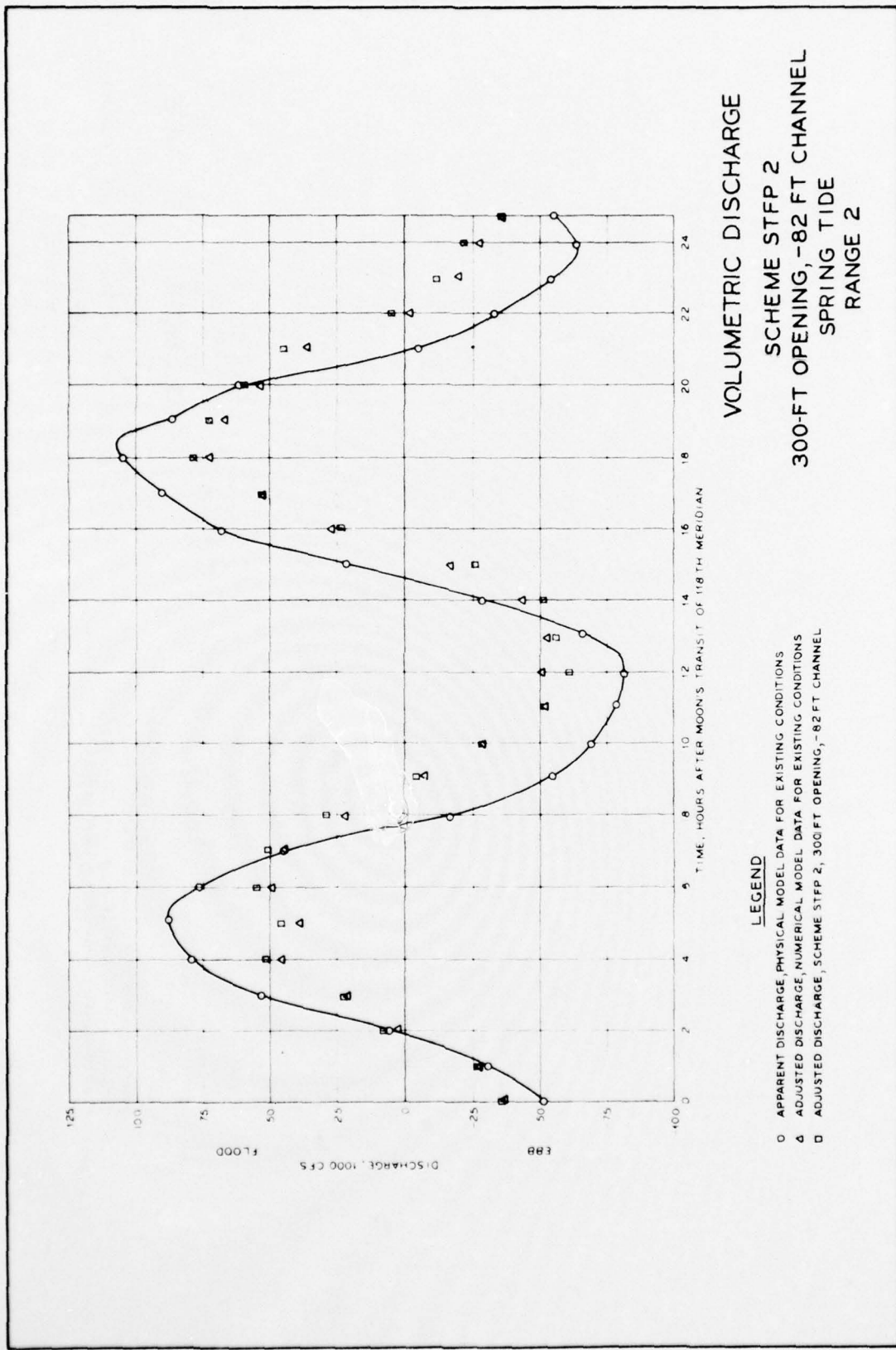
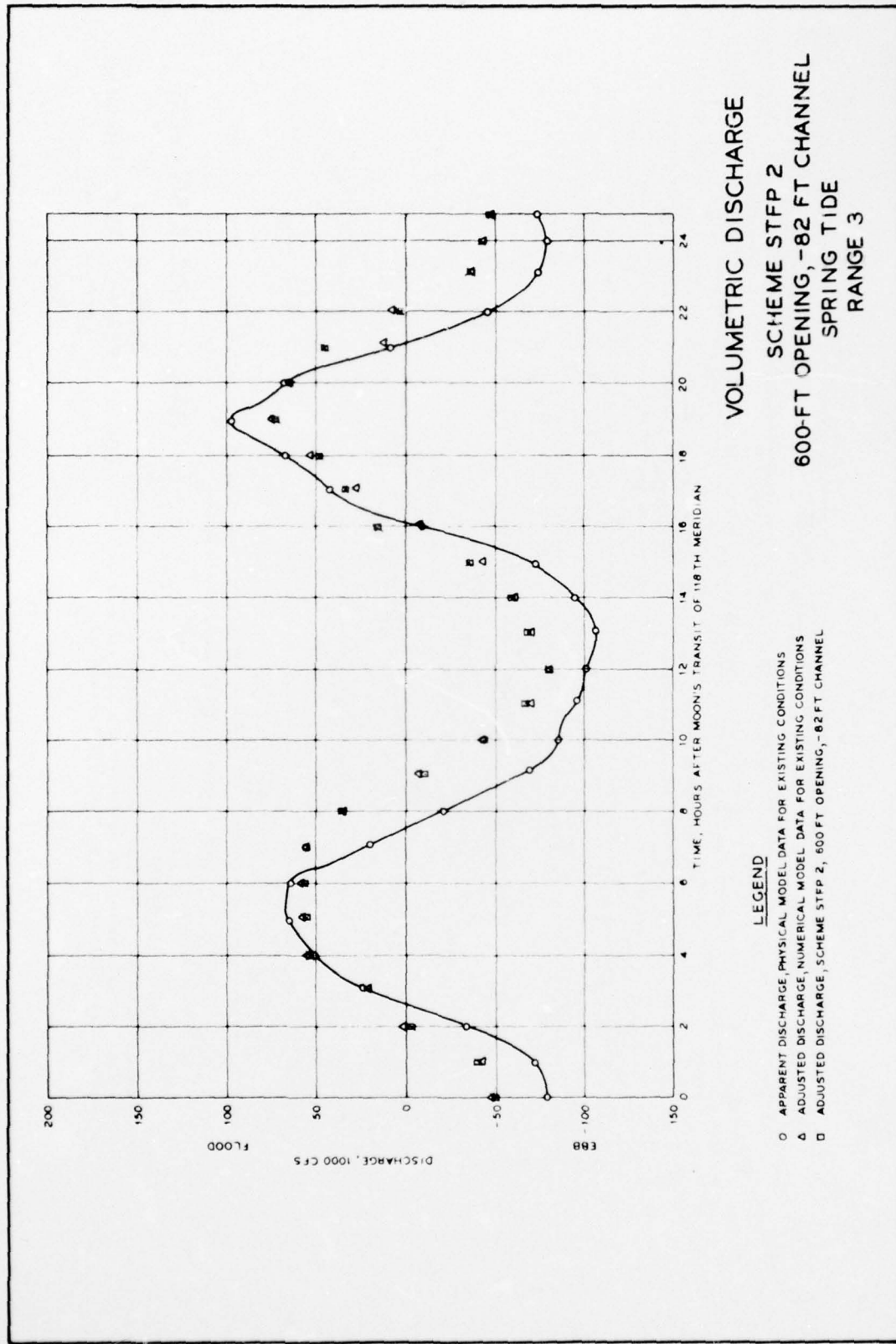


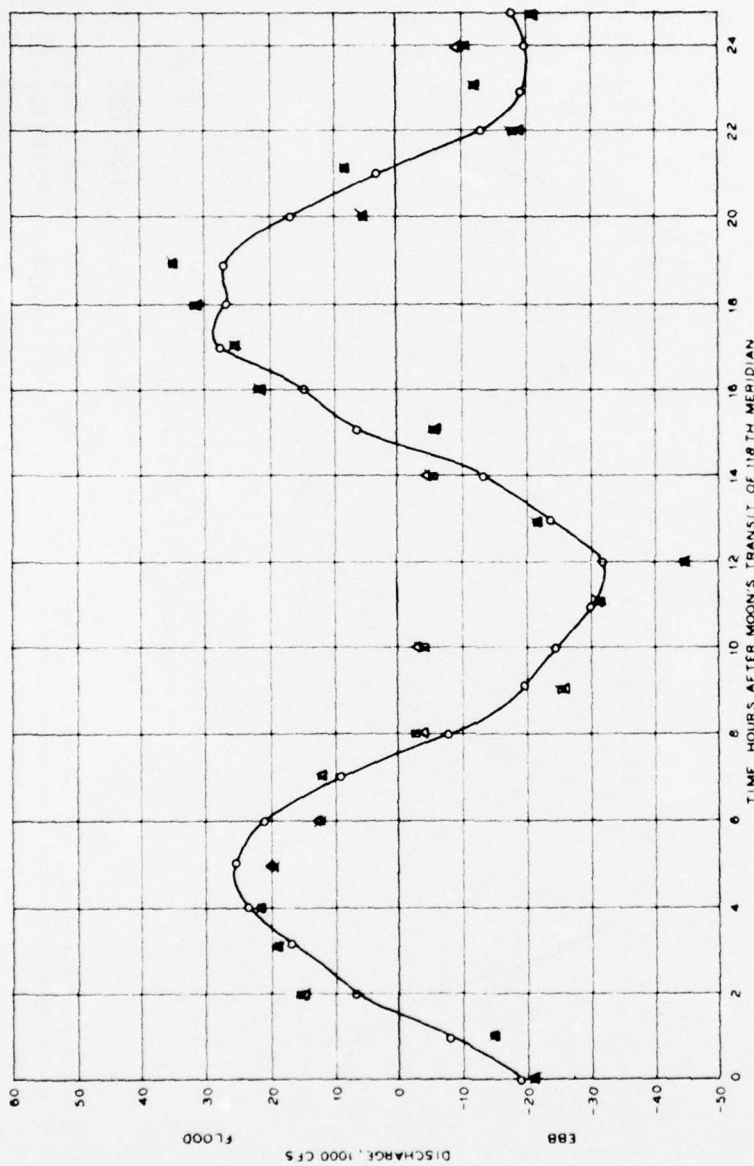
PLATE 94

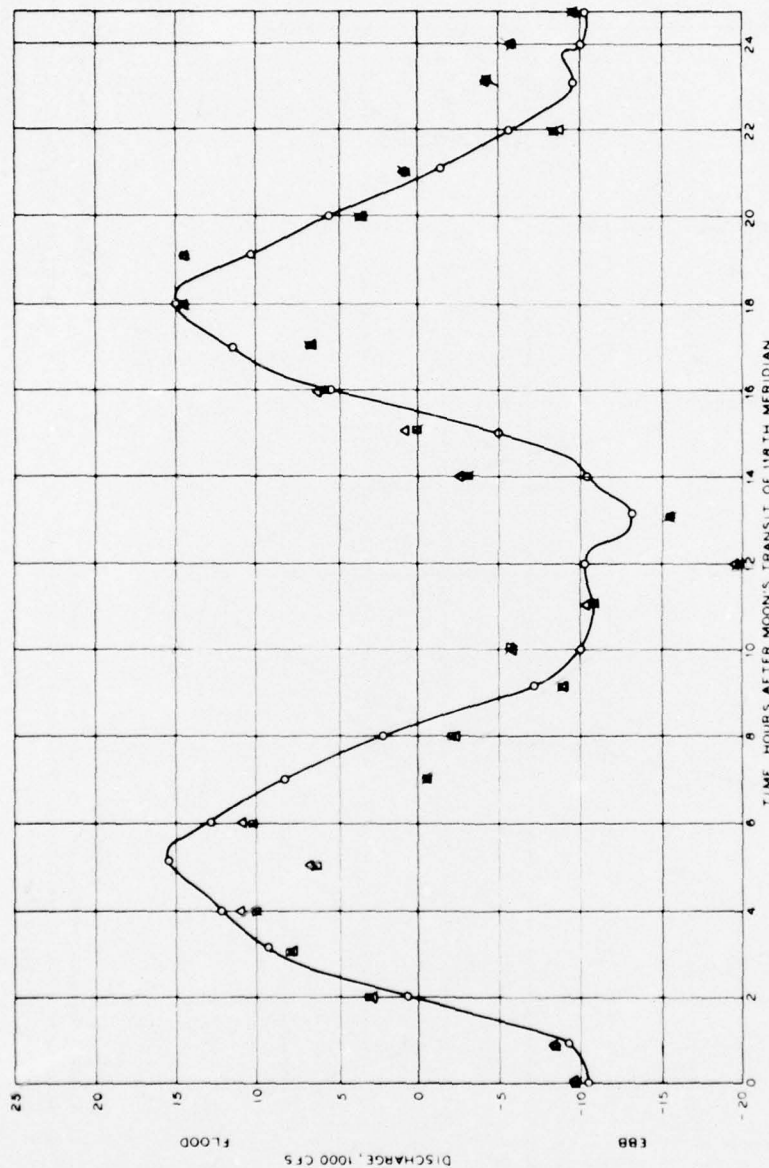


VOLUMETRIC DISCHARGE
 SCHEME STFP 2
 600-FT OPENING, -82 FT CHANNEL
 SPRING TIDE
 RANGE 5

LEGEND

- APPARENT DISCHARGE, PHYSICAL MODEL DATA FOR EXISTING CONDITIONS
- △ ADJUSTED DISCHARGE, NUMERICAL MODEL DATA FOR EXISTING CONDITIONS
- ADJUSTED DISCHARGE, SCHEME STFP 2, 600 FT OPENING, -82 FT CHANNEL





VOLUMETRIC DISCHARGE

SCHEME STFP 2
600-FT OPENING, -82 FT CHANNEL
SPRING TIDE
RANGE 8

LEGEND

- APPARENT DISCHARGE, PHYSICAL MODEL DATA FOR EXISTING CONDITIONS
- △ ADJUSTED DISCHARGE, NUMERICAL MODEL DATA FOR EXISTING CONDITIONS
- ADJUSTED DISCHARGE, SCHEME STFP 2, 600 FT OPENING, -82° CHANNEL
- ADJUSTED DISCHARGE, SCHEME STFP 2, 600 FT OPENING, -82° CHANNEL, RANGE 8

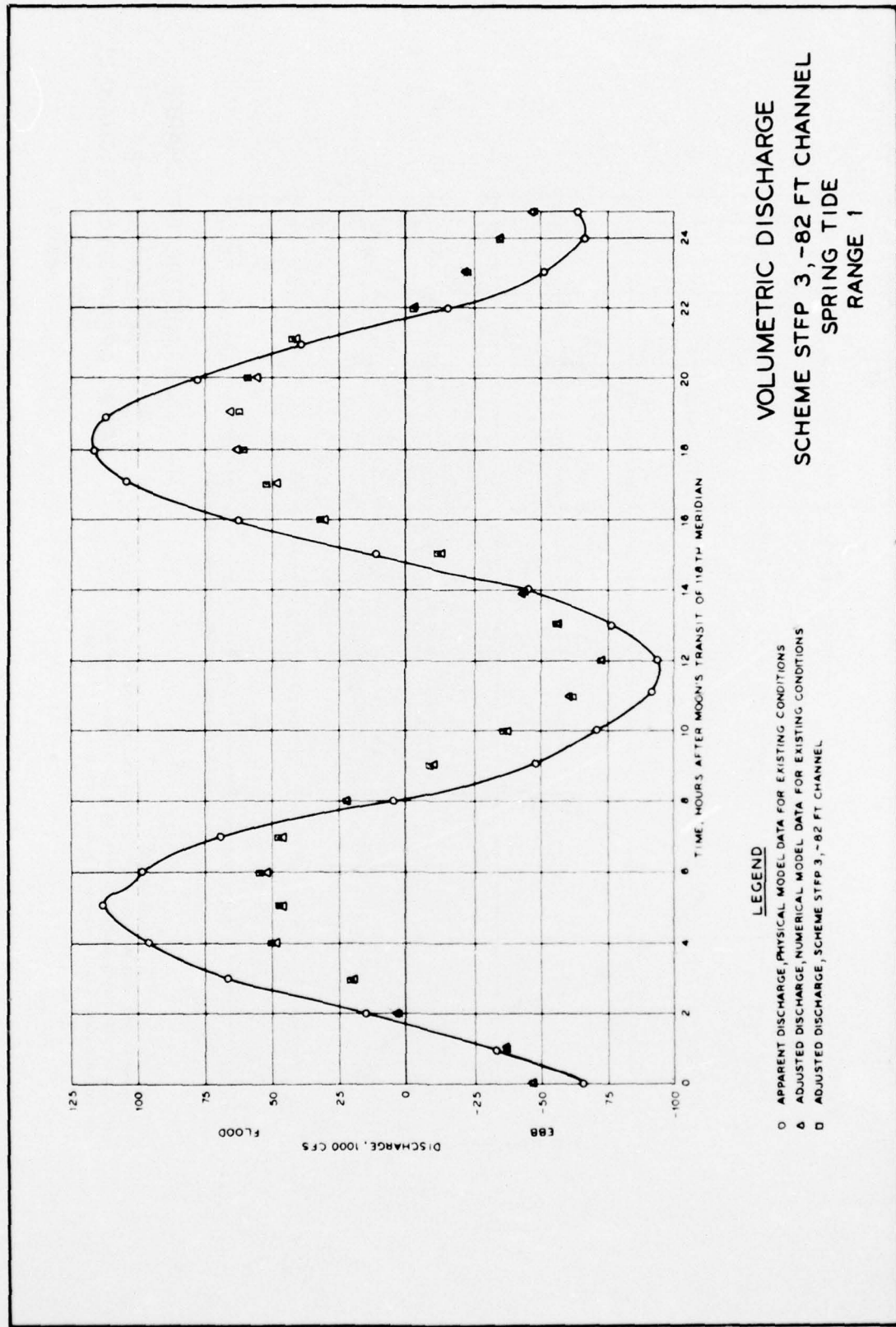
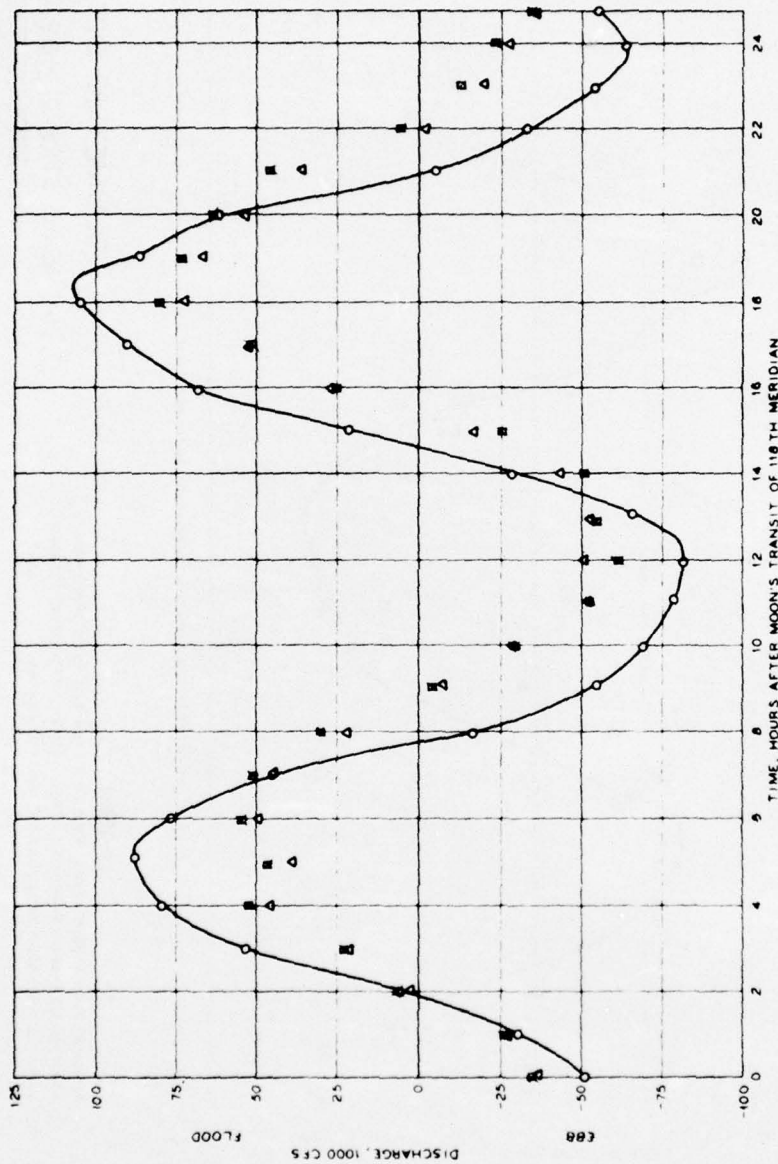


PLATE 98

VOLUMETRIC DISCHARGE
SCHEME STFP 3, -82 FT CHANNEL
SPRING TIDE
RANGE 2

LEGEND
○ APPARENT DISCHARGE, PHYSICAL MODEL DATA FOR EXISTING CONDITIONS
△ ADJUSTED DISCHARGE, NUMERICAL MODEL DATA FOR EXISTING CONDITIONS
□ ADJUSTED DISCHARGE, SCHEME STFP 3, -82 FT CHANNEL



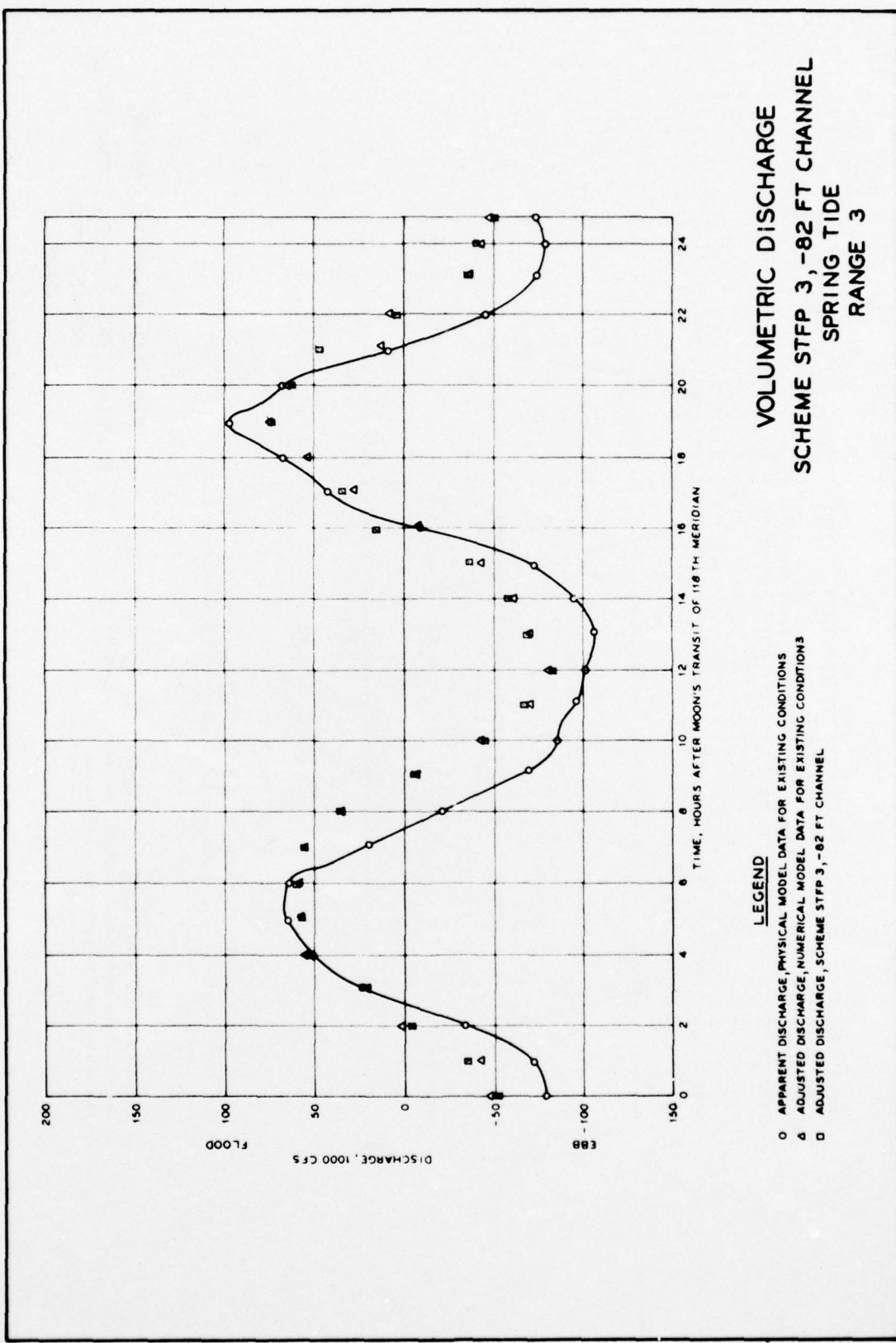
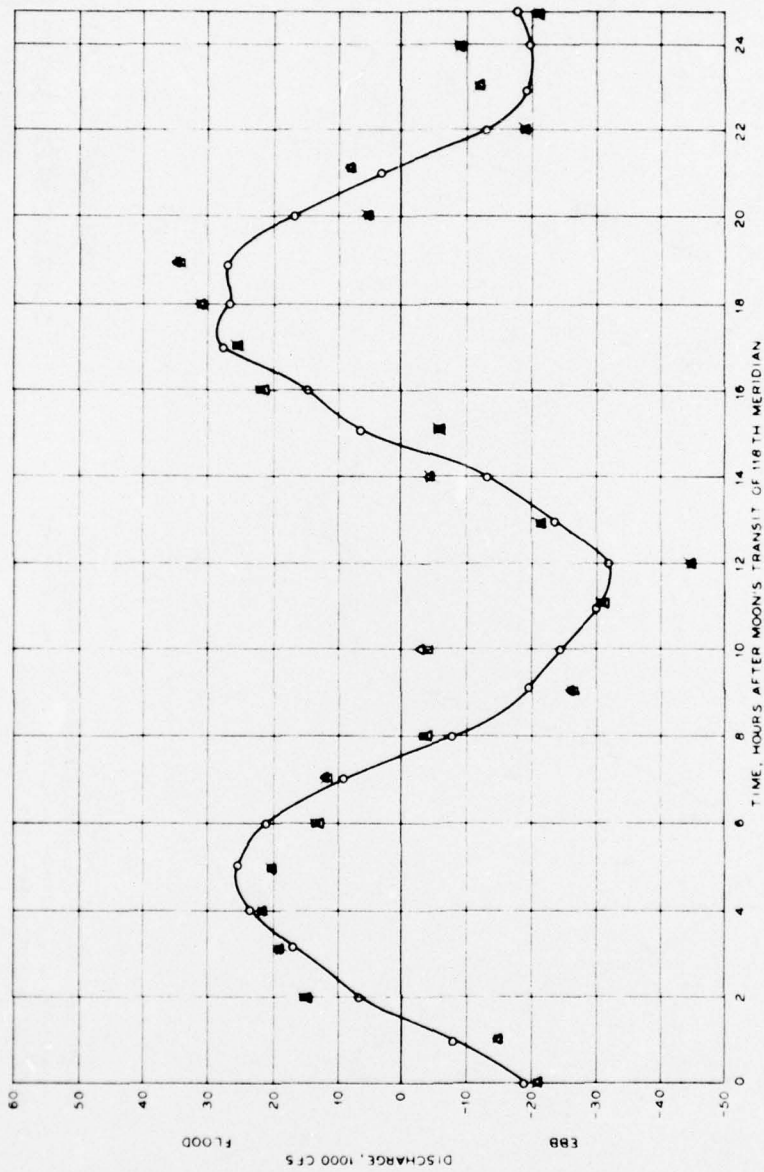


PLATE 100

VOLUMETRIC DISCHARGE
SCHEME STFP 3, -82 FT CHANNEL
SPRING TIDE
RANGE 5

LEGEND

- APPARENT DISCHARGE, PHYSICAL MODEL DATA FOR EXISTING CONDITIONS
- △ ADJUSTED DISCHARGE, NUMERICAL MODEL DATA FOR EXISTING CONDITIONS
- ADJUSTED DISCHARGE, SCHEME STFP 3, -82 FT CHANNEL



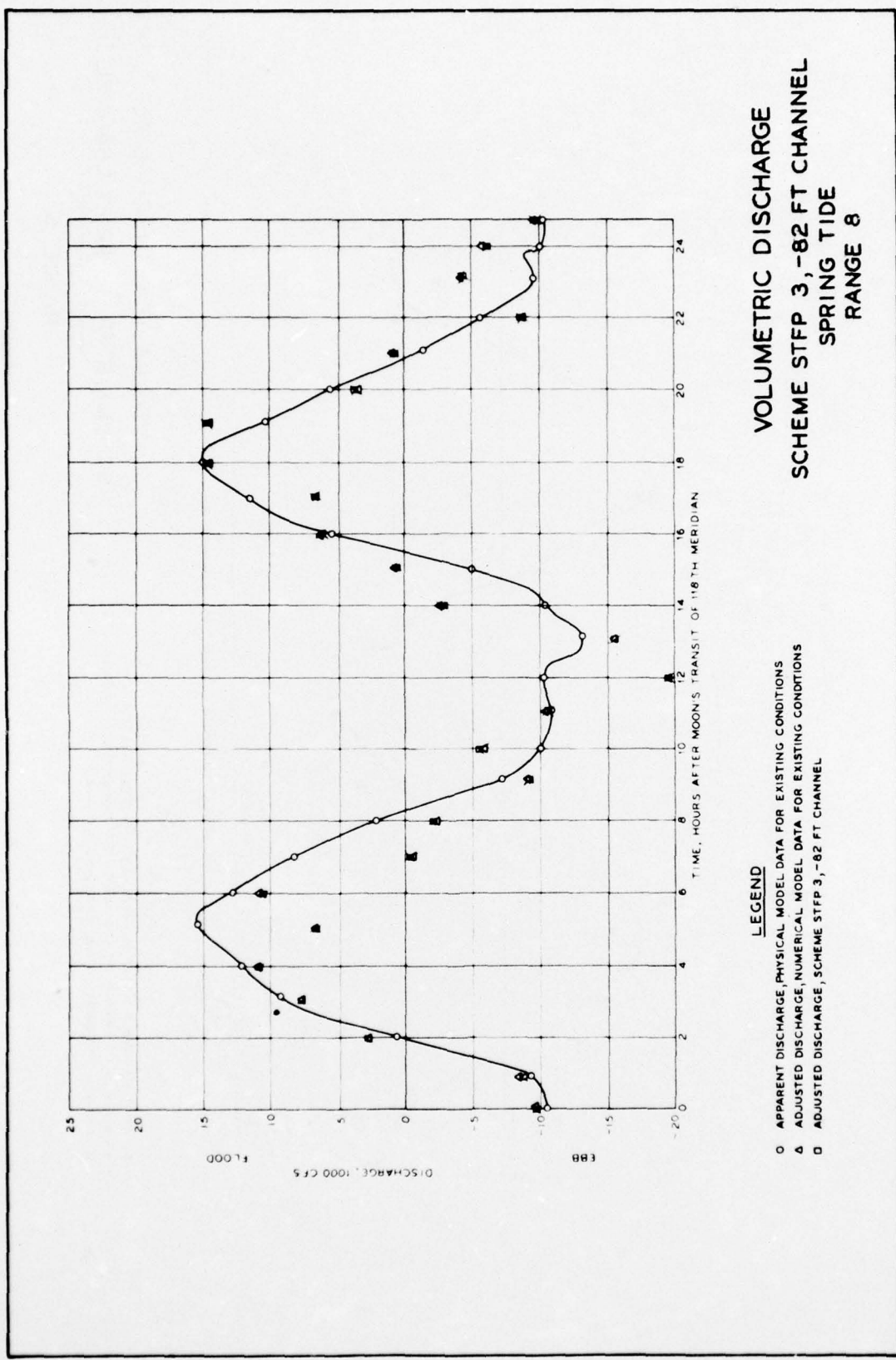


PLATE 102

APPENDIX A: NOTATION

C	Chezy coefficient
f	Coriolis parameter
g	Acceleration due to gravity
h	Water depth
j,k	Grid lines
L_x, L_y	Acceleration effect of the wind stress acting on the water surface in the x and y directions.
n	Integer defining the calculation time step
R_x, R_y	Effect of bottom roughness in x and y directions
t	Time
T_x, T_y	Wind stress components acting on the water surface
u	$u(x,y,z,t)$
v	Depth-averaged velocity component in the y direction
\bar{V}_n	Normal component of velocity
w	Depth-averaged velocity component in the x direction
x	Longitudinal coordinate measured along the estuary axis
x,y	Rectangular coordinate variables
y	Transverse coordinate
z	Vertical coordinate
η	Water-level displacement with respect to datum elevation
ρ	$\rho(x,y,z,t)$

In accordance with ER 70-2-3, paragraph 6c(1)(b),
dated 15 February 1973, a facsimile catalog card
in Library of Congress format is reproduced below.

Raney, Donald C

Numerical analysis of tidal circulation for Long Beach Harbor; Report 3: Existing conditions and alternate plans for Pier J completion and tanker terminal study with -82 ft channel, by Donald C. Raney. Vicksburg, U. S. Army Engineer Waterways Experiment Station, 1976.

1 v. (various pagings) illus. 27 cm. (U. S. Waterways Experiment Station. Miscellaneous paper H-76-4, Report 3)

Prepared for Port of Long Beach, Long Beach, California.
Includes bibliography.

1. Harbors. 2. Long Beach Harbor. 3. Numerical analysis. 4. Piers (Docks). 5. Tanker terminals. 6. Tidal circulation. 7. Tides. I. Port of Long Beach.
(Series: U. S. Waterways Experiment Station, Vicksburg, Miss. Miscellaneous paper H-76-4, Report 3)
TA7.W34m no.H-76-4 Report 3